



Argonne National Laboratory
Center for Transportation Research
9700 South Cass Avenue
IL-60439 Argonne, USA

Diesel Hybridization and Emissions

A Report to DOE from the ANL Vehicle Systems and Fuels Team



For the U.S. Department of Energy
Office of Advanced Automotive Technologies



Contacts:
Maxime Pasquier and Gilles Monnet
Argonne National Laboratory
9700 South Cass Avenue, Bldg. 362
Argonne, IL 60439



Argonne National Laboratory, a U.S. Department of Energy Office of Science laboratory, is operated by The University of Chicago under contract W-31-109-Eng-38.

DISCLAIMER

This report was prepared as an account of work sponsored by an agency of the United States Government. Neither the United States Government nor any agency thereof, nor The University of Chicago, nor any of their employees or officers, makes any warranty, express or implied, or assumes any legal liability or responsibility for the accuracy, completeness, or usefulness of any information, apparatus, product, or process disclosed, or represents that its use would not infringe privately owned rights. Reference herein to any specific commercial product, process, or service by trade name, trademark, manufacturer, or otherwise, does not necessarily constitute or imply its endorsement, recommendation, or favoring by the United States Government or any agency thereof. The views and opinions of document authors expressed herein do not necessarily state or reflect those of the United States Government or any agency thereof.

Available electronically at <http://www.osti.gov/bridge/>

Available for a processing fee to U.S. Department of Energy and its contractors, in paper, from:

U.S. Department of Energy

Office of Scientific and Technical Information

P.O. Box 62

Oak Ridge, TN 37831-0062

phone: (865) 576-8401

fax: (865) 576-5728

e-mail: reports@adonis.osti.gov

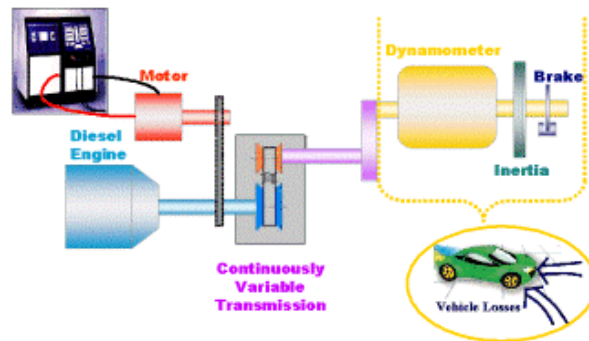


Executive Summary — Diesel Hybrid Shows Impact of Control Strategy on Fuel Economy and Emissions

Description of the Project

The CTR Vehicle Systems and Fuels team tested a diesel hybrid powertrain. Our goal was to investigate and demonstrate the potential of diesel engines in hybrid electric vehicles (HEVs) to improve fuel economy and reduce emissions.

The test setup consisted of a diesel engine coupled to an electric motor driving a Continuously Variable Transmission (CVT). This hybrid drive was connected to a dynamometer and a DC electrical power source, thereby creating a vehicle context by combining advanced computer models and emulation techniques.



The experiment focused on the impact of the hybrid control strategy on fuel economy and emissions — in particular, nitrogen oxides (NO_x) and particulate matter (PM). We used the same hardware and test procedures throughout the entire experiment to assess the impact of different control approaches.

Exploration of Different Control Approaches

Engine operation is key to hybrid vehicle control strategy, because it is directly related to fuel efficiency and gaseous emissions. The CVT parallel hybrid configuration provides tremendous flexibility in the choice of both engine torque and speed operation. The electric motor can replace, assist, or absorb the engine torque independently from driver expectations. In addition, the CVT allows decoupling between engine and wheel speeds.

Conventional Vehicle Operation Provides Experimental Reference

To obtain a fuel economy and emissions reference, we operated the vehicle in conventional mode, which yielded the first test results. Therefore, the electric motor was disabled, and the CVT acted as a manual transmission.

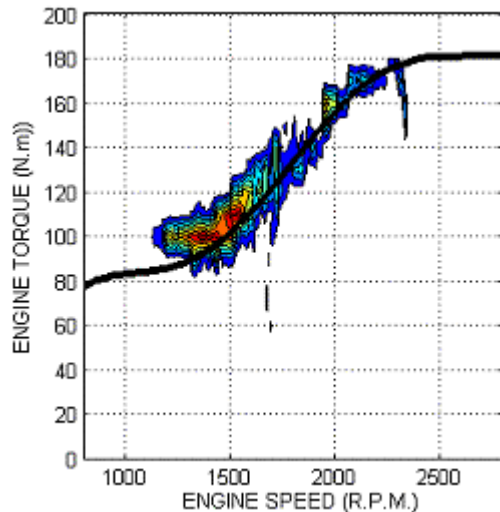
Hybrid Vehicle Control Using Best Engine Efficiency Curve

The best efficiency curve describes the optimal engine operating point for each power demand from an energy perspective. Therefore, the engine torque and the CVT ratio were both controlled to operate the engine at the most efficient point while satisfying the power demand. However, when the engine operates on its best efficiency curve, it produces excessive NO_x emissions. We used simulation to design a trade-off between fuel economy and NO_x emissions.

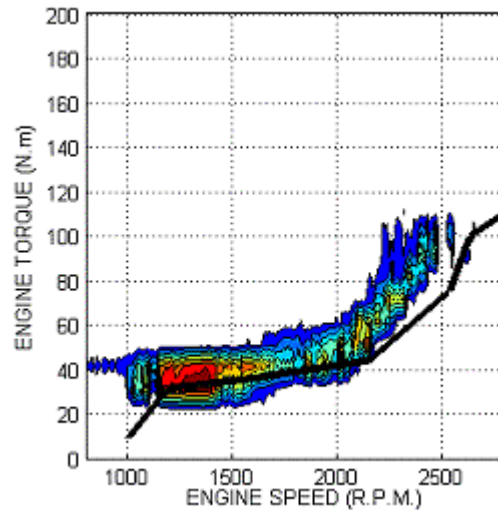
Hybrid Vehicle Control Using Best Engine Trade-Off Curve

For each engine power demand, we interpreted NO_x emissions and fuel consumption data to define the best trade-off curve. The engine torque and the CVT ratio were controlled to operate the engine on this curve while satisfying engine power demand.

Best efficiency operation



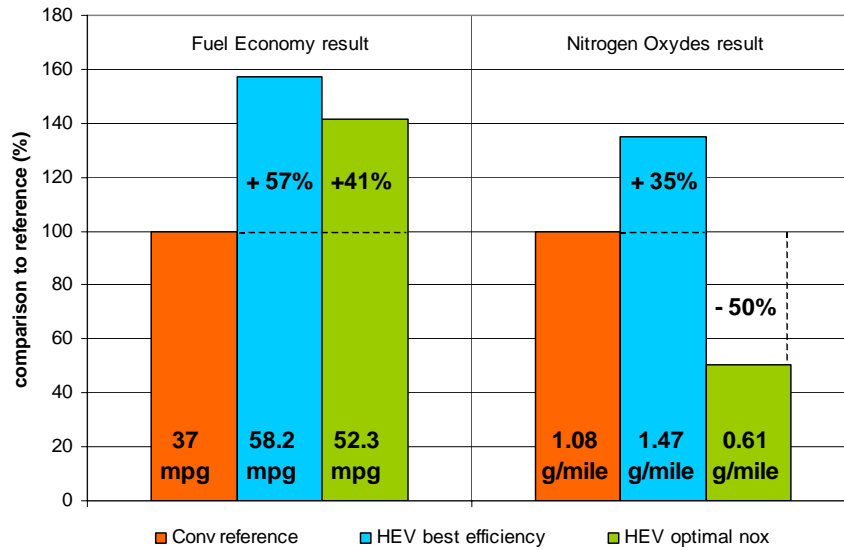
Best trade-off operations



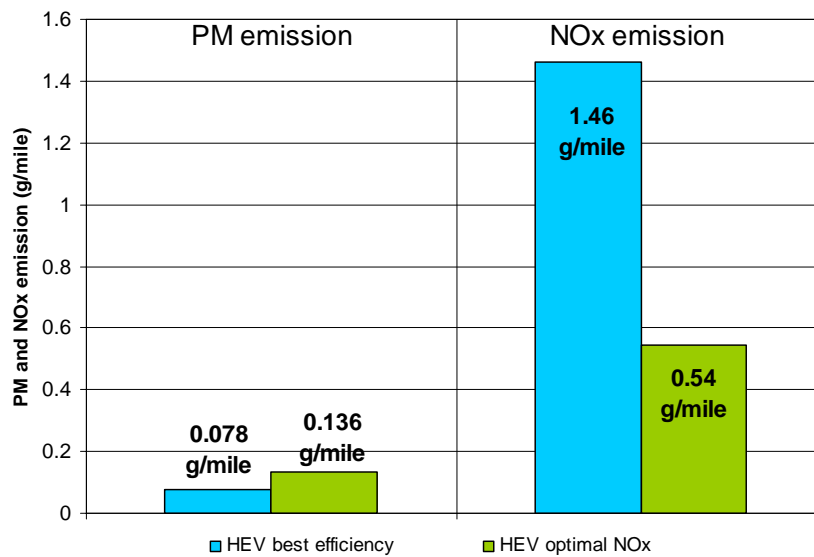
These figures display engine operating points during testing of the two hybrid control strategies. Color is based on duration of engine operation at a given operating point. Both curves were determined by using steady-state engine data. Control was developed in simulation and then implemented in a controller set up for experimental testing.

Experimental Results, Comparison, and Analysis

Operating the engine at optimal efficiency increased fuel economy by 57%. This efficient engine utilization results in a 35% increase in NO_x emissions. The best trade-off approach yielded a 50% NO_x reduction and yet improved fuel economy by 41%. However, it also resulted in an increase in PM emissions.



Summary of fuel economy and NO_x results



Summary of PM and NO_x results

Those results refer to an emulated conventional vehicle, which is actually penalized by (1) the inefficiency of a CVT acting as a manual transmission and (2) the losses and inertia of a disabled electric motor.



Conclusion

This experiment demonstrated and quantified the impact of control strategy on fuel economy and emissions for diesel hybrid vehicles. To complete the evaluation of diesel hybrid technology, after-treatment devices should also be considered. At this time, particulate filter technology is more mature than a NO_x absorber. However, the development of an after-treatment control integrated into the vehicle control strategy would complete the demonstration of a diesel hybrid as a short-term bridge to a hydrogen economy.

Sponsor

U.S. Department of Energy, Office of Energy Efficiency and Renewable Energy, FreedomCAR and Vehicle Technologies Program

Contacts

Maxime Pasquier or Gilles Monnet



Table of Contents —

1.	Description of the Project	9
1.1.	Objective and Approach	9
1.2.	Description of the Tools	9
1.3.	Simulation: Hybridization of the Baseline Vehicle	10
1.4.	Emulation: Control and Assembly of the Hybrid Powertrain.....	15
1.5.	Validation: Component Models, and Emissions Measurement.....	25
2.	Conventional Diesel.....	33
2.1.	Conventional Diesel Vehicle	33
2.2.	Conventional Diesel Powertrain	37
2.2.1.	Control Development.....	37
2.2.2.	Baseline Testing.....	40
2.2.3.	Impact of Engine Speed Transients	41
2.2.4.	Impact of Transmission Efficiency	43
2.2.5.	Impact of Engine Operation.....	45
3.	Hybrid Diesel.....	49
3.1.	Control Description.....	49
3.2.	Impact of Control on Fuel Economy	51
3.3.	Trade-Off between Fuel Economy and NO _x Emissions.....	56
4.	Conclusion	62
5.	Recognition.....	64
6.	Acknowledgments.....	66
7.	References.....	67
8.	Appendixes	69
8.1.	PSAT-PRO© User Guide	70
8.2.	Instrumentation	100
8.3.	Design of the Constant Velocity Sampler.....	101
8.4.	Data Acquisition Code to Calculate g/mi Emissions	108
8.5.	A, B, C Coefficients Calculation	110
8.6.	Different Mode of Operation of the Powertrain.....	113
8.7.	Engine Torque and Speed Using Best Efficiency Control.....	115
8.8.	NO _x Emissions Results from Engine Steady-State Tests.....	116
8.9.	Simulation Results Trade-Off Control Operation	117
8.10.	Engine Torque and Speed Using Trade-Off Control	118



1. Description of the Project

1.1. Objective and Approach

The main objective of the project was to determine the impact of hybridization and powertrain system control on diesel engine emissions and efficiency. Argonne National Laboratory (ANL) completed the design and installation of a hybrid electric powertrain in ANL's Advanced Powertrain Research Facility (APRF); the powertrain consisted of a CIDI engine and electric motor in parallel driving through a continuously variable transmission (CVT).

We simulated the components and the hybrid powertrain system by using our in-house developed simulation tool (PSAT©), which is translated to the ANL control software (PSAT-PRO©) to control the components individually and as a system. Several control strategies were developed, tuned, and tested. We used the powertrain test cell to study the trade-off between fuel economy and emissions by using powertrain controls and a validated Hardware-In-the-Loop (HIL) emulation technique.

1.2. Description of the Tools

The Center for Transportation Research (CTR) offers a unique integrated process based on powerful simulation tools and experimental facilities to perform system-level tests quickly and cost-effectively. ANL's unique combination of capabilities, expertise, and facilities reduce wasted effort in progressing from simulation to control implementation, component emulation, testing, and validation by removing the barriers associated with communication, data transfer, unnecessary code generation, or software changes. CTR's integrated process is based on three advanced tools: PSAT© simulation, HIL emulation, and APRF validation. [1]

The ANL-developed, forward-looking vehicle modeling software PSAT© is used to optimize control strategies that will be further translated to PSAT-PRO© and integrated in a micro-controller for hardware control. [2][3]

PSAT-PRO©, designed for use in the APRF, is a Matlab©-based program that uses dSPACE© prototyper to link PSAT© control strategy and real hardware control. This direct connection between modeling and simulation software, control software, and the APRF offers the opportunity to streamline technology development through continual feedback and refinement. Control implementation bridges the modeling and experimental hardware testing programs (see Figure 1). [4] (APPENDIX 1)

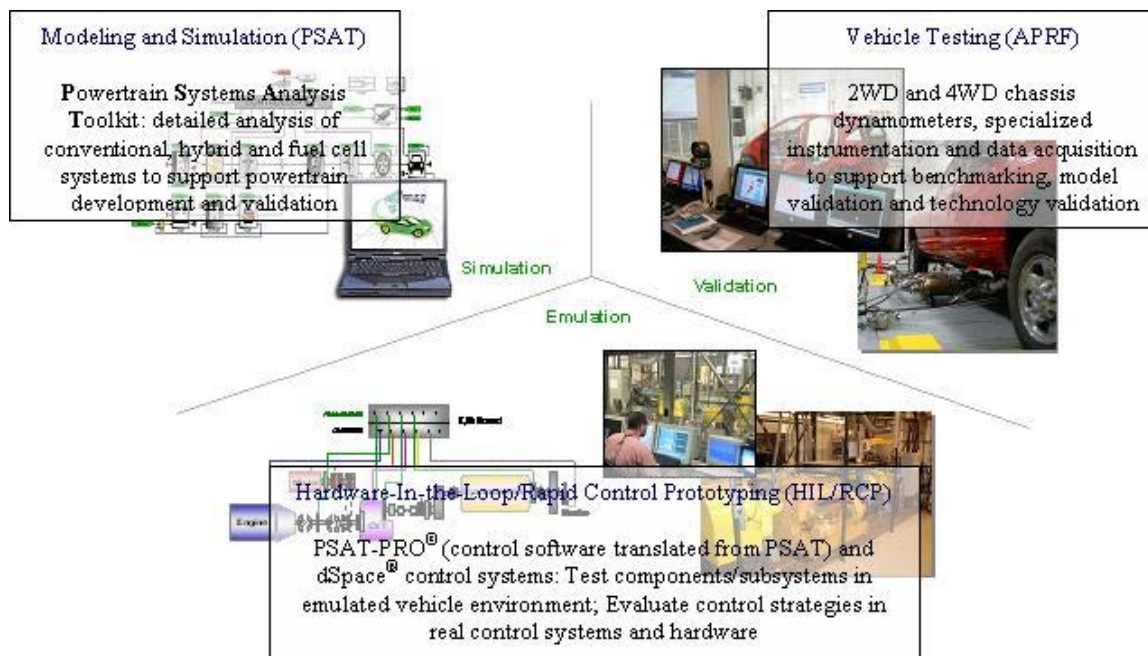


Figure 1: Argonne’s integrated vehicle system program

HIL is used at ANL as a unique, advanced testing methodology that combines hardware and computer models to emulate virtual components of the hybrid vehicle. HIL emulation provides a cost-effective way to validate technology.

The APRF is a flexible, controlled test environment that can be used to assess any powertrain technology, including engines, fuel cells, electric drives, and energy storage. State-of-the-art performance and emissions measurement equipment (listed below) are available to all component and vehicle test cells to support model development, HIL, and technology validation. [5] [6]

- Light- and heavy-duty dynamometers
- 2WD and 4WD chassis dynamometers
- Battery/fuel cell emulator (150 kW)
- Precision-controlled environment
- SULEV emissions measurement capability
- Low-emissions raw emissions bench
- Ultra-fast (<5 ms) HC and NO_x measurement
- Fast (10 Hz) direct fuel measurement
- Fast (10 Hz) particulate measurement;
- Unique laser-induced incandescence (LII)
- Mini-dilution PM measurement
- Scanning mobility particle sizer

1.3. Simulation: Hybridization of the Baseline Vehicle

To evaluate the performance of a conventional diesel vehicle available in the market, we used a Mercedes C-class C 220 CDI as our baseline. The vehicle specifications are summarized in the table below:



Vehicle Parameter	Specification
Model Year	1999
Body Style	4-door sedan
Transmission	5-speed manual
Tires	P195/65R15
Engine Type	2.2 L I-4 intercooled turbo-diesel
Fuel System	Electronically controlled, high-pressure common rail with pilot injection
Wheelbase	2,690 mm
Length/width/height	4,516 mm /1,723 mm/1,427 mm
Curb weight	1,410 kg
Top track speed	198 km/h (123 mph)
Acceleration 0–100 km/h	10.5 s
Rated Fuel Consumption (City + Highway)	6.1 l/100 km (38.5 mpg)
Engine Parameter	
Cylinders/arrangement	4/bank, 4 valves per cylinder
Displacement (bore × stroke)	2,151 cm ³ (88.0 mm × 88.4 mm)
Compression ratio	19.0:1
Rated output	92 kW (125 hp) @ 4,200 rpm
Rated torque	300 Nm @ 1,800–2,600 rpm
Aftertreatment	“Lean NO _x ” catalyst
Drivetrain Parameter	
Gear ratios	4.10/2.18/1.38/1.00/0.80/4.27
1st/2nd/3rd/4th/5th/reverse	
Final drive	3.07

The “lean NO_x” catalyst after-treatment technology installed on this vehicle relies on low-sulfur fuel to be effective. Therefore, we performed all of our experiments by using “California Low-Sulfur Commercial 2-D Diesel Fuel.”

The baseline vehicle (Mercedes C-class C 220 CDI) was simulated by using PSAT and then tested in a 4-wheel-drive chassis dynamometer environment at the APRF for validation purposes.

To assess the effect of hybridization and control on diesel emissions, we hybridized in simulation the Mercedes-Benz C 220 CDI vehicle (including engine downsizing).



By using PSAT, we were able to study a suitable hybrid version of the Mercedes C-class diesel. The Mercedes-Benz 2.2 L I-4 intercooled turbo-diesel engine used in the C-class vehicle has been downsized to a Mercedes-Benz 1.7-L engine from the same technology and generation. The engine power went from 92 kW (125 hp) @ 4,200 rpm for the conventional vehicle to 66 kW (88 hp) @ 4,200 rpm for its hybrid version. The engine downsizing corresponds to a power reduction of 26 kW (28%).

The results of the simulation suggest that, to compensate for this power reduction an electric motor of approximately 32 kW, coupled to the engine shaft, should be added. This recommended power is slightly higher than the power reduction to keep the vehicle at iso-performances and compensate for the gain in weight.

The control strategy uses the motor as a prime mover when the engine is off. The battery must provide enough power to start moving the vehicle as an electric vehicle. Engine start/stop decision is based on battery state of charge (SOC). The power requirement and battery choice depend on motor utilization. Simulation was used to select the most suitable battery for our application.

Since realistic vehicle performances are expected, utilization of commercially available existing battery technology is a requirement for the battery choice.

In simulation, a custom-made battery pack can be designed by using existing commercially available battery cells that are available in PSAT. The number of cells is calculated to meet a minimum total-pack requirement of 30 kW. The number of cells then sets pack characteristics (voltage, mass, etc). Battery capacity is also a key issue because it is directly related to engine utilization.

We used PSAT to design two battery packs matching our power requirement. The battery models were then submitted in simulation to the power profile extracted from test results.

Figures 2 and 3 show voltage, current, and SOC variation of the batteries when submitted to the test power profile.

Figure 2: Pack A — Cylindrical Ni-Mh from Panasonic (Japanese Prius cells technology)
Cell Characteristics: 1.2 V/6 Ah/200 g
Pack: 240 cells, 288 V, 6 Ah, 50 kg

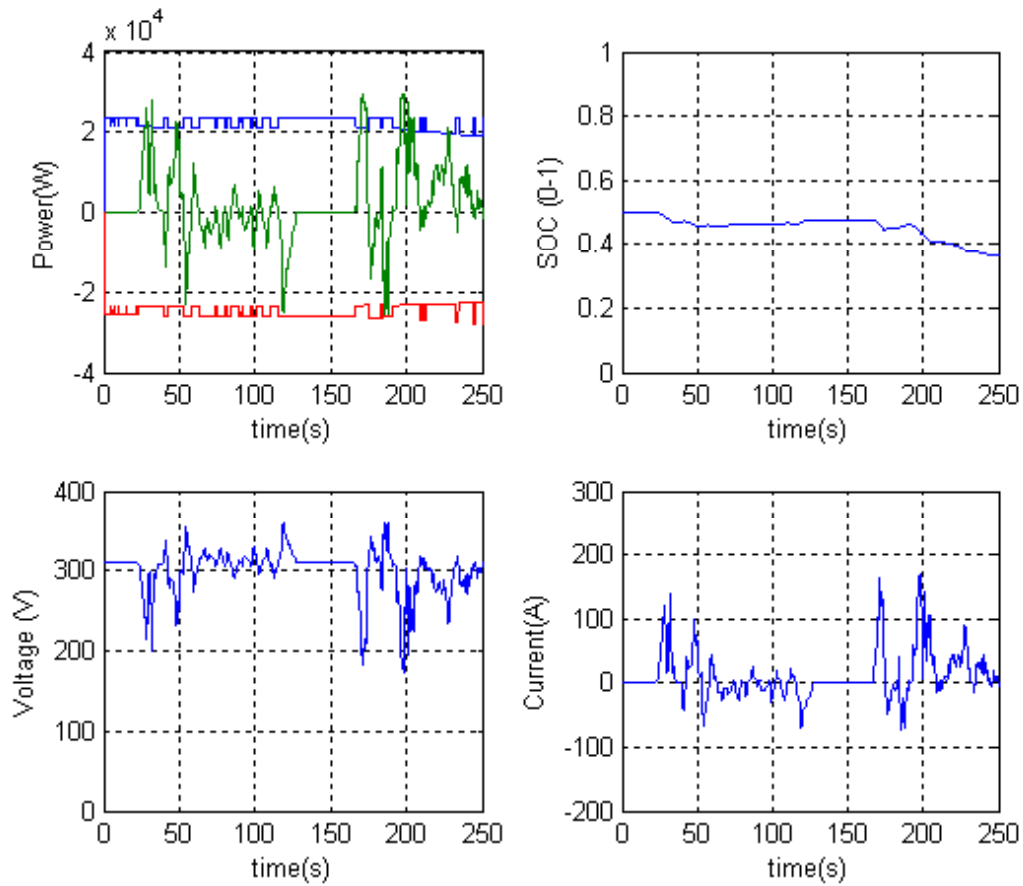
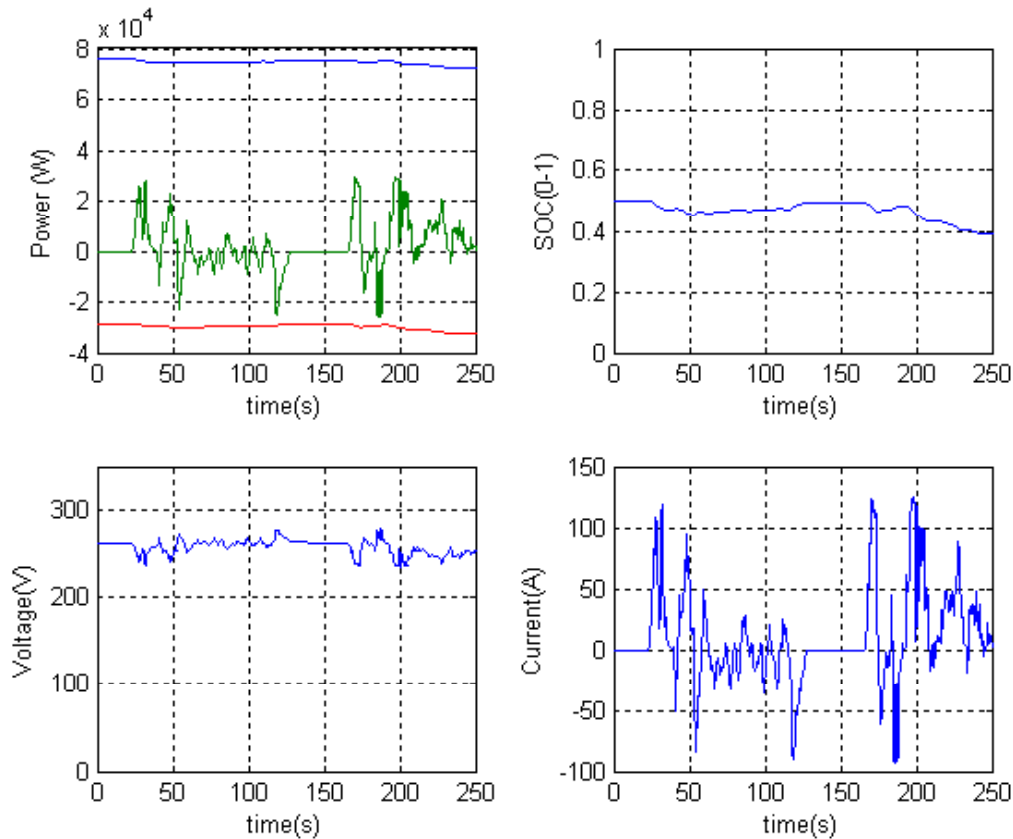


Figure 3: Pack B — Li-ion from SAFT

-Pack B: Li-ion from SAFT

Cell Characteristics: 3.8 V/6 Ah/550 g (estimated)

Pack: 6 modules of 12 cells, 72 cells total, 276 V, 6 Ah, 45 kg



Those results show that the SAFT Li-Ion technology is more suitable for our application: The main advantage is better power and energy density and the higher available power to handle regenerative event. This battery offers more flexibility to motor utilization and therefore more options to design control strategy.

The components have been sized to eliminate any unnecessary constraints and limitations and ultimately to increase the possibility of system control. For those reasons, a fixed ratio has been introduced between the engine shaft and the motor shaft. The ratio has been selected to adapt the motor speed range to the engine speed range. The maximum speed of the engine is 4,800 rpm, and so assuming a maximum speed of 8,000 rpm for the motor, this gives us a ratio of approximately 1.7.

Different types of transmission have been studied in simulation, and it appears that a continuous variable transmission (CVT) provides more possibilities in terms of control than an automatic or a manual transmission. One of the benefits of using a CVT is that the engine speed is decoupled from the vehicle speed. The CVT ratio allows the engine to be kept at a target operating speed. On the other hand, simulation results show that a CVT has a lower efficiency than a manual transmission. Because one of the objectives of the project is to demonstrate the impact of control on fuel economy and emissions, we decided to use a CVT and to modify it to increase its efficiency.

1.4. Emulation: Control and Assembly of the Hybrid Powertrain

To evaluate the potential of Diesel engines in a Hybrid Electric Vehicle (HEV) environment, we used a unique advanced testing methodology that combines hardware and computer models, thereby providing a cost-effective way to validate technology. We can apply a PSAT© control strategy to efficiently use a diesel engine in a complex hybrid configuration while the battery and the vehicle are being emulated using Hardware-In-the-Loop (HIL).

The term HIL is derived from the common practice of testing an electronic control unit (hardware) with a real-time computer that behaves like a system or vehicle (virtual) in a closed loop. [7]

HIL is often confused with rapid control prototyping, or RCP, which is the practice of testing control software with a real system, because both often use the same control software development approach.

In this project, because we actually used some elements of both HIL and RCP, there is potential for confusion. We used a real-time computer to control the dynamometer to react as a vehicle and a DC power source to act as a battery, but we also controlled the components of the hybrid powertrain.

The hybrid powertrain was controlled with PSAT-PRO[®]. Specifically, the computer-based PSAT-PRO[®] vehicle controller controlled the torque of the powertrain to track a vehicle speed profile. The speed of the transmission output shaft (corresponding to the wheels) was measured. We fed this measured speed to the vehicle model to determine vehicle losses under these conditions. To simulate the torque losses that would be produced in reality by the vehicle's aerodynamics, the calculated vehicle losses were sent to the dynamometer as a torque command. The powertrain control computer is shown in Figure 4, and the overall concept is shown in Figure 5.



Figure 4: HIL hybrid powertrain control computer using PSAT-PRO[®]

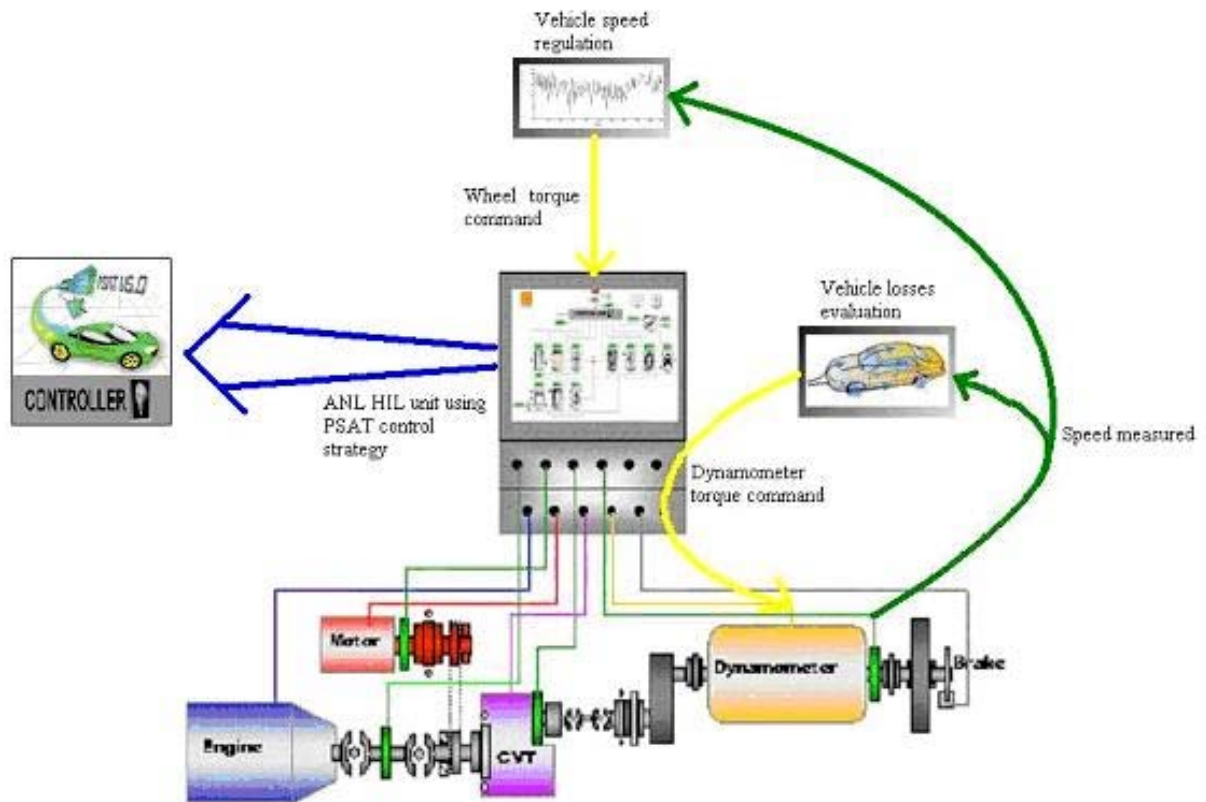


Figure 5: Powertrain control concept using the ANL HIL computer system

We designed a hydraulic friction brake to provide the resisting torque that a vehicle would need during an aggressive driving cycle. Two calipers were used on the same disk so that no radial force was applied to the rotating shaft, and the calipers teamed their effort. The calipers, disk, and master cylinder were automotive aftermarket units, typically used in racing applications. To translate this to a brake pressure (and resulting torque), we designed an air control system to operate the hydraulic automotive master cylinder. A high-precision pneumatic regulating valve took the analog command from the PSAT-PRO[®] computer and provided a proportional air pressure output. The output pressure then entered a pneumatic cylinder that provided the mechanical force to the automotive hydraulic master cylinder. The hydraulic pressure from the master cylinder actuated the calipers (see Figure 6).

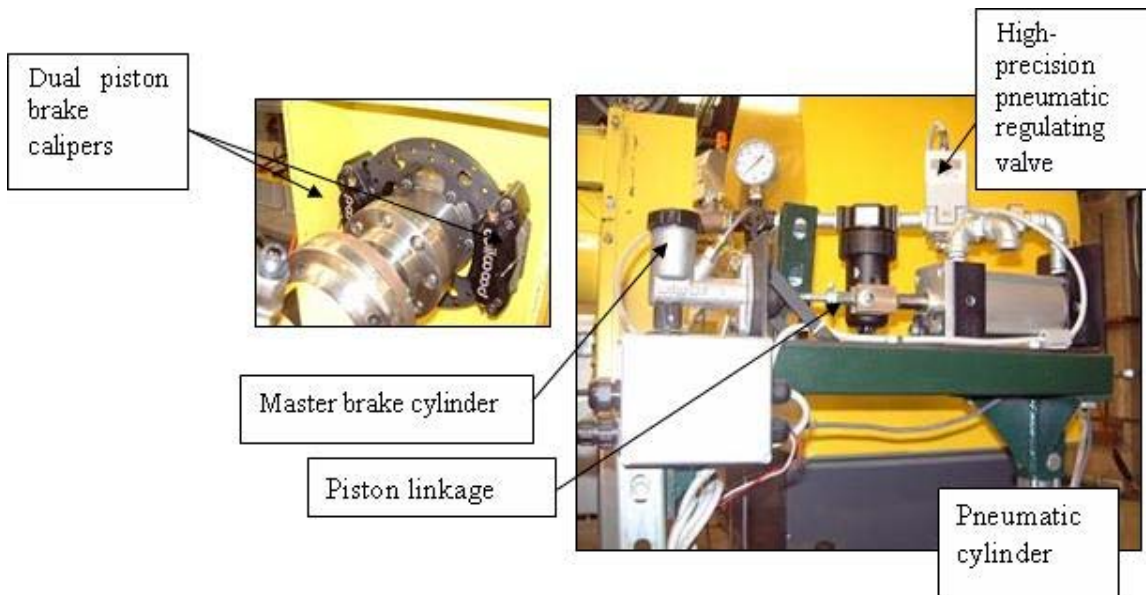


Figure 6: Disc Brake and Controller

Flywheels were added to one shaft of the both-ended dynamometer to provide the inertia required for the mass of the emulated vehicle (see Figures 7 and 8).

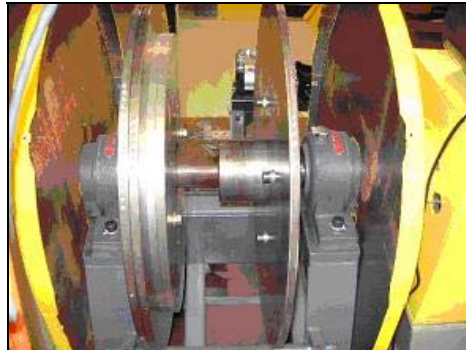


Figure 7: Inertia flywheels

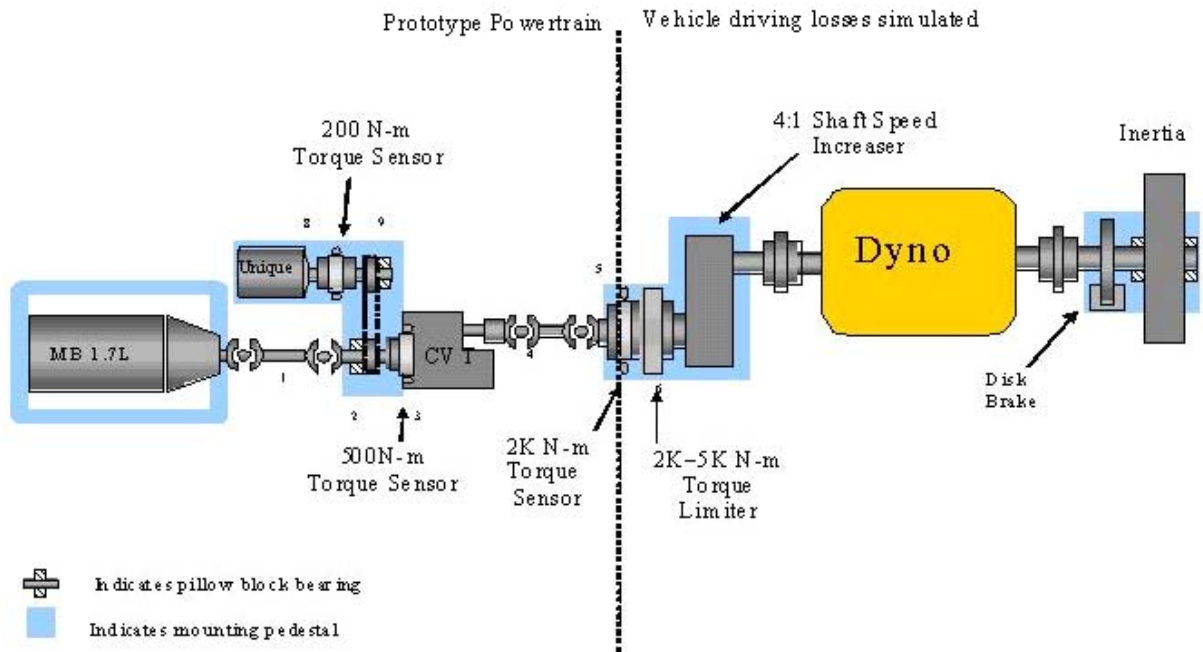


Figure 8: Layout of major components of the hybrid powertrain

The transmission was a modified Nissan CK-2 CVT, which uses a Van Doorne push-type belt that is commercially available in several Japanese production vehicles. Mechanical and electrical modifications were made to the CVT, both internal and external to the transmission. In stock trim, an off-board transmission control unit that controls torque converter lock-up, CVT ratio, and hydraulic pressure accompanies the CVT. In its original design, the mechanical hydraulic pump is connected to the engine through the torque converter.

Hybridization requires disconnecting the engine from the transmission by using a clutch, temporarily allowing the electrical motor alone to propel the vehicle. The torque converter was replaced by a clutch. The clutch benefits system efficiency because clutch efficiency is better than torque converter efficiency.

The reverse planetary gear was removed because HEVs with electric-only capabilities can use the electric motor for reverse.

All CVT control is done with the ANL-developed PSAT-PRO© control software; additional hardware has been added to support this approach. But the main modification to the CVT was the removal of the internal high-pressure hydraulic pump. We replaced it with an off-board pump. The pump is a key component of the CVT because it provides adequate belt/pulleys clamping. By using an external pump, much higher power transmission efficiencies can be achieved because an electrically driven pump allows the optimal control of hydraulic clamping pressure by decoupling the pump from the transmission input shaft (see Figures 9 and 10).



Figure 9: Removal of the CVT oil



Figure 10: Modified Nissan CVT

Supply clamping pressure is a key parameter for efficient use of this type of transmission. Ideally, the pressure should always be minimized to allow efficient torque transmission while avoiding belt slipping (if pressure is too low) or overheating and abnormal wear (if pressure is too high).

For this reason, a dynamic control algorithm has been integrated into the powertrain controller to allow optimal CVT operation. This algorithm uses instantaneous CVT input shaft torque and ratio measurement to calculate optimum supply pressure and accordingly command hydraulic pump.

Figure 11 shows in parallel the CVT pressure, the input torque used to dynamically control the hydraulic pump, and the vehicle wheel speed during a test.

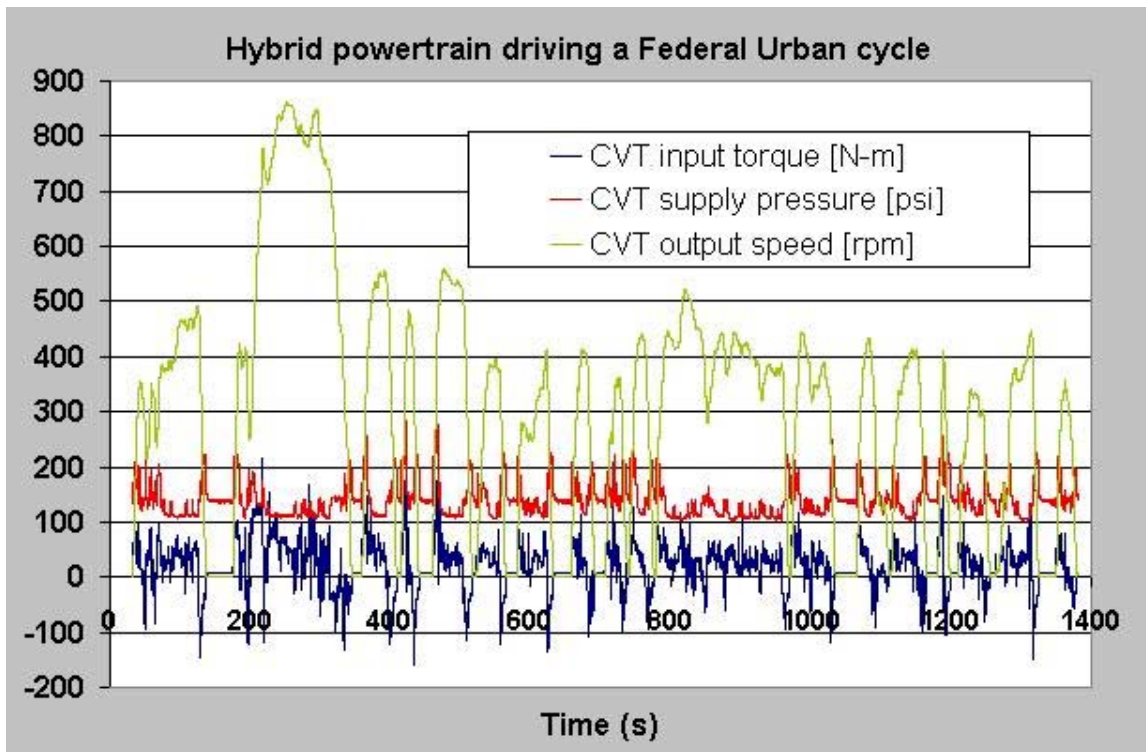


Figure 11: CVT pressure control

The test data show a substantial improvement in the efficiency of the transmission.

The hydraulic pump was instrumented to evaluate its energy use. This parameter needs to be taken into account to validate the actual gain in efficiency of the dynamic pressure control. Therefore, the power consumed by the auxiliary pump was taken into account. The electric power consumed by the pump was drawn from the emulated battery to reflect its impact on fuel economy (see Figure 12).

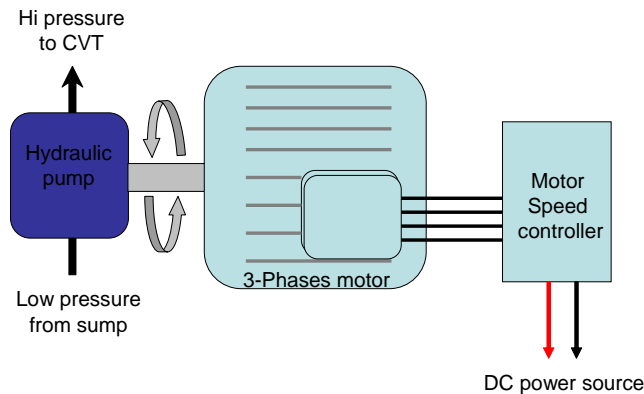


Figure 12: Off-board hydraulic pump

We used pump specifications to evaluate its instantaneous power. The manufacturer specifies pump shaft torque and speed according to operating pressure and flow. A constant efficiency is used to convert pump drive power into electrical power. The power is then drawn from the battery to discharge it and ultimately impact fuel economy, which is corrected according to battery state of charge.

The efficiency of the modified CVT was measured on the complete speed, torque, and ratio range of the transmission. The results of this mapping are shown in Figure 13.

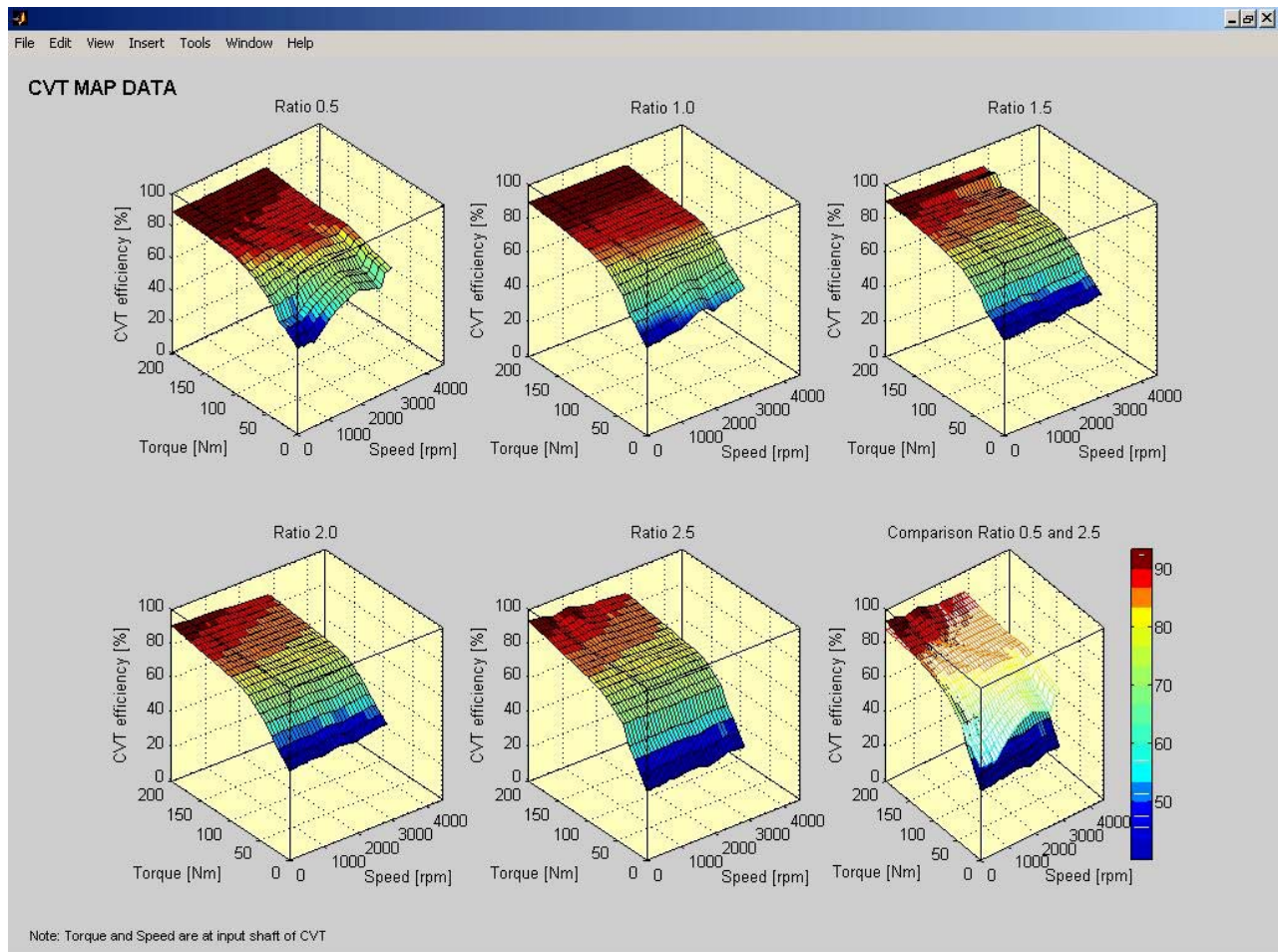


Figure 13: Modified CVT efficiency map

Figure 14 shows a comparison with a similar transmission commercially available in the Toyota Opa CVT. This vehicle has been previously tested at APRF for a different purpose, but the vehicle was instrumented with an engine torque sensor and an axle torque sensor. Therefore, data could be extracted from the tests for CVT efficiency comparison. [8]

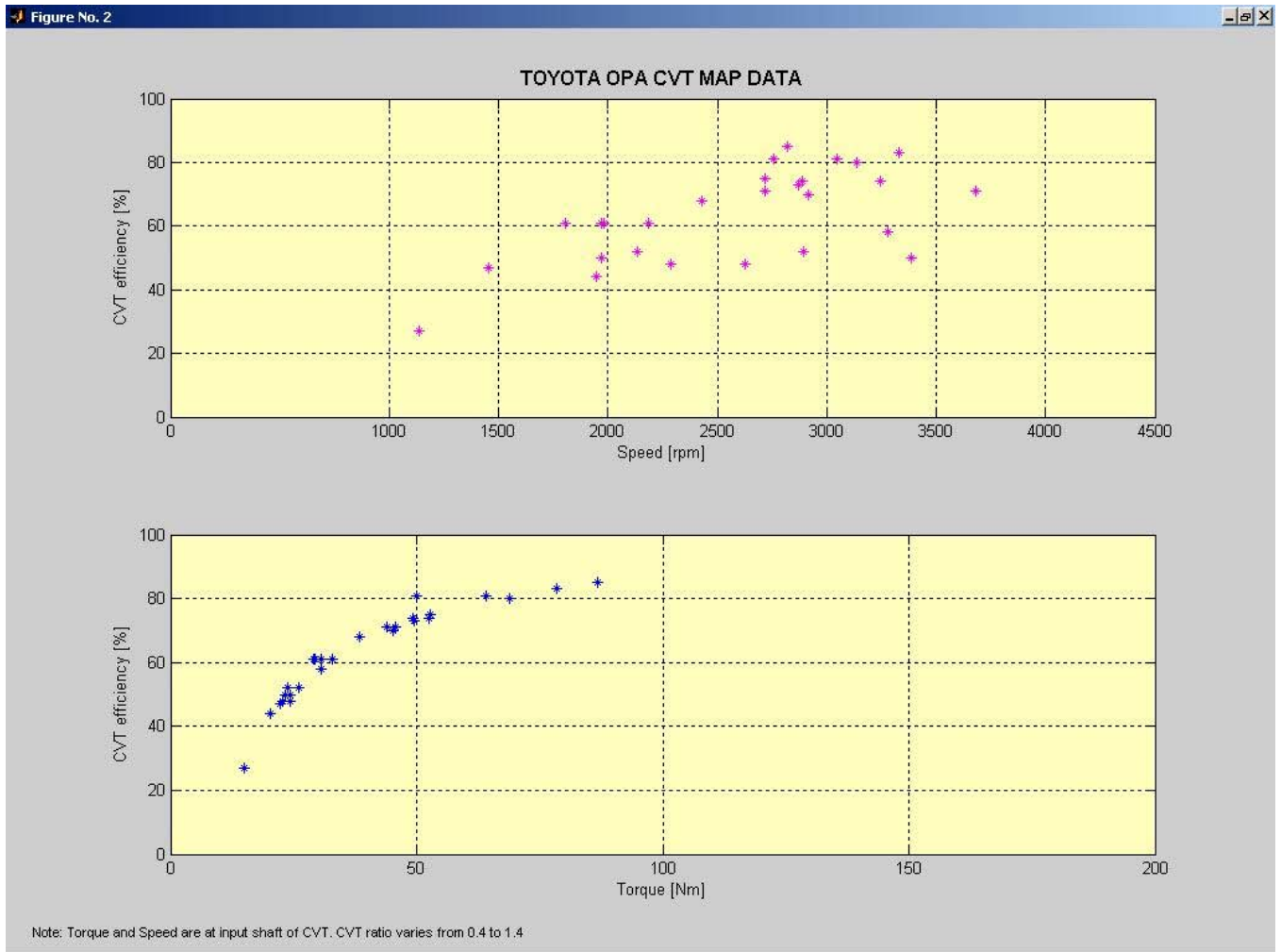


Figure 14: Toyota Opa CVT efficiency data

As discussed earlier, the simulation study recommends an engine downsizing from 92 kW (125 hp) @ 4,200 rpm for the conventional vehicle to 66 kW (88 hp) @ 4,200 rpm for its hybrid version. A Compression-Ignition Direct-Injection (CIDI) engine from a Mercedes-Benz A170 CDI vehicle was removed from a research vehicle and prepared for testing as part of this HEV powertrain configuration (see Figure 15).



Figure 15: CIDI 1.7-L engine

The motor, a 32-kW continuous (45-kW peak) DC brushless permanent magnet traction drive system from Unique Mobility (UQM), introduced the electrical torque into the powertrain by the use of a flat-toothed belt. The belt was a Woods QT Power Chain specifically made for high-torque applications. For greater accuracy in simulating the components in an actual vehicle, the components were designed to keep the inertia to a minimum (see Figure 16).



Figure 16: DC brushless permanent magnet electric motor

The battery was emulated by using a DC power source (ABC150). Emulation was used to replace a real battery and to gain flexibility over the type of battery used.

Several options were available to emulate the battery, but the best option was a power-based constant voltage battery emulation.

With this option, the electric motor is powered by using a constant nominal 180 V. The current drawn and the voltage are used to calculate instantaneous electrical power. The predicted voltage from the battery model and the measured power give the current that would be drawn from the real battery. This calculated current is used to feed the battery model and predict voltage variations (see Figure 17).

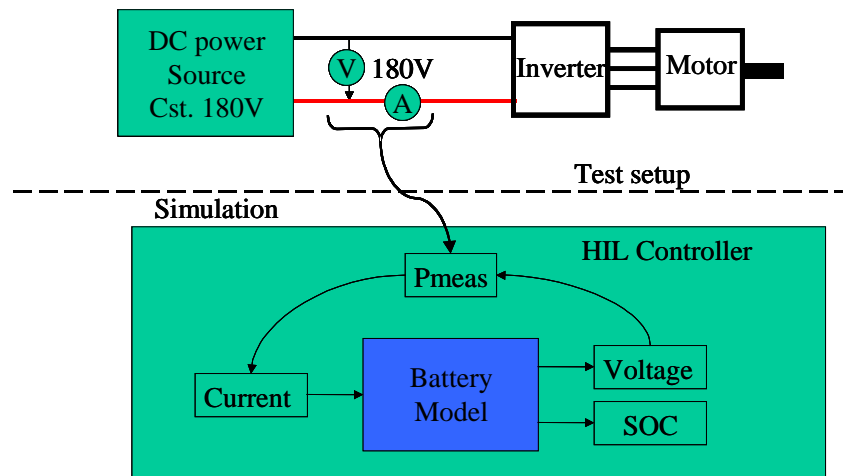


Figure 17: Battery emulation principle

With this solution, the actual inverter DC voltage range does not limit battery choice, and we could choose the battery independently from the inverter's specifications. In addition, the SOC calculation is as realistic as the current measurement is accurate because there is no delay in the control of the ABC150. In fact, there is no need for dynamic control of the DC power source.

One can argue that battery voltage is different from inverter voltage, but we can hypothesize that in an actual HEV, inverter hardware should be designed to interface/match motor and battery characteristics. Furthermore, inverter losses are still taken into account since the inverter is physically integrated into the test setup. Also, it has been demonstrated that motor inverter efficiency is not significantly affected by a variation in DC voltage. The emulation is as realistic as the battery model. Therefore, adequate effort should be dedicated to the validation of the component models used for emulation.

1.5. Validation: Component Models, and Emissions Measurement

Validation of component models is an integral part of the emulation process. Through validation, researchers are able to compare hardware development/testing with data from modeling. The enablers for the integrated process are the tools that ANL has developed to generate data, feed component models, analyze vehicle powertrain systems, perform testing by using control tools, and produce results that validate the models. An important common thread of these tools is model validation. The usefulness of a model can only extend to the limits of confidence, which are based upon rigorous validation of the models. [9][10][11][12]

We consider a vehicle model validated only when all of the component model predictions agree with the test data. To validate a single component, the data measured during a drive cycle are fed directly into the component model, and the simulated output is compared with the measured data. If there are errors in individual component models, this method will easily expose them.

Before using the battery model for emulation purposes, we validated the model by using this methodology by tracking voltage and current throughout the drive cycle. The battery model predictions were compared to the actual battery data from the ANL Battery Test Facility by using actual discharge profiles from the previously tested Toyota Prius.

Once the components had been validated independently, the last step was to integrate the control strategy developed with PSAT and compare the powertrain reactions to the results of simulation.

The whole drivetrain was instrumented to allow this comparison. Three torque and speed sensors are necessary: one on the motor shaft, one on the input shaft of the CVT, and one on the output shaft of the CVT, as shown in Figure 18.

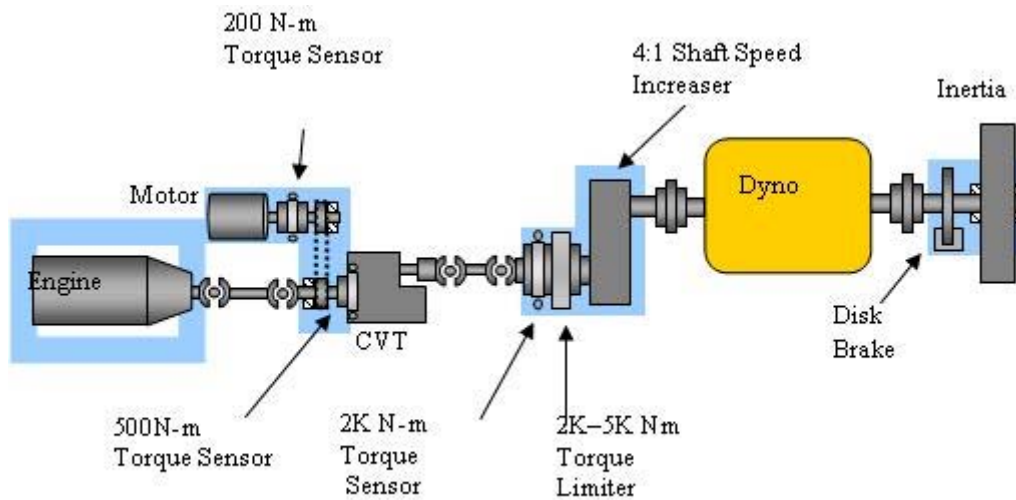


Figure 18: Instrumentation of the powertrain

To measure the CVT inputs without modifying the behavior of this component, we integrated a flat torque sensor. The bell housing of the CVT transmission had to be modified to mount the HBM T-10F flat torque sensor to measure CVT input torque. Flanges that mated to the splined shaft and the engine output were also machined (see Figure 19).

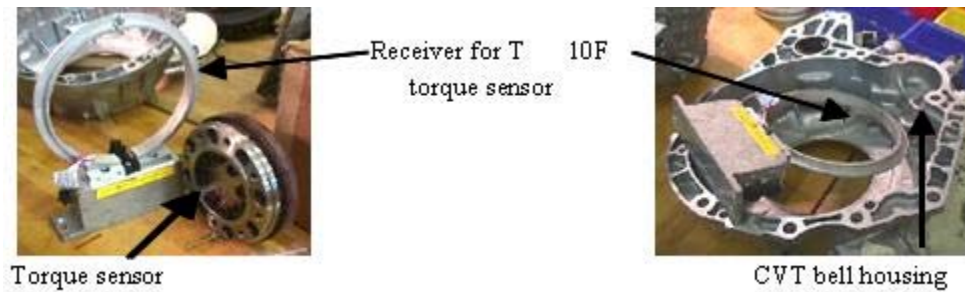


Figure 19: Instrumentation of the CVT

The extensive instrumentation (listed in APPENDIX 2) was connected to a central Data Acquisition System (DAQ). The DAQ system consisted of a National Instrument chassis connected to a desktop computer. Instrument output signals were routed to the DAQ chassis and to the DAQ computer. An internally developed LabView program was running on the DAQ computer. The emission concentration bench was connected to the computer as well via series communication.

The LabView program performed several functions. For example, the program graphical interface design allowed the operator to monitor powertrain instrument and status during a test. The program also recorded over-sampled and averaged raw data at a 10-Hz rate. Therefore, the operator could record complete test phases while monitoring the powertrain behavior. At the end of each test phase, the program launched a post-processing routine that automatically calculated fuel economy and emission pollutants mass for the recorded phase.

Emission mass was preferred to evaluate control benefit of the pre-transmission diesel hybrid powertrain. A Pierburg 2000 emission bench provided emission samples concentration. But, to calculate total emission mass, sample flow had to be monitored, in addition to concentration. Initially, sample flow was evaluated on the basis of the mass conservation equation of intake airflow and fuel flow in order to evaluate exhaust gas flow. This method was not optimal because air and fuel flow are transient and depend on engine operating points. Therefore, the accuracy of mass emission depended highly on fuel and airflow sensor accuracy, as well as on time response.

To address this issue, we designed a Constant Velocity Sampler (C.V.S.) associated with the dilution of exhaust. The purpose of this device was to replace the previous transient flow calculation with a constant flow of diluted tailpipe exhaust and ambient air. As a result, total emission mass could be estimated more accurately. The design of the CVS is described step by step in Appendix 3.

In addition, a port could be fitted in the CVS to get particulate mass on the same diluted sample by using a Tapered Element Oscillating Microbalance (T.E.O.M.). This instrument enhances exhaust sample analysis by providing information about particulate matter.



The CVS system was set up and all instruments have been calibrated. A propane injection test and an engine steady-state test were performed to validate the emission measurement system.

This test consisted of injecting propane in the dilution tunnel by using a calibrated flow meter. Therefore, the mass of injected propane was known and could be compared with the CVS measured mass. This test confirmed that the CVS operated properly and, in particular, that critical flow was correct.

CVS PROPANE TEST		
Propane Concentration	Venturi Number	Bag Flow Rate (Lpm)
99.99%		
CVS flowrate	0.157697311	Normalized cubic meters
Sample time	1.0	seconds
THC Sample	33.625092	ppm C3
THC Background	2.382933	ppm C3
Propane Shot Meas. THC	31.24	ppm C3
Barometric Pressure	29.02	inHg
Line Gage Pressure	59.0	psig
Panel Gage Pressure	50.0	psig
Orifice Temperature	74.4	Deg. F
Absolute Pressure	64.25	psia
CFO Propane Flow Rate	0.01018839	CFM
CVS Total Flow Rate	334.14	CFM Average
Calculated Concentration	30.49	ppm C3
System Error	2.463%	

The propane recovery indicated that propane-injected mass was within 2.5%.

Concerning the engine steady-state test, the emissions measurement system was used to calculate brake-specific fuel consumption and pollutant mass emission while the engine was operated at constant load and speed. The results of that test were compared with published reference values. The emission-based calculated fuel consumption could also be compared with the fuel-scale-measured value.

The engine speed was set up by using the dynamometer; the engine load was set up by using a pedal position sensor. Once speed and torque were at desired levels (1900 rpm, 68 Nm), a warming-up period allowed all temperatures to reach steady values.

The first step of the validation process consisted of verifying that the dilute exhaust volume (V_{mix}) stays constant during the test.

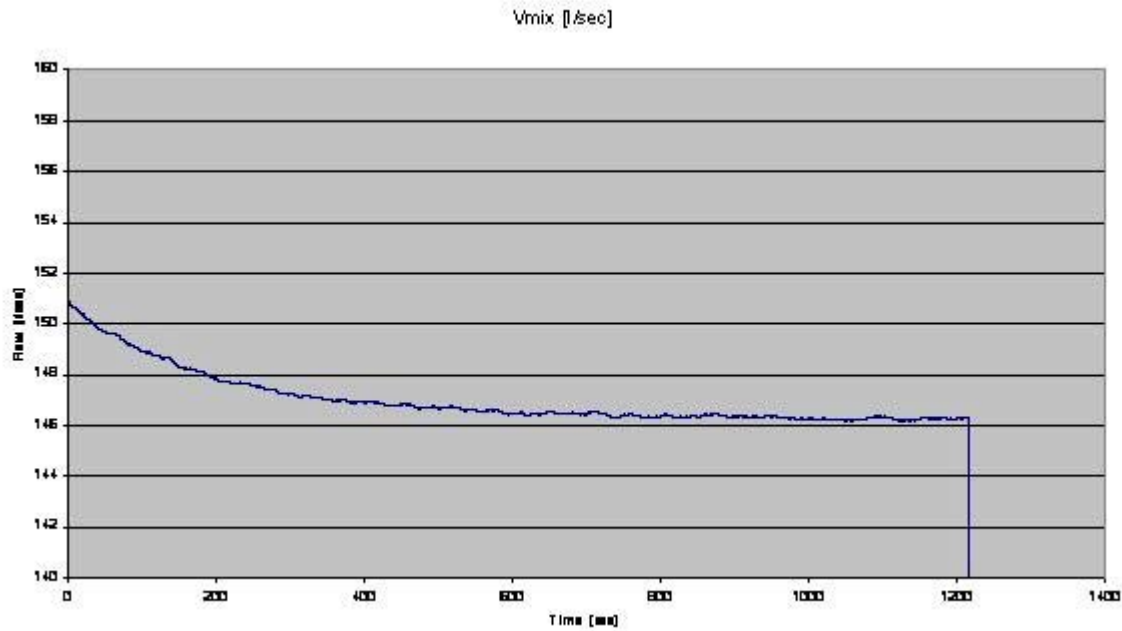


Figure 20: Dilute exhaust volume during engine steady-state test

To have a constant V_{mix} , we used only the data generated after the first 500 s of test.

V_{mix} was used to calculate the emitted mass of the pollutant in g/s. Figure 21 shows the calculated mass of THC in g/s from concentration in ppm.

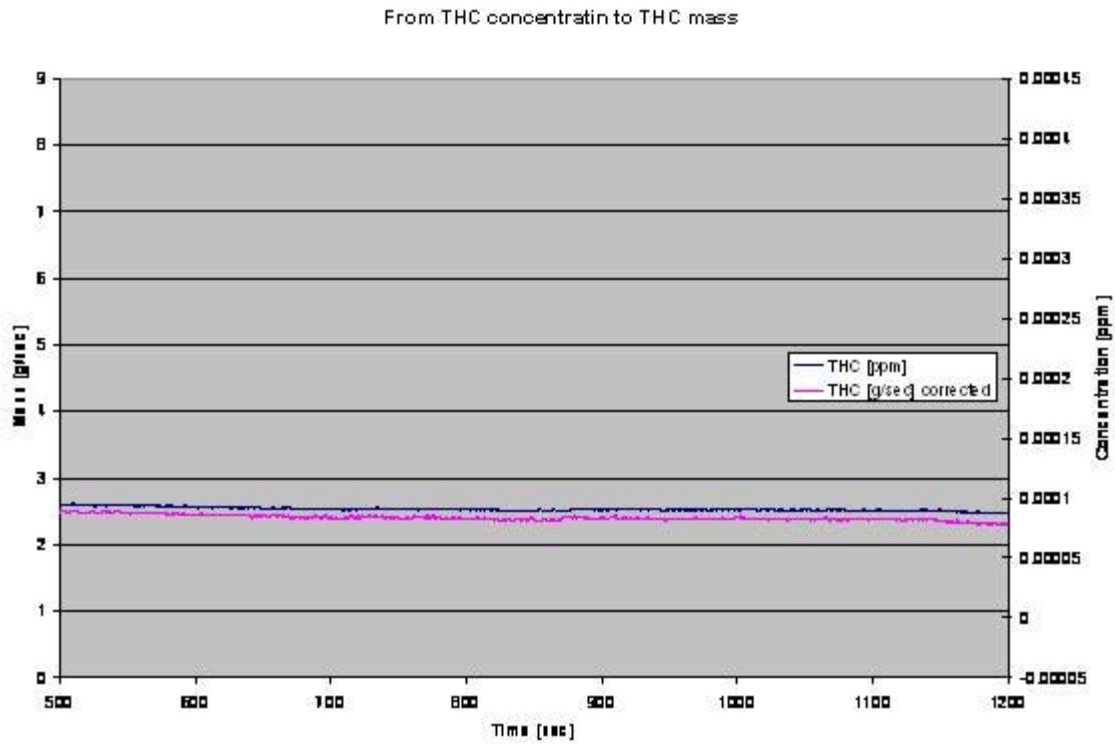


Figure 21: Conversion of THC concentration to THC mass

We could also calculate the diesel fuel rate from emissions data and compare it to the measured fuel rate to validate our emissions measurement system.

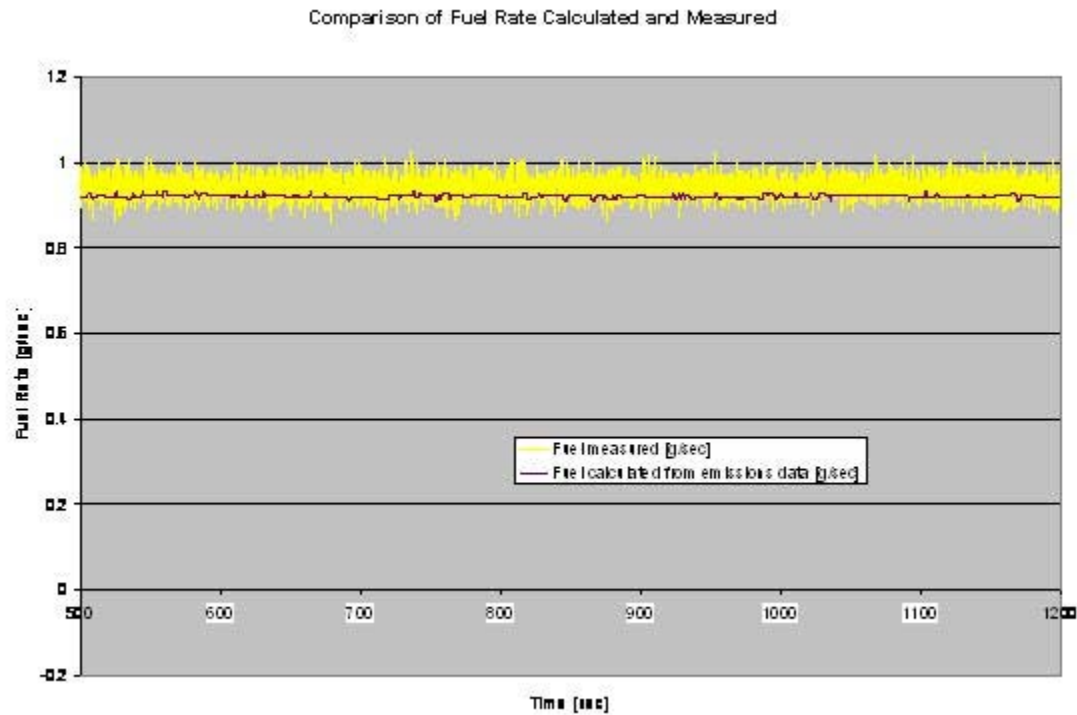


Figure 22: Fuel rate calculated from emissions data and fuel rate measured

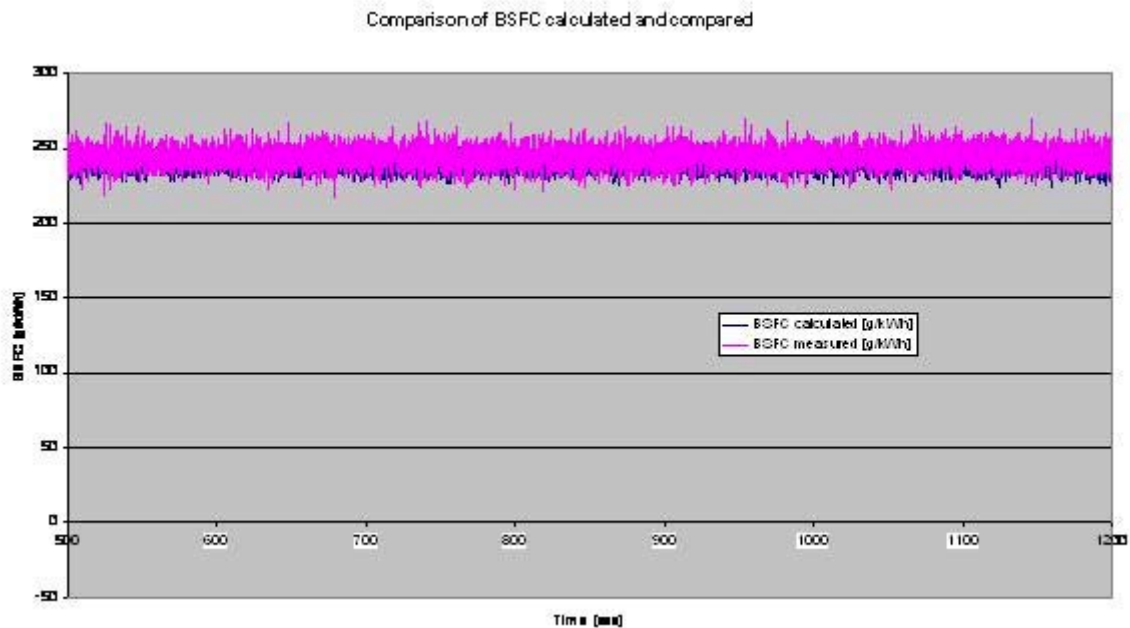


Figure 23: BSFC calculated from emissions data and BSFC measured



The average brake-specific fuel consumption (BSFC) measured at this engine torque and speed was 244 g/kWh and 239 g/kWh for the calculated average. The difference of about 2% is consistent with the propane shot test. The following tables provide BSFC results for the same engine at the same operating point tested in different test cells. Our BSFC measurements were compared with those from DaimlerChrysler, Oak Ridge National Laboratory (ORNL), and the engine and emissions research group at ANL. [13]

Organization	Speed (rpm)	Torque (Nm)	BSFC (g/kWh)
ANL-HIL	1900	70	244 (measured); 239 (calculated)
ANL-Engine	1900	70	245
DaimlerChrysler	1900	70	230
ORNL	1900	70	247

The fuel used was “California Low-Sulfur Commercial 2-D Diesel,” which is the same as that used by the Engine and Emissions Research group at Argonne.

The CVS associated with the data acquisition system that supports it provides transient emission readability and allows accurate calculation of pollutant g/mi. The calculations of pollutant mass and fuel consumption have been validated and are based on CFR 40 Part 86. The system successfully passed a propane injection procedure, and the results correlated with those of engine steady-state testing (APPENDIXES 3 and 4).

By validating the emissions and fuel measurement system, we have confidence in the conclusions were drawn from the entire experiment. Similarly, validating the component models ensured (1) the authenticity of the emulated components reaction and (2) the effectiveness of the hybridization effort performed in simulation.

2. Conventional Diesel

2.1. Conventional Diesel Vehicle

Using the emulation principle, we are able to evaluate the hybrid powertrain in the Mercedes-Benz C 220 CDI vehicle environment. However, the dynamic of our dynamometer controller is less than desirable to emulate vehicle losses. Therefore, the testing conditions and the simulation parameters were modified so that the simulation and testing results of the baseline vehicle could be compared with the results obtained on the hybrid powertrain. The appropriate process was to:

Evaluate the actual losses being applied by the dynamometer emulating the vehicle;

Calculate the corresponding A, B, C coefficients;

Test and simulate the Mercedes-Benz C220 CDI with those coefficients; and

Compare the results of tests and simulations of the conventional vehicle with those of the hybrid powertrain in the identical but emulated vehicle (see Figure 24).

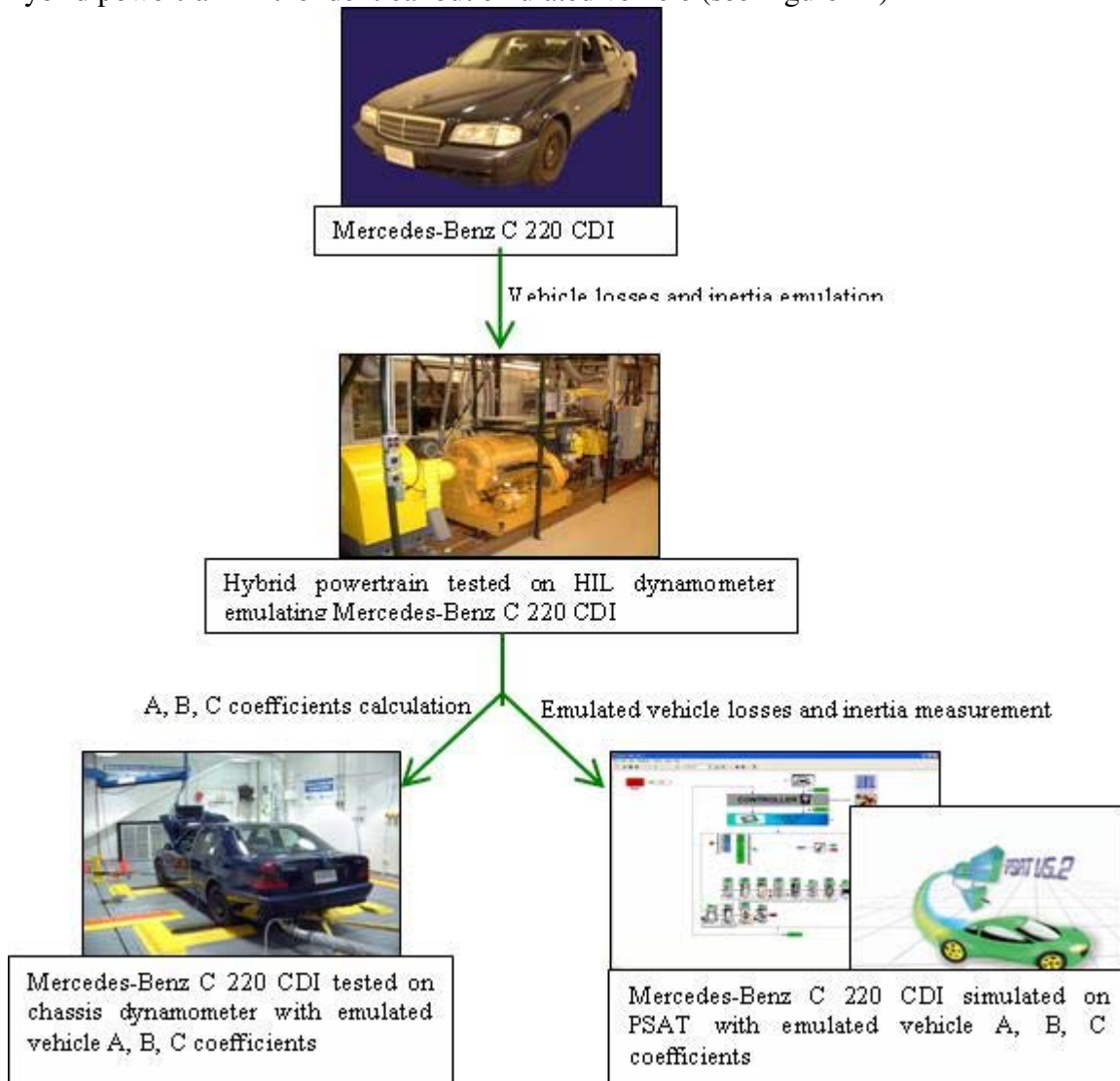


Figure 24: A, B, C coefficients of the baseline vehicle are based on the emulated vehicle

To simulate and test the vehicle and the powertrain under the same conditions, we needed to define the A, B, C coefficients of the emulated vehicle, which could eventually be slightly different from the real baseline vehicle coefficients. A, B, and C are the polynomial coefficients of the powertrain pound force curve. We did not measure the force losses; however, by using coast-down data, we could calculate those coefficients knowing the exact inertia of the emulated vehicle.

To measure the inertia, we used the following procedure. The emulated vehicle was disconnected from the HIL hybrid powertrain by disengaging the torque limiter located after the transmission (see Figure 25).

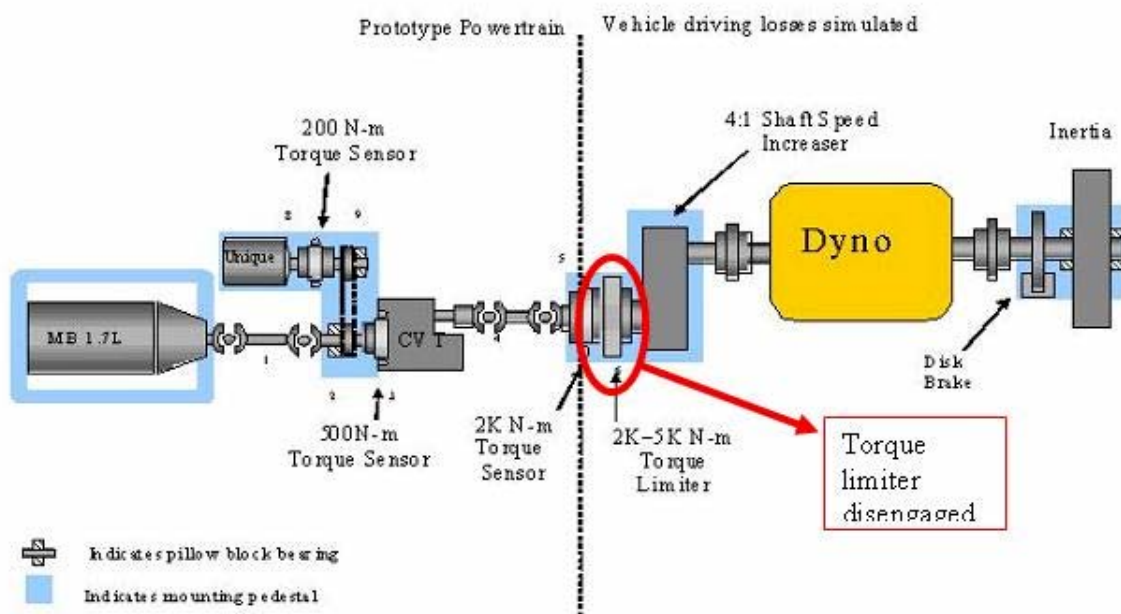


Figure 25: Torque limiter is disengaged to evaluate inertia of the emulated vehicle

A ramp up and down test was performed by using the dynamometer to propel the emulated vehicle. The principle of the inertia calculation is showed in Figure 26.

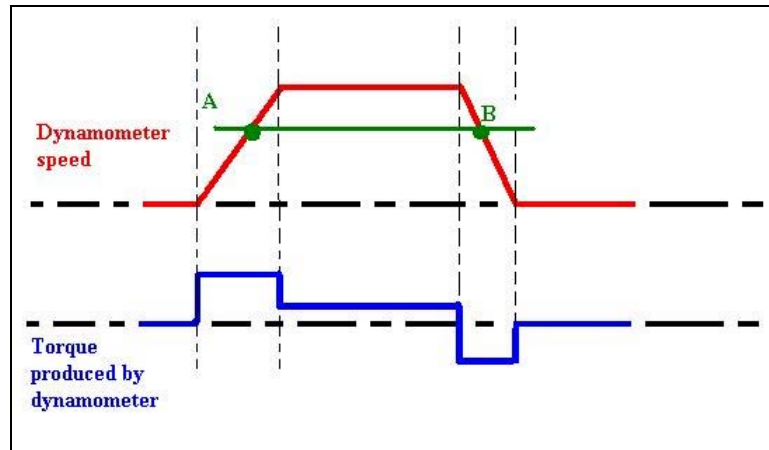


Figure 26: Inertia calculation principle

Dynamometer speed and torque are monitored. At point A, we have:

$$T_{\text{dyno_a}} - T_{\text{friction_a}} = J (dW/dt)_{\text{a}} \quad (1)$$

$T_{\text{dyno_a}}$: Torque produced by the dynamometer at point A

$T_{\text{friction_a}}$: Friction torque at point A

J : emulated vehicle inertia

$(dW/dt)_{\text{a}}$: Rotational acceleration at point A

We can then write the same equation for B:

$$-T_{\text{dyno_b}} - T_{\text{friction_b}} = -J (dW/dt)_{\text{b}} \quad (2)$$

$$(1)-(2) \text{ gives: } J = (T_{\text{dyno_a}} + T_{\text{dyno_b}}) / ((dW/dt)_{\text{a}} + (dW/dt)_{\text{b}})$$

For repeatability purposes, we used this procedure on two different sets of data (see Figures 27 and 28).

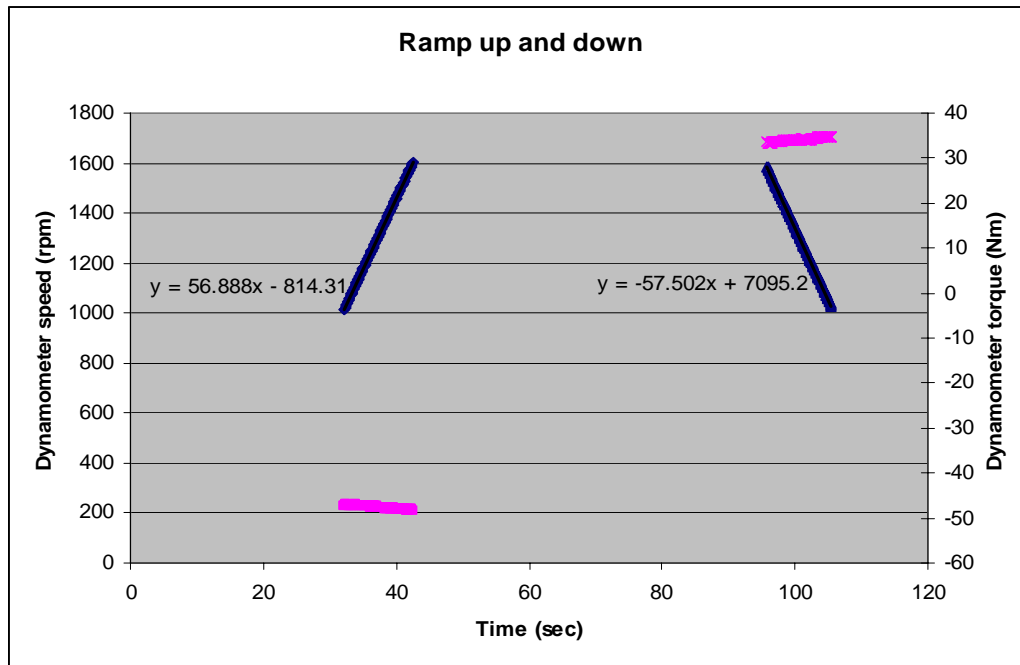


Figure 27: Torque and speed measured during ramp up and down test 1.

$(dW/dt)_a = 56.9 \text{ rpm/s}^2 = 6 \text{ rad/s}^2$

$(dW/dt)_b = 57.5 \text{ rpm/s}^2 = 6 \text{ rad/s}^2$

$T_{\text{dyno_a}} = 47 \text{ Nm (average)}$

$T_{\text{dyno_b}} = 34 \text{ Nm (average)}$

$J = 6.75 \text{ kg/m}^2 \text{ at dyno shaft}$

$J = 112.5 \text{ kg/m}^2 \text{ at wheel}$

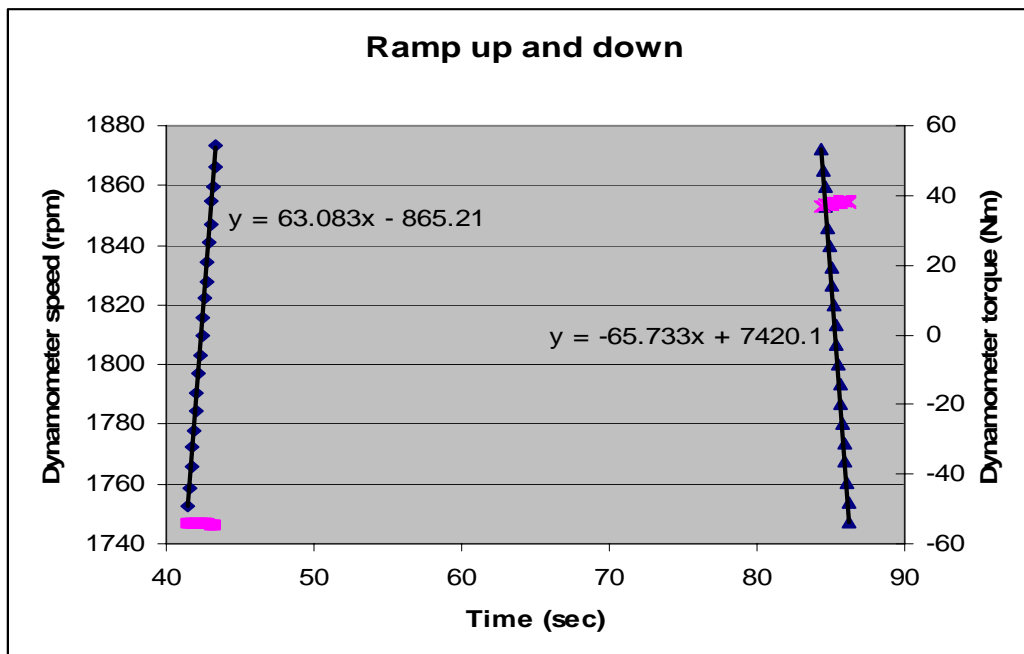


Figure 28: Torque and speed measured during ramp up and down test 2.



$$(dW/dt)_a = 63 \text{ rpm/s}^2 = 6.6 \text{ rad/s}^2$$
$$T_{\text{dyno}_a} = 54 \text{ Nm (average)}$$

$$(dW/dt)_b = 65.7 \text{ rpm/s}^2 = 6.9 \text{ rad/s}^2$$
$$T_{\text{dyno}_b} = 38 \text{ Nm (average)}$$

$$J = 6.81 \text{ kg/m}^2 \text{ at dyno shaft}$$

$$J = 113.5 \text{ kg/m}^2 \text{ at wheel}$$

Calculated emulated vehicle inertia = 113 kg/m²

The calculated emulated vehicle inertia can be used to calculate the pound force curve and the corresponding A, B, C coefficients from the coast-down test ($F = J/R^2 dV/dt$). Those coefficients were used in the entire study to set the simulation and testing parameters. For accurate comparison of the results and to maintain the integrity of our integrated program, it was crucial to use the same A, B, C coefficient in simulation, emulation, and testing. (APPENDIX 5)

2.2. Conventional Diesel Powertrain

To compare the prototype with the baseline conventional vehicle, we decided to operate the powertrain as if it would be a conventional vehicle powertrain. To do so, the electric motor was disabled for the duration of the experiment. This “Conventional Diesel Powertrain experiment” also helped us to understand CVT transmission operation and benefit hybridization of the powertrain. The vehicle controller had to be implemented to automatically drive the powertrain over a complete driving cycle. Several components had to be simultaneously controlled to achieve proper vehicle operation: engine on/off, engine torque, clutch displacement, CVT ratio, and mechanical brake. We used the same hardware setup throughout the entire experiment.

2.2.1. Control Development

-Engine on/off

Like in a conventional vehicle, the engine starts before the driving cycle and stops after completion. The controller uses a turnkey system that automatically turns the engine on before the drive cycle starts. The engine keeps on idling as the vehicle comes to a stop. Physically, ignition and starter commands are two voltage signals sent to the Engine Control Unit (ECU) by the vehicle controller.

Clutch engagement: vehicle launches and stops

The clutch realizes the coupling of the engine shaft with the CVT input shaft. It needs to be controlled to achieve proper vehicle operation. This function must be integrated into the vehicle controller as part of the automated driving control. The clutch control intervenes for vehicle launch and when the vehicle comes to a stop. When the vehicle comes to a stop, the engine shaft keeps idling while the transmission input shaft stops. The algorithm that was implemented in the vehicle controller simply disengages the



clutch, allowing the engine to idle when the controller detects that the transmission input shaft falls below idle speed during vehicle deceleration.

The clutch engagement process required at vehicle launch is more delicate. Vehicle launch is critical in the sense that CVT input shaft, linked to vehicle inertia, is initially stopped, and the engine must provide launching power by using clutch friction. As a consequence, engine power and clutch engagement must be controlled simultaneously to achieve smooth vehicle launch without stalling the engine. The control algorithm engages the clutch and monitors engine speed. When this speed drops, because of initial clutch friction, the accelerator pedal is used to provide launching power that quickly accelerates the vehicle (clutch engagement is slower during this phase). Finally, when the engine shaft and transmission shaft speeds are close and high enough for the engine to sustain torque, clutch engagement is completed. Physically, the vehicle controller sends a voltage that sets the position of a servomotor connected to the clutch hydraulic command line. [14]

Engine torque

For the vehicle to follow the driving cycle, the controller compares speed profile with instantaneous vehicle speed and uses Proportional Integral (PI) speed regulation. Physically, engine torque is controlled by sending a voltage signal to the ECU that emulates pedal position sensor.

Mechanical brake

Mechanical braking is necessary to meet the driving cycle trace during deceleration phases. The PI speed regulation is used to operate the brake actuator. This actuator is an air cylinder that pushes on the brake master cylinder. Physically, the vehicle controller translates torque into voltage that regulates air cylinder pressure.

CVT ratio

Transmission ratio can be changed continuously during operation. The ratio ranges from 2.5 to 0.5 and is physically controlled by using a stepper motor through RS232 series communication. There are several possibilities to operate the ratio during a driving cycle. Ratio control is a key parameter of the way the vehicle will perform on a given driving cycle. The ratio can be controlled to provide the most efficient engine operation at all times.

Because the ratio can vary continuously, the engine speed is decoupled from the vehicle speed (see Figure 29).

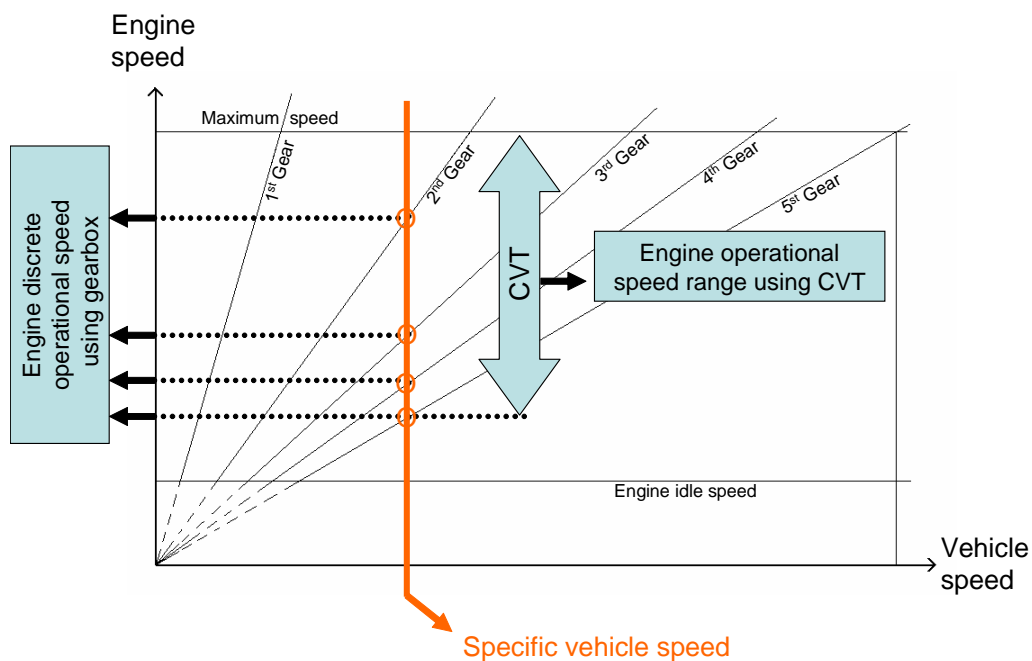


Figure 29: Continuously variable ratio compared with discrete ratio



At each given vehicle speed, engine speed can be set to any value allowed by the ratio range. For a manual or automatic transmission, discrete engine speed must be chosen among a limited number of gear sets.

As a consequence, engine operating point (instantaneous engine torque and speed) can be set freely (within range limits) while the vehicle is being driven over a cycle. Setting the engine operating point freely can greatly benefit fuel economy and emissions. Adequate continuous control of the CVT ratio can keep the engine running at a preferred efficiency operating range, resulting in better fuel economy. This continuous ratio change may also limit transient operation of the engine, thus lowering pollutant emission.

2.2.2. Baseline Testing

For this experiment, the CVT was operated at five discrete ratios; each ratio corresponded to one gear of the manual transmission of the baseline vehicle. An engine speed based shifting schedule was used to determine adequate ratios during vehicle operation. The clutch was fully disengaged before and fully reengaged after a shifting event. Although the durations of shifting events were higher and CVT efficiency was lower than those characteristic of an actual manual transmission (despite the torque converter removal), using this shifting approach recreated engine operation as it would be in the context of a manual transmission vehicle.

-Results

Test 103080/#	/11	/12	/13	Average	Standard Deviation	95% confidence interval
F.E. meas. (mpg)	36.47	36.77	37.84	37.03	0.42	[36.2;38.0]
F.E. calc. (mpg)	36.24	36.78	37.95	36.99	0.51	[36.0;38.1]
NO _x (g/mi)	1.09	1.09	1.07	1.08	0.007	[1.06;1.11]
CO ₂ (g/mi)	277.73	273.54	265.28	272.18	3.66	[268.04;276.32]
CO (g/mi)	1.95	1.98	1.80	1.91	0.06	[1.84;1.98]
THC (g/mi)	3.03E-3	3.16E-3	2.67E-3	2.95E-3	1.47E-4	[2.78E-03;3.12E-03]

Test consisted of a Federal Urban Driving Schedule (duration, 1372 s; distance, 7.45 mi)

In the table, “F.E. meas.” denotes the fuel economy directly measured, while “F.E. calc.” denotes the fuel economy calculated from emissions data. The average of the three tests was used as a basis for comparison during the entire study. The average provided an estimate, but it was important to calculate the standard error from the mean to evaluate the dispersion from the mean. The 95% confidence interval indicates how close the average was from the true value. With a 95% level of confidence, the actual value is within the given interval independently from measurement variability. The interval calculation was made under an assumption of normal distribution around the average.

Figure 30 shows engine operating points from test data during a FUDS cycle while emulating a manual transmission with the CVT.

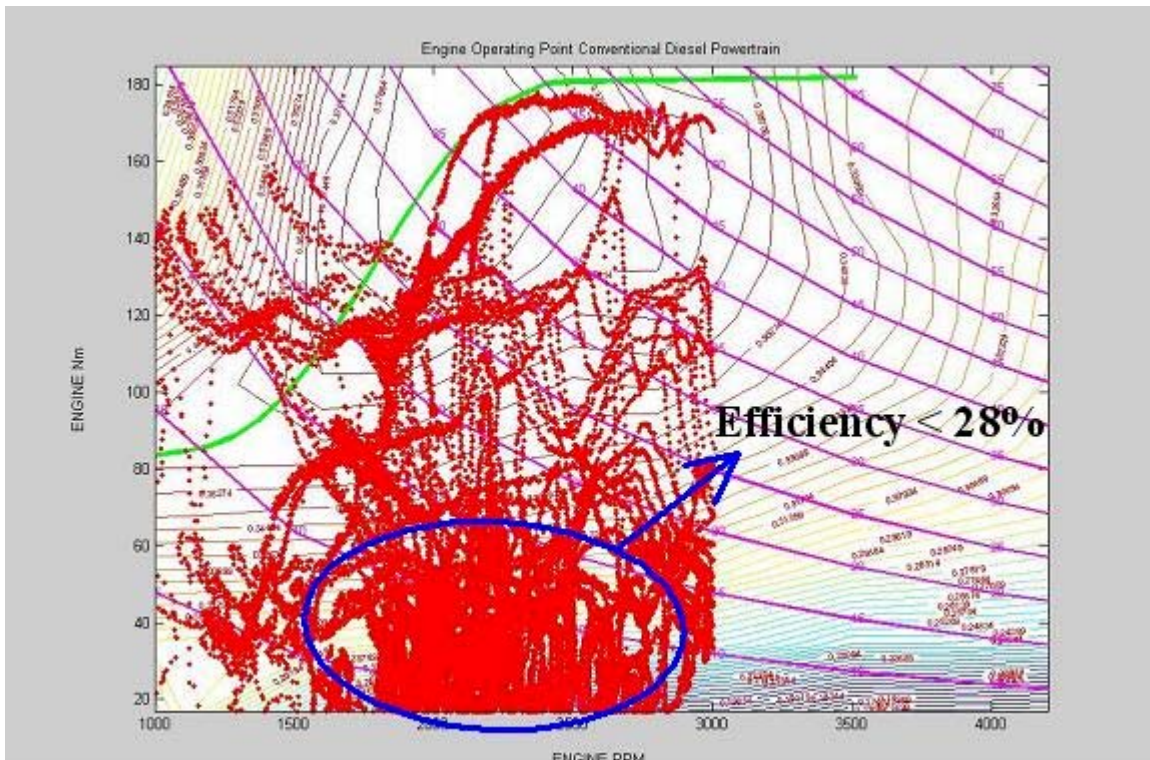


Figure 30: Engine operating point

The engine operated at low efficiency ($< 28\%$) most of the time. Moreover, we noticed important speed and torque variations that had a negative impact on emissions. In the next experiment, we used the CVT to maintain the engine at a constant speed and assess the impact of transients on emissions.

2.2.3. Impact of Engine Speed Transients

To put a figure on the impact of engine speed transients on fuel economy and emissions, the CVT ratio was operated continuously to keep the engine at a constant operating speed of 2000 rpm during this experiment. Therefore, CVT ratio operation was proportional to vehicle speed during the cycle to minimize engine speed transients.

Results

Test 103080/#	/17	/19	/20	Average	Standard Deviation	95% confidence interval	% gain
F.E. meas. (mpg)	40.64	41.37	41.69	41.23	0.54	[40.6;41.8]	11%
F.E. calc. (mpg)	40.33	39.11	41.67	40.37	1.28	[38.9;41.8]	9%
NOx (g/mile)	0.90	0.87	0.89	0.89	0.02	[0.87;0.90]	-18%
CO ₂ (g/mile)	249.99	257.54	241.88	249.80	7.83	[240.94;258.67]	-8%
CO (g/mile)	1.47	1.67	1.49	1.54	0.11	[1.42;1.67]	-19%
THC (g/mile)	2.44E-3	2.68E-3	2.46E-3	2.53E-3	1.3E-4	[2.38E-3;2.68E-3]	-14%

The test consisted of a Federal Urban Driving Schedule (duration, 1372 s; distance, 7.45 mi)

% Gain compared with previous experiment

This experiment involved using a very simple control algorithm that is not realistically applicable in a real-vehicle context. However, the results show the impact of engine speed transients. We observed a gain of 10% in fuel economy and a substantial reduction in emissions. Limiting engine transients improved both fuel efficiency and emissions without a trade-off. This inference will be used in the development of a hybrid control strategy because the electric motor could compensate for a driver’s high dynamics demands while limiting engine transients.

Figure 31 shows engine operating points from test data during a FUDS cycle while maintaining engine speed constant.

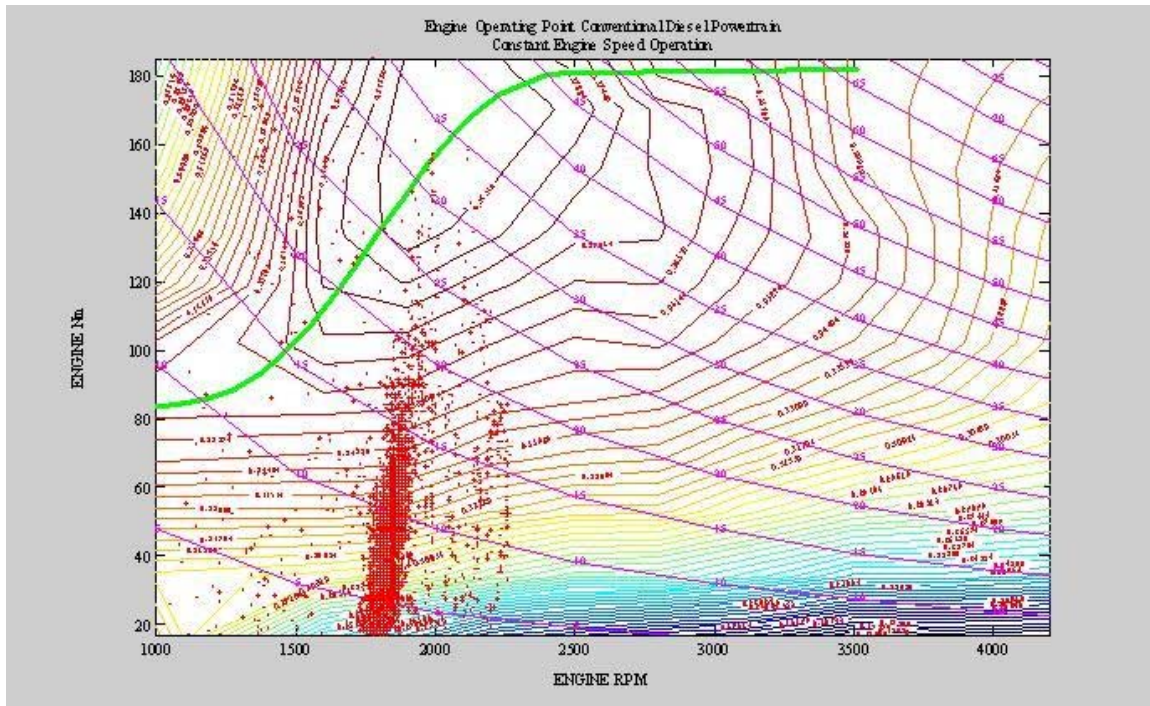


Figure 31: Engine operating point – Constant speed operation

2.2.4. Impact of Transmission Efficiency

As described previously, the main modification of the CVT was to replace the mechanical hydraulic pump, which was connected to the engine through a torque converter. The pump is a key component of the CVT because it provides adequate belt/pulleys clamping. The torque converter was replaced by a clutch, and the CVT gear pump was replaced by an auxiliary electrically driven pump. These changes benefited system efficiency because clutch efficiency is better than torque converter efficiency and also because an electrically driven pump allows optimal control of hydraulic clamping pressure by decoupling the pump from the transmission input shaft. Moreover, compared with the existing pump, an electrically driven pump can be operated when the engine is off and the vehicle is propelled electrically.

Transmission input torque, speed, and ratio allowed calculation of the optimal clamping pressure, as described in Section 1.4 (Emulation: Control and Assembly of the hybrid powertrain). Closed loop control of the pump provided adequate clamping pressure.



Results

Test 103080/#	/14	/15	/16	Average	Standard Deviation	95% confidence interval	% gain	% gain cumul.
F.E. meas. (mpg)	43.30	43.56	43.04	43.30	0.26	[43.01;43.59]	5%	17%
F.E. calc. (mpg)	42.54	44.28	41.88	42.90	1.24	[41.50;44.30]	6%	16%
NO _x (g/mile)	0.88	0.86	0.85	0.86	0.02	[0.85;0.88]	-3%	-20%
CO ₂ (g/mi)	236.24	227.30	239.88	234.47	6.47	[227.15;241.80]	-6%	-14%
CO (g/mi)	1.89	1.60	1.60	1.70	0.17	[1.51;1.89]	10%	11%
THC (g/mi)	2.68E-3	2.49E-3	2.52E-3	2.56E-3	1E-4	[2.45E-3;2.68E-3]	1%	13%

The test consisted of a Federal Urban Driving Schedule (duration, 1372 s; distance, 7.45 mi)

% Gain compared with previous experiment

% Gain cumulative compared with baseline experiment

This experiment was the same than the constant engine speed operation, except for the control of the clamping pressure. In the previous experiment, the clamping pressure was set to a high value to avoid any belt slippage. In this experiment, we wanted to evaluate the benefit of operating the pump at a lower pressure by using our pump control algorithm. In the table, the “% gain” column represents the gain compared with the previous experiment, while “%gain cumul.” is the percentage gain compared with the baseline experiment.

As expected, applying an optimal clamping pressure increased CVT efficiency and consequently improved fuel economy by 5%. We also noticed a general trend toward decreasing NO_x and CO₂ emissions. Concerning CO and THC, the average results show higher level of emissions. However, because of the uncertainties associated with emissions data collection, we should also look at the confidence interval for an accurate comparison. The CO interval and THC interval for both experiments show an important superposition, demonstrating that the comparison of averages is of limited accuracy. If we look at the individual test data, the first test of the second experiment generated 1.89 g/mi of CO. This value is higher than that of the other tests and contributed to a 10% increase in average CO emissions. Concluding that, on the basis of a single test, pressure control of the CVT causes an increase in CO emissions would be erroneous. Because of its benefit on fuel economy, the control algorithm was used for the remainder of the study.

2.2.5. Impact of Engine Operation

As we explained earlier, the CVT allows engine speed to be set to any value within the ratio range. Thus, we had an additional degree of freedom (compared with a manual or automatic transmission) to operate the engine. During this experiment, to improve fuel economy, we applied continuous control of the CVT ratio to keep the engine running near its most efficient operating point for any given power demand.

The most efficient operating area for each engine's power demand yields the best engine efficiency curve, as shown in the Figure 32.

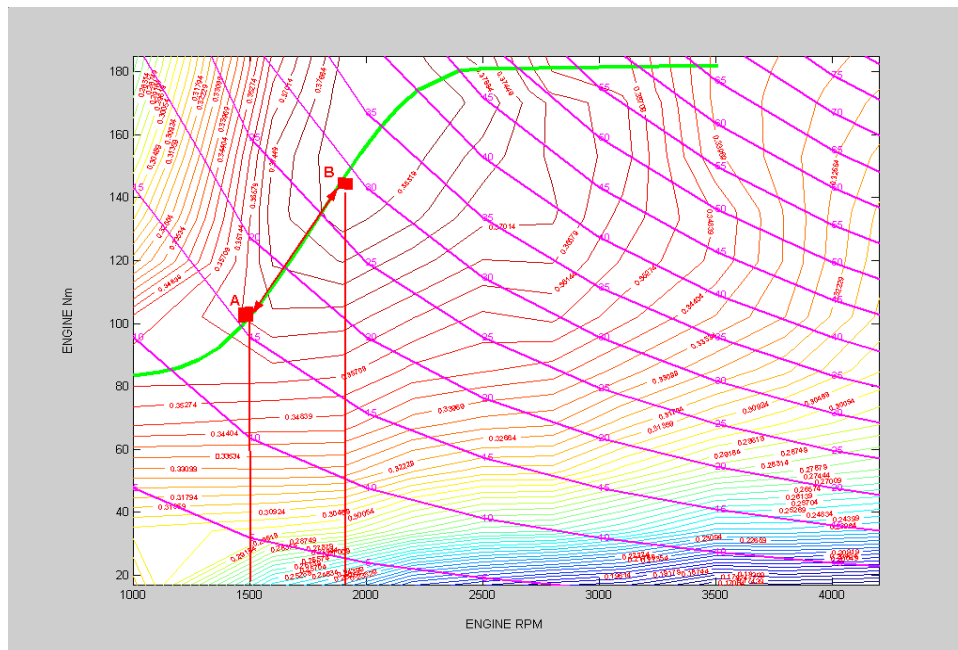


Figure 32: Engine best efficiency operating curve

CVT offers additional control opportunities to maintain the engine on its best efficiency curve. However, for a low power-level requirement (below 15 kW), the engine would have to operate at a low speed (below 1500 rpm) to stay on the curve (point A). Thus, we needed to impose a low engine speed limit so that engine torque could leave the curve to satisfy driver's demand. This engine speed limit was selected by using simulation, and an example of the simulation analysis is discussed below for two different engine speed limits (1500 rpm and 1900 rpm).

If the minimum engine speed is set at 1500 rpm, for an engine power (1) below the intersection between 1900 rpm and the best efficiency curve (point B) and (2) above the intersection between 1500 rpm and the best efficiency curve (point A), the engine is kept on the best efficiency curve (see Figure 32).

If the low engine speed limit is set at 1900 rpm, for the same engine power requirement, the engine stays at a speed of 1900 rpm and the torque decreases to match power demand. The engine operates between points B and C, as shown in Figure 33. However, when comparing the area between A and B with the area between B and C, we can conclude that the difference in efficiency is not significant.

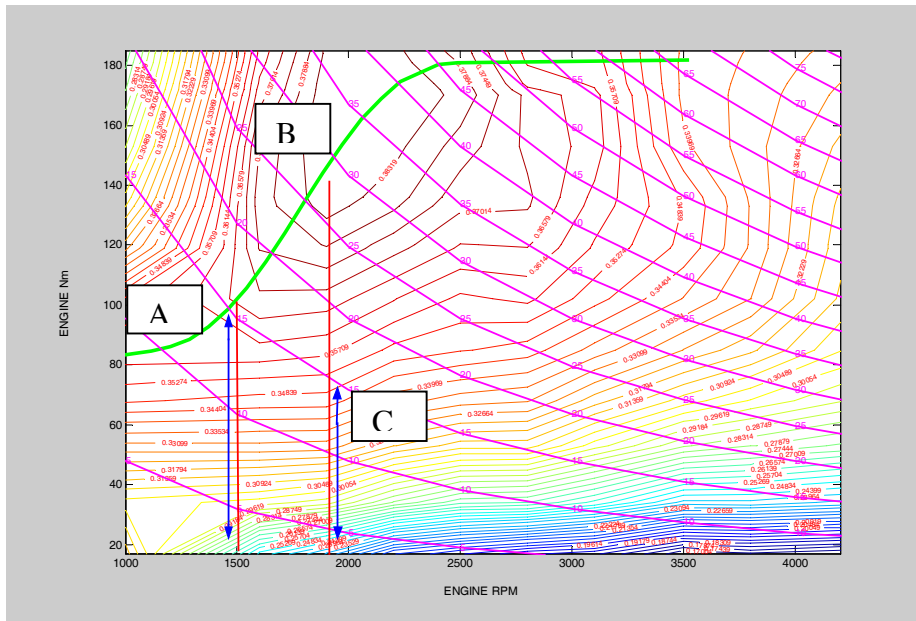


Figure 33: Selection of lower operating speed

To complete the analysis, we can compare the efficiency in the low power area at 1500 rpm with the low power area at 1900 rpm (blue arrows in Figure 33). Similarly, the difference in efficiency is not significant and, therefore, according to the results of the simulation, we should only expect a modest improvement in fuel economy by setting the low engine speed limit at 1500 rpm instead of 1900 rpm.

However, if we impose a low engine speed limit at 1500 rpm, for low vehicle speed and low acceleration demand conditions, we will generate more engine torque transient than if the limit is set at 1900 rpm. Figure 33 shows that it takes more torque variation to go from 10 kW to 15 kW if the engine is at 1500 rpm than if the engine is at 1900 rpm.

Even if the engine stays longer on its best efficiency curve and the low engine speed limit is 1500 rpm, the fuel economy impact is not significant. However, imposing a low engine speed limit of 1900 rpm reduces engine torque transient under conditions of low vehicle power. Therefore, for subsequent research, we operated the engine above 1900 rpm.

Figure 34 shows engine operating points from test data during a FUDS cycle as the engine is maintained on its best efficiency curve.

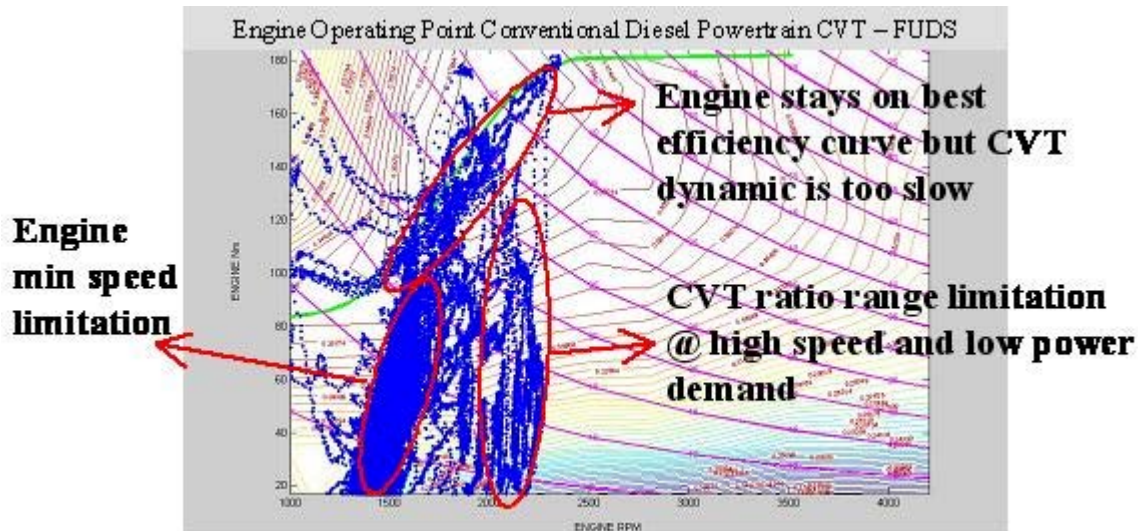


Figure 34: Engine operating point – Best efficiency curve operation

Figure 34 shows that the control does not maintain the engine at its best efficiency all of the time. This test was performed at a low engine speed of 1500 rpm to confirm the impact of torque transient on emissions predicted by simulation. Therefore, when the power level required was below 15 kW, the control reduces the engine torque and leaves the curve. Moreover, at high vehicle speed, the CVT ratio range becomes a constraint. At high vehicle speed, once the ratio reaches its minimum, the engine speed keeps accelerating with vehicle speed. Acceleration becomes particularly problematic when the power demand decreases because we have to operate the engine at low efficiency. Moreover, if we are not limited by the CVT ratio range, we still have difficulties in controlling the ratio dynamically enough to follow the power variations.

Results

Test 103090/#	/01	% gain	% gain cumul.
F.E. meas. (mpg)	42.22	-2%	14%
F.E. calc. (mpg)	44.45	4%	20%
NO _x (g/mi)	1.05	22%	-3%
CO ₂ (g/mi)	226.55	-3%	-17%
CO (g/mi)	1.49	-12%	-22%
THC (g/mi)	2.51E-3	-2%	-15%

The test consisted of a Federal Urban Driving Schedule (duration, 1372 s; distance, 7.45 mi)

% Gain compared with previous experiment

% Gain cumul compared with baseline experiment

This experiment demonstrates that we can achieve the same fuel economy by operating the engine on its best efficiency curve as by operating the engine at 2000 rpm. We can assume that the higher-efficiency operating point compensates for the transient effect on fuel economy. However, NO_x emissions increase. When performing the steady-state emissions map of the engine, we noticed that the best efficiency curve is at a very high level of NO_x . Nevertheless, looking at the measured engine operating point in Figure 34, it is difficult to determine if the 22% increase in NO_x was due to engine operating area or engine transients.

Figure 35 shows a summary of the study of the conventional powertrain.

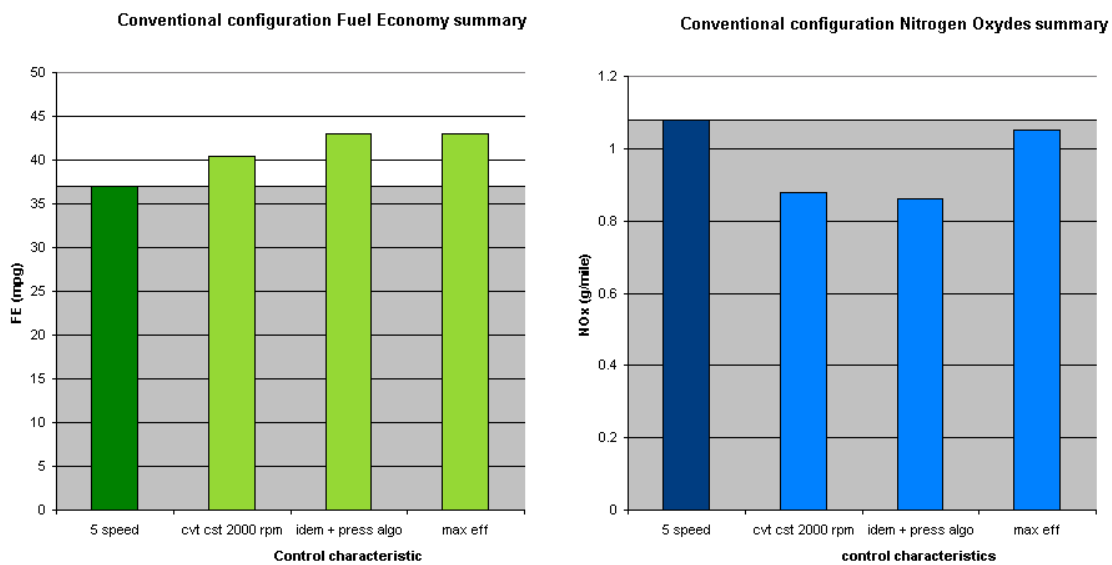


Figure 35: Comparison between the different conventional powertrain control approaches

Those experiments introduced the notion of a trade-off between fuel economy and emissions. They also demonstrated two limitations of the CVT in a conventional vehicle: ratio range and CVT dynamics.

Those issues can be addressed in a hybrid environment where the electric motor can compensate for the slow CVT dynamic and charge the battery to store energy when it is more efficient to operate the engine at a higher load.

3. Hybrid Diesel

The CVT parallel hybrid configuration provides tremendous flexibility in the choice of both engine torque and speed operation. Because of the engine and electric motor combination, engine torque can be replaced, assisted, or absorbed by the electric motor independently from a driver's expectations. In addition, the transmission's continuous ratio variation allows engine speed to be decoupled from wheel speed independently of power flow.

Engine operating point is a key parameter of the vehicle control strategy. Engine operation is directly related to fuel efficiency and gaseous emissions, as demonstrated in the following discussion.

3.1. Control Description

Each component of the hybrid powertrain is independently controlled by using the control strategy developed in simulation. The control strategy can be described as the logic that supervises components depending on their status, and driver input while the vehicle is being driven on a test cycle. The control strategy is critical as it manages energy resources (fuel and battery state of charge) and therefore impacts powertrain efficiency.

The driver has been automated and embedded in the control system as a driver model. The driver model function is emulating a real driver by using a PI control, which compares actual vehicle speed to a driving trace. The driving trace consists of a standard velocity versus time driving cycle, such as the Federal Urban Driving Schedule (FUDS). The driver model outputs a wheel torque/power demand, which may be positive or negative, depending on the variation in the instantaneous driving schedule. The torque/power demand is then interpreted by the vehicle control strategy to optimally operate each component while meeting the driving trace.

Battery State Of Charge (SOC) indicates the availability of electrical energy stored in the battery, and its preservation is a key feature of a hybrid control strategy. Not only must the SOC be maintained so that motor torque is available to drive the vehicle, but SOC must also allow energy recovery from the wheels during deceleration by regenerative braking. Battery life may be affected if state of charge goes out of a defined range or instantaneous power exceeds theoretical limitations. Therefore, in addition to SOC preservation, the control strategy must ensure that electrical power flows are not affecting battery life. A solution is to (1) constantly monitor and limit SOC and (2) limit motor torque.

All vehicle launches are made by using pure EV mode. EV mode will be used temporarily while cruising if driver demand does not require the engine to supply power. When the engine is on, the motor can supply additional torque and enhance vehicle performance. The motor can also absorb a part of the engine torque by acting as a generator while cruising. This mode is used to charge the battery.

The electric motor allows the vehicle’s inertial energy to be recovered during deceleration. Regenerative braking energy stored in the battery may be reused later. Mechanical braking is used when the motor cannot alone decelerate the vehicle. The mechanical brake is then operated to ensure that the vehicle meets the driving trace.

Because the electric motor alone can temporarily supply power, the engine is not required all of the time. The strategy must decide when engine must be fired or killed. This engine on or off decision is based on power demand. The engine will be fired when the power demand exceeds an acceptable level. Power demand is based on both driver input and battery state of charge. Similarly, the engine will be killed when its power is no longer required.

The control strategy logic is described in the Figure 36 and in the table below.

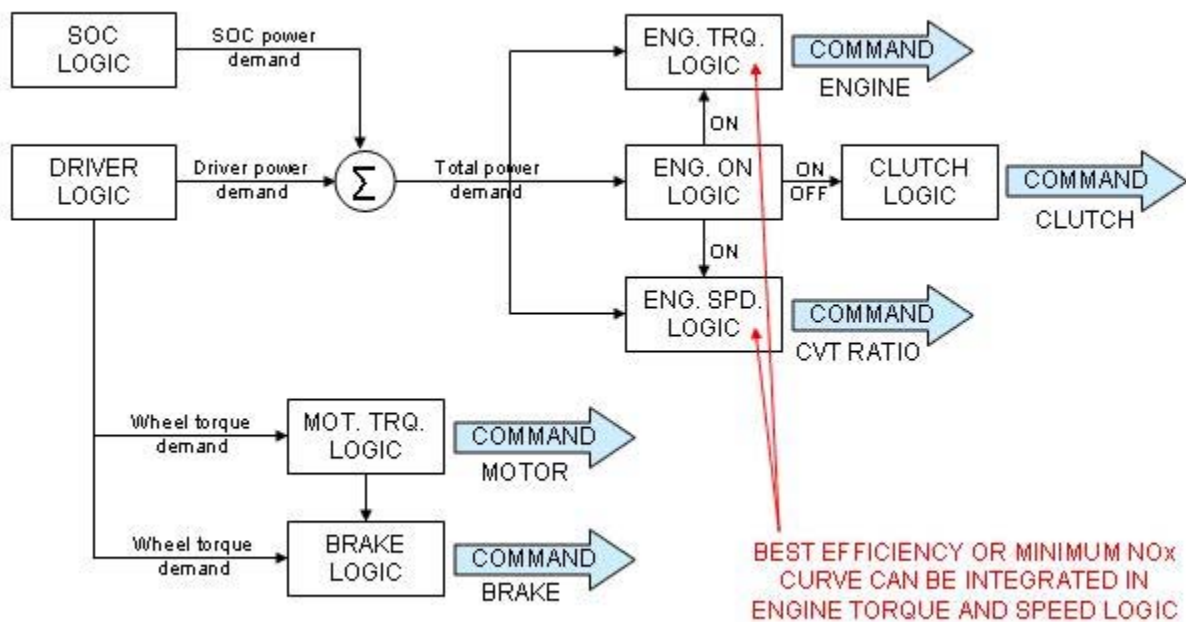


Figure 36: Simplified control strategy logic

The following table describes the outputs of the strategy functions

Output	Logic	Description
Wheel torque demand	DRIVER LOGIC	Torque required at the wheel is calculated by using closed-loop Proportional Integral PI speed regulation.
Driver power demand	DRIVER LOGIC	Power required for vehicle to follow the cycle is calculated by using vehicle speed and wheel torque demand.
SOC power demand	SOC LOGIC	Power required to maintain fixed SOC target is calculated by using closed loop Proportional P regulation.
Total power demand		Sum of both driver and SOC power demand.
Engine ON command	ENG. ON LOGIC	If total power demand exceeds 20 kW, engine turns ON. If power demand is lower than -20 kW, engine turns OFF.
Clutch command	CLUTCH LOGIC	Clutch is engaged when engine is ON. Clutch is disengaged before the engine shuts off.
Engine torque command	ENG. TRQ. LOGIC	Engine torque command is calculated by using engine target torque according to total power demand.
Motor torque command	MOT. TRQ. LOGIC	Motor torque command is based on wheel torque demand, measured engine torque, and measured CVT ratio.
CVT ratio command	ENG. SPD. LOGIC	CVT ratio command is calculated by using engine target speed according to total power demand.
brake command	BRAKE LOGIC	Brake supplies negative torque at the wheel if motor torque reaches limits and to match wheel torque demand.

(APPENDIX 6)

3.2. Impact of Control on Fuel Economy

Data on engine brake specific fuel consumption allow engine efficiency to be calculated. Therefore, it is possible to determine the most efficient engine operating point for each power. The best efficiency curve describes optimal operation. When the engine is on, its torque and the CVT ratio are controlled to operate the engine at the most efficient point while satisfying engine power demand (see Figure 37).

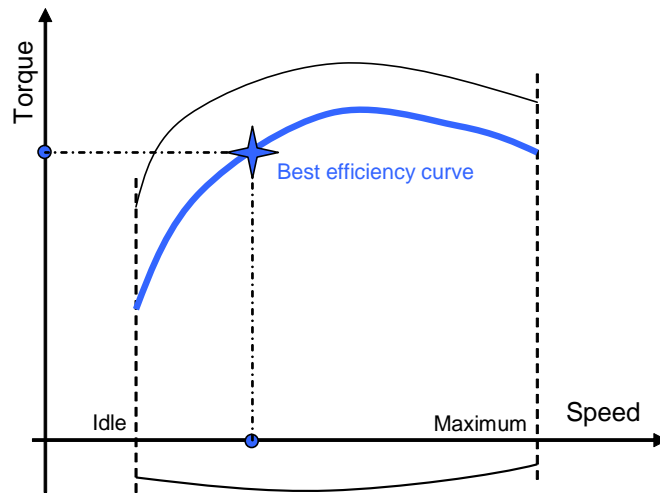


Figure 37: Engine best efficiency curve

Hybridization brings a second degree of freedom compare to a conventional powertrain with a CVT. The electric motor can compensate for the slow dynamic of the CVT ratio change but also allows the engine to operate at a higher power than that demanded by the driver. The excessive power can be used to recharge the battery by using the motor as a generator. If the battery state of charge (SOC) becomes too high or the driver's power demand too low, an option is to turn off the engine and propel the vehicle in electric-only mode. Consequently, the control of the engine is more accurate than with a conventional powertrain with CVT.

Figure 38 displays typical engine operation during a test that was performed with the best efficiency strategy. Engine power demand is calculated to match driver expectations and SOC requirement. The engine power required is then interpreted by the control strategy in order to set engine torque command and CVT ratio command. As a result, the engine operates near the best efficiency curve.

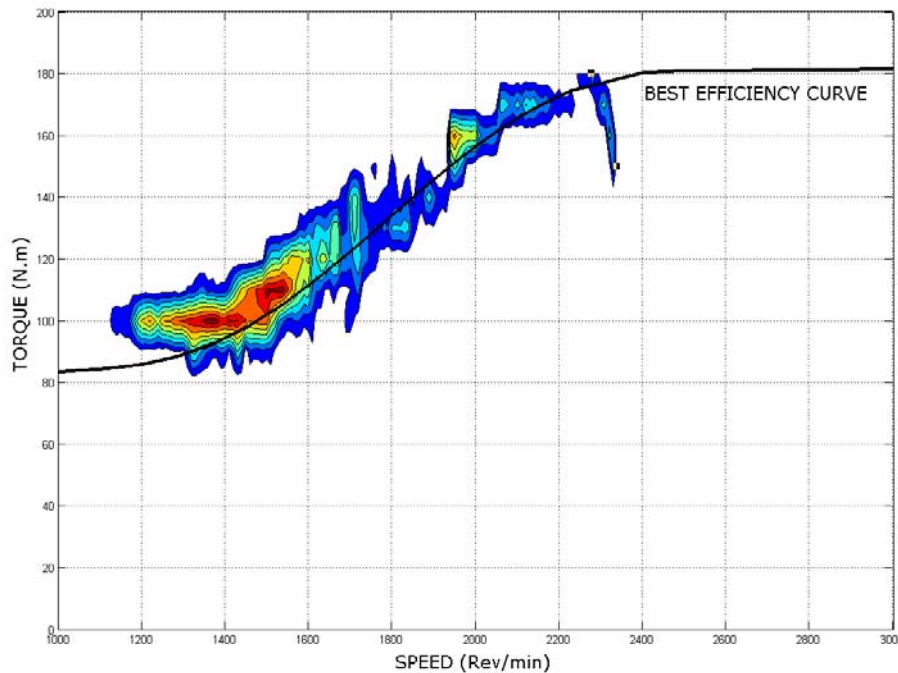


Figure 38: Engine operation point using the best efficiency strategy

The color density on this plot is proportional to the time spent by the engine on the operating area. By comparing Figure 34 with Figure 38, we notice that the engine stays closer to the best efficiency curve. At high load and an engine speed above 2300 rpm, the control reduces the engine torque because the motor cannot absorb all of the excessive power generated by the engine. Because the motor is above its base speed, it is limited in maximum negative torque capacity. The driver’s power demand takes priority on the best efficiency curve, and the control has to leave the optimal (in terms of fuel consumption) mode of operation. We also notice that we can operate the engine at a lower speed than in conventional configuration and stay on the curve.

Results

Test 103110/#	/01	/02	/03	/06	/12	/15
F.E. meas. (mpg)	45.23	58.33	67.23	52.69	48.38	69.95
F.E. calc. (mpg)	44.50	61.19	69.39	55.63	50.69	76.08
Delta SOC (%)	+29.8	-1.91	-19.33	+9.71	+18.48	-21.06
NOx (g/mi)	1.77	1.29	1.12	1.59	1.84	1.13
PM (g/mi)	NA	NA	NA	0.086	0.087	0.061
CO2 (g/mi)	228.7	166.3	146.6	182.8	200.4	133.8
CO (g/mi)	43E-3	22E-3	29E-3	82E-3	#NV#	#NV#
THC (g/mi)	#NV#	3.3E-3	3.8E-3	9.4E-3	4.9E-3	9.4E-3

Test consisted of a Federal Urban Driving Schedule (duration, 1372 s; distance, 7.45 mi)

Both fuel usage and battery SOC must be taken into account when calculating or measuring the fuel economy (FE). Figure 39 shows how to estimate the corrected FE (i.e., what the fuel economy would be in case of SOC equalization over the test cycle).

Best efficiency strategy Fuel Economy (FE)

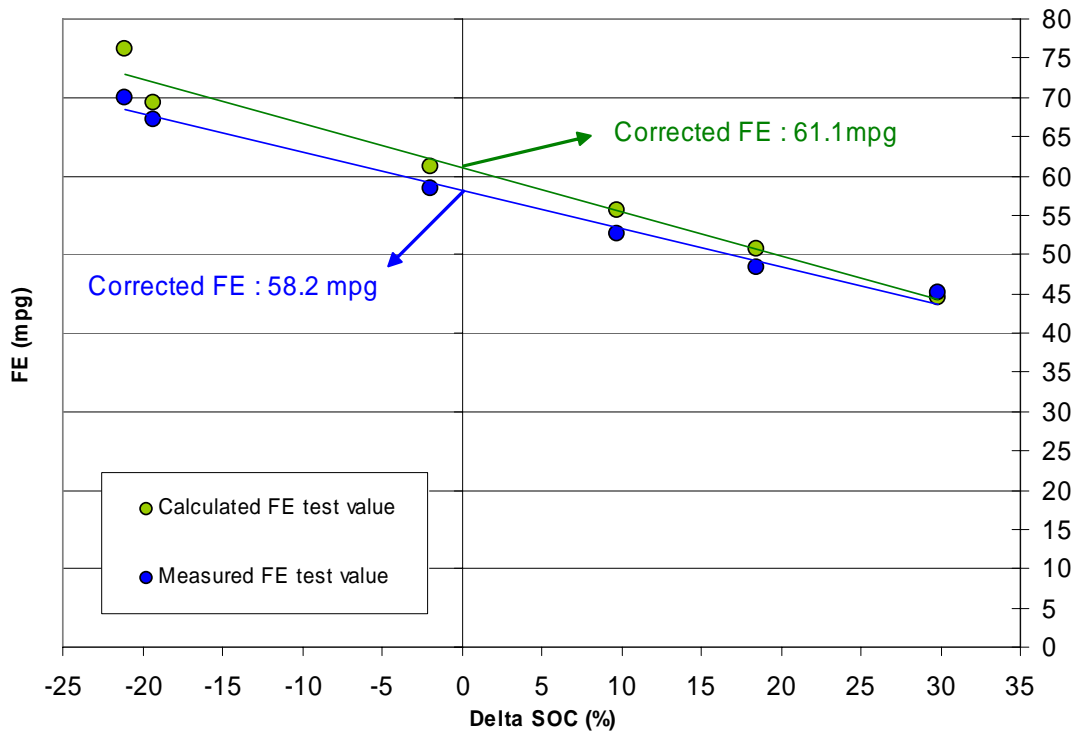


Figure 39: Regression of fuel economy versus delta SOC – Best efficiency strategy

This regression analysis studies how fuel economy varies across different tests indexed by delta SOC. It assumes that this relationship is linear on average. We need to estimate this linear relationship to make predictions (such as fuel economy with SOC equalization). With the use of statistical theory, we can make inferences about those predictions (such as confidence interval).

The concept is that the coefficients of the regression line are estimators of the real coefficients since we have a limited number of tests. The corrected FE is an estimate for the average fuel consumption. Thus, we can calculate its standard deviation and confidence interval to quantify the variability due to the test.



Results summary

Test 103110/#	/01	/02	/03	/06	/12	/15	Corrected FE	Average	Standard Deviation	95% confidence interval	% gain	% gain cumul.
F.E. meas. (mpg)	45.23	58.33	67.23	52.69	48.38	69.95	58.2	57.0	1.4 for corrected FE	[54.4; 62.1] for corrected FE	38%	57%
F.E. calc. (mpg)	44.50	61.19	69.39	55.63	50.69	76.08	61.1	59.6	2.3 for corrected FE	[54.8; 67.3] for corrected FE	37%	65%
Delta SOC (%)	+29.8	-1.91	-19.33	+9.71	+18.48	-21.06	0	+2.62	NA	NA	NA	NA
NOx (g/mi)	1.77	1.29	1.12	1.59	1.84	1.13	NA	1.46	0.32	[1.20; 1.71]	39%	35%
PM (g/mi)	NA	NA	NA	0.086	0.087	0.061	NA	0.078	0.015	[0.066; 0.090]	NA	NA
CO2 (g/mi)	228.7	166.3	146.6	182.8	200.4	133.8	NA	176.4	35.1	[148.4; 204.5]	-22%	-35%
CO (g/mi)	43E-3	22E-3	29E-3	82E-3	#NV#	#NV#	NA	0.044	0.027	[0.023; 0.065]	#NV#	#NV#
THC (g/mi)	#NV#	3.3E-3	3.8E-3	9.4E-3	4.9E-3	9.4E-3	NA	0.0062	0.0030	[0.0037; 0.0086]	#NV#	#NV#

The test consisted of a Federal Urban Driving Schedule (duration, 1372 s; distance, 7.45 mi)
 % Gain compared with previous experiment
 % Gain cumul compared with baseline experiment

The 95% confidence interval for fuel economy is wider in hybrid mode because, in addition to the test variability, we introduce a second variability by predicting the fuel consumption at a deltaSOC = 0 with a linear regression.

With the assistance of the electric motor in hybrid mode, the engine operates closer to its best efficiency curve. As a consequence, fuel economy increases by 38%, in comparison with the same control principles used in a conventional mode with CVT and by 57% in comparison with the baseline 5-speed manual emulated conventional powertrain. This experiment is critical to demonstrating the potential of hybridization and control. The 57% improvement in fuel economy denotes the impact of hybridization, but the same components were used in both experiments (baseline and hybrid). The baseline powertrain uses all of the components of the complete hybrid powertrain. To consider only the control aspect, the baseline is penalized by the CVT transmission operating as a manual transmission (which would be more efficient) and by the electric motor inertia and bearing losses.

Despite the improvement in fuel economy, we also noticed a 39% increase in NO_x emissions. We already observed this tendency in conventional operation, but now that the engine is always operating on the best efficiency curve, we can correlate this increase in NO_x emissions to the engine operating point. Figure 40 shows the engine operating points on the NO_x emissions map of the engine.

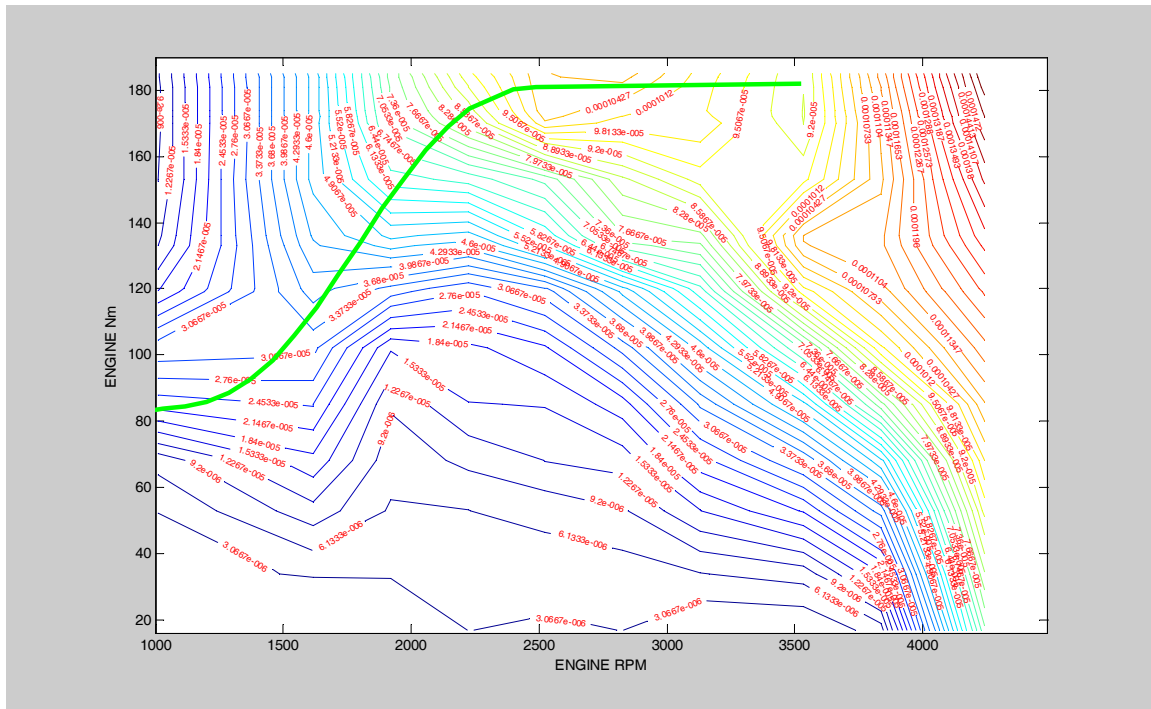


Figure 40: NO_x emissions map based on steady-state data

This map has been established by using ANL test data of steady-state engine operation. The best efficiency curve is located in high NO_x -emissions areas.

This experiment demonstrates the need for a trade-off between fuel economy and harmful NO_x emissions.
(APPENDIX 7)

3.3. Trade-Off between Fuel Economy and NO_x Emissions

Nitrogen Oxide (NO_x) emission data allow definition of a minimal NO_x curve that can be used to determine the lowest NO_x production at each power. For each power, if several NO_x minima exist, the controller selects the most efficient operating point. The engine torque and the CVT ratio are controlled to operate the engine on this NO_x /FE trade-off curve while satisfying engine power demand. Figure 41 shows the trade-off curve that has been calculated in simulation. (APPENDIX 8)

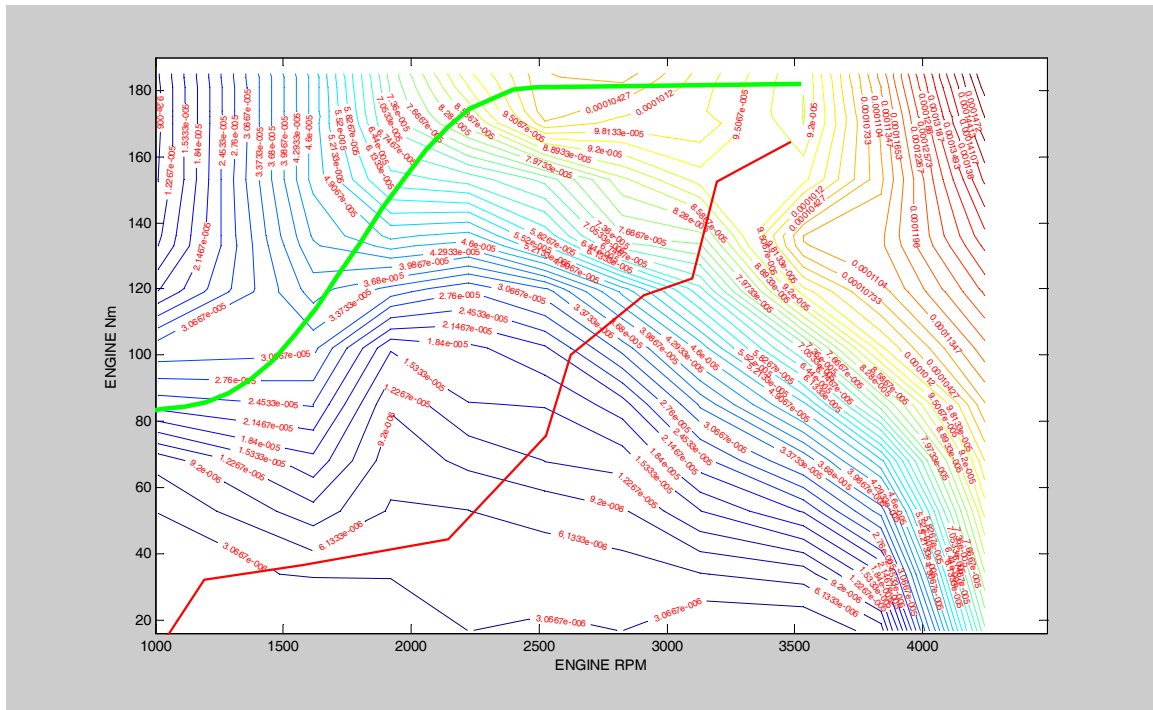


Figure 41: NO_x/FE trade-off curve

Figure 42 displays typical engine operation during a test that was performed with the trade-off strategy. Engine power demand is calculated to match driver expectations and the battery SOC requirement. The engine power required is then interpreted by the control strategy in order to set engine torque command and CVT ratio command. As a result, the engine operates near the trade-off curve. (APPENDIX 9)

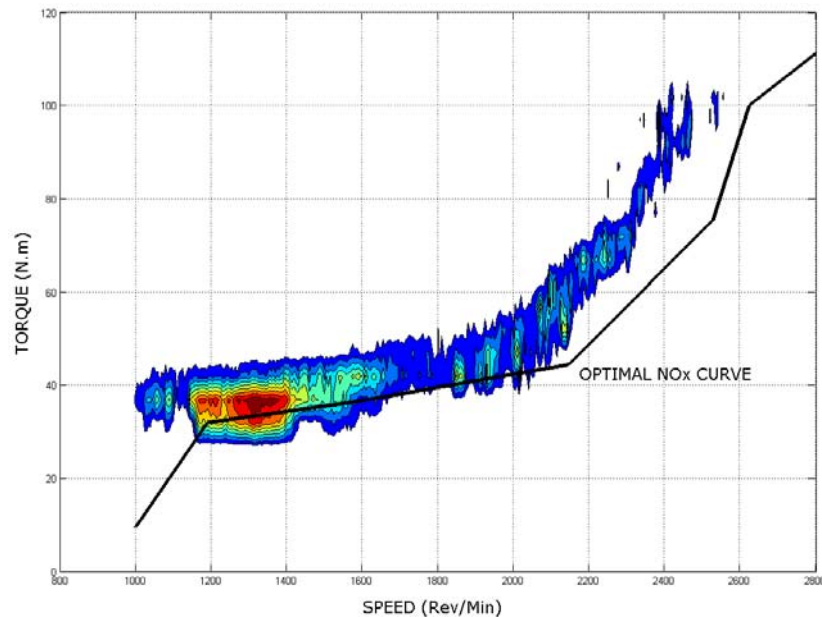


Figure 42: Engine operation point using the trade-off strategy

The color density on this plot is proportional to the time spent by the engine in the operating area. By comparing Figure 37 with Figure 42, we see that the engine is operating at lower load and higher speed. Consequently, the motor is able to absorb the excess power generated by the engine and is not limited by its negative torque.

Each test consists of the Federal Urban Driving Schedule. The vehicle’s performance is evaluated over several tests to check test repeatability. Initial and target battery SOC is changed before each test. As a result, we have a range of SOC variation that allows a corrected FE calculation.

Results

Test 103110/#	/08	/10	/11	/16	/17
F.E. meas. (mpg)	51.97	50.36	42.97	59.98	60.25
F.E. calc. (mpg)	54.11	52.48	44.64	59.55	61.09
Delta SOC (%)	+1.26	+2.7	+21.53	-16.86	-17.33
NOx (g/mi)	0.521	0.559	0.819	0.407	0.409
PM (g/mi)	0.119	0.125	0.211	0.112	0.112
CO2 (g/mi)	187.2	193.4	227.4	170.3	165.6
CO (g/mi)	0.372	0.260	0.272	0.293	0.456
THC (g/mi)	80.7E-3	22.2E-3	24.3E-3	19.7E-3	76E-3

Both fuel use and battery SOC must be taken into account when calculating or measuring the fuel economy (FE). Figure 43 shows how to estimate the corrected FE (i.e., what the fuel economy would be in case of SOC equalization over the test cycle).

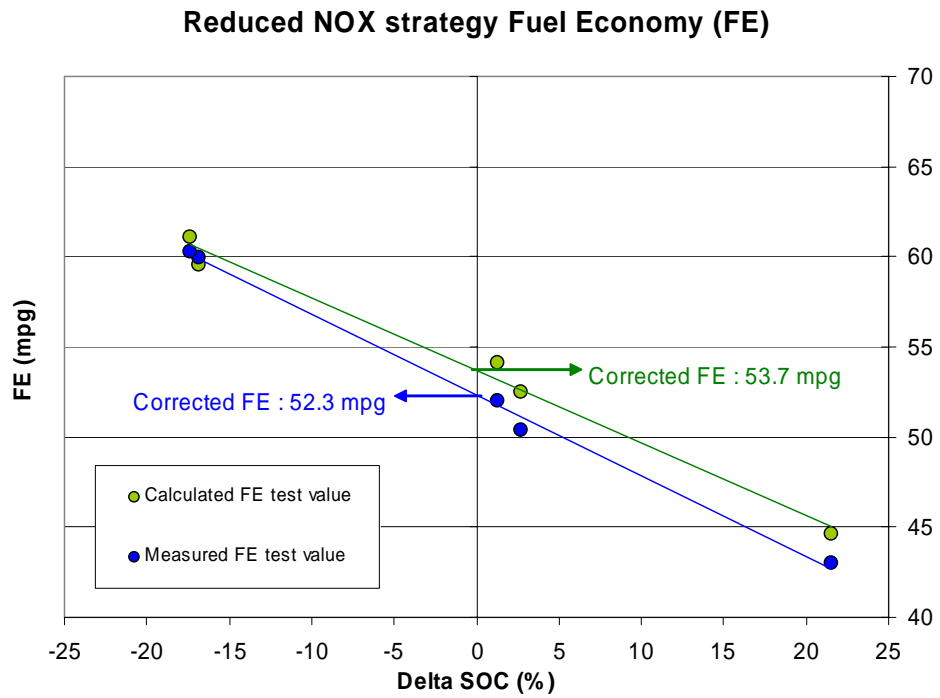


Figure 43: Regression of fuel economy versus delta SOC – trade-off strategy



Results summary

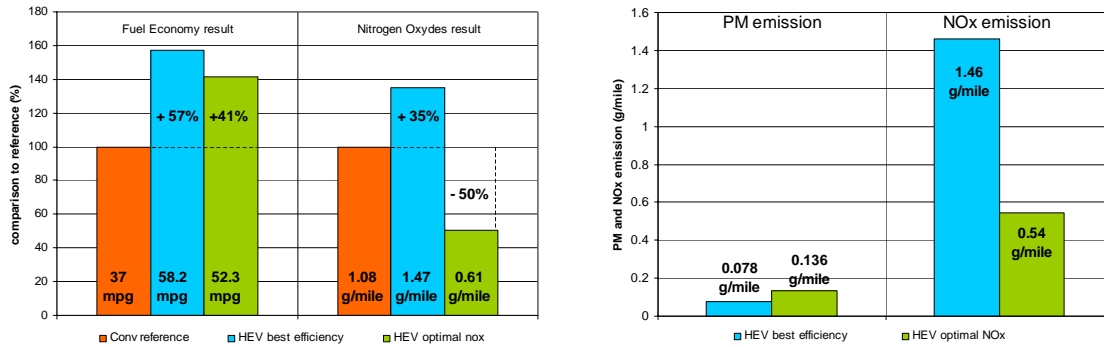
Test 103110/#	/08	/10	/11	/16	/17	Corrected FE	Average	Standard Deviation	95% confidence interval	% gain	% gain cumul.
F.E. meas. (mpg)	51.97	50.36	42.97	59.98	60.25	52.3	53.1	0.5 for corrected FE	[50.6; 54.0] for corrected FE	-10%	41%
F.E. calc. (mpg)	54.11	52.48	44.64	59.55	61.09	53.7	54.4	0.9 for corrected FE	[50.8; 56.6] for corrected FE	-12%	45%
Delta SOC (%)	+1.26	+2.7	+21.53	-16.86	-17.33	0	-1.74	NA	NA	NA	NA
NOx (g/mi)	0.521	0.559	0.819	0.407	0.409	NA	0.543	0.17	[0.395; 0.691]	-63%	-50%
PM (g/mi)	0.119	0.125	0.211	0.112	0.112	NA	0.136	0.042	[0.099; 0.173]	NA	NA
CO2 (g/mi)	187.2	193.4	227.4	170.3	165.6	NA	188.8	24.5	[167.3; 210.2]	7%	-31%
CO (g/mi)	0.372	0.260	0.272	0.293	0.456	NA	0.331	0.083	[0.258; 0.403]	NA	NA
THC (g/mi)	80.7E-3	22.2E-3	24.3E-3	19.7E-3	76E-3	NA	0.0446	0.0309	[0.017; 0.071]	NA	NA

The test consisted of a Federal Urban Driving Schedule (duration, 1372 s; distance, 7.45 mi)

% Gain compared with previous experiment

% Gain cumul compared with baseline experiment

Compared with the previous experiment, we have a fuel economy penalty, but NO_x emissions are reduced. Figure 44 shows a comparative analysis of the baseline experiment and the two hybrid modes of operation.



FE and NO_x result summary chart

Hybrid operation PM and NO_x summary

Figure 44: Comparison analysis

Operating the engine with the best efficiency approach increases fuel economy by 57%. This efficient engine utilization results in a 35% increase in NO_x emissions. The NO_x/fuel economy trade-off approach yields a 50% reduction in NO_x and yet improves fuel economy by 41%. However, it also results in an increase in PM emissions.

Those results refer to an emulated conventional vehicle, which is actually penalized by the inefficiency of a CVT acting as a manual transmission, as well as the losses and inertia of a disabled electric motor. The NO_x and PM emissions results are averages of the tests performed and are not SOC corrected. Consequently, the average delta SOC should be considered in order to interpret the analysis correctly.

(APPENDIX 10)

4. Conclusion

In this study, we presented two different hybrid control strategies. The objective of the study was not to optimize the control strategy but to assess the impact of hybridization and control and to demonstrate the potential of diesel to minimize the fuel economy penalty and yet meet emissions regulations. Figure 45 shows a comparison of our results for the experiments in conventional mode, and Figure 46 shows the results for the experiments in hybrid mode.

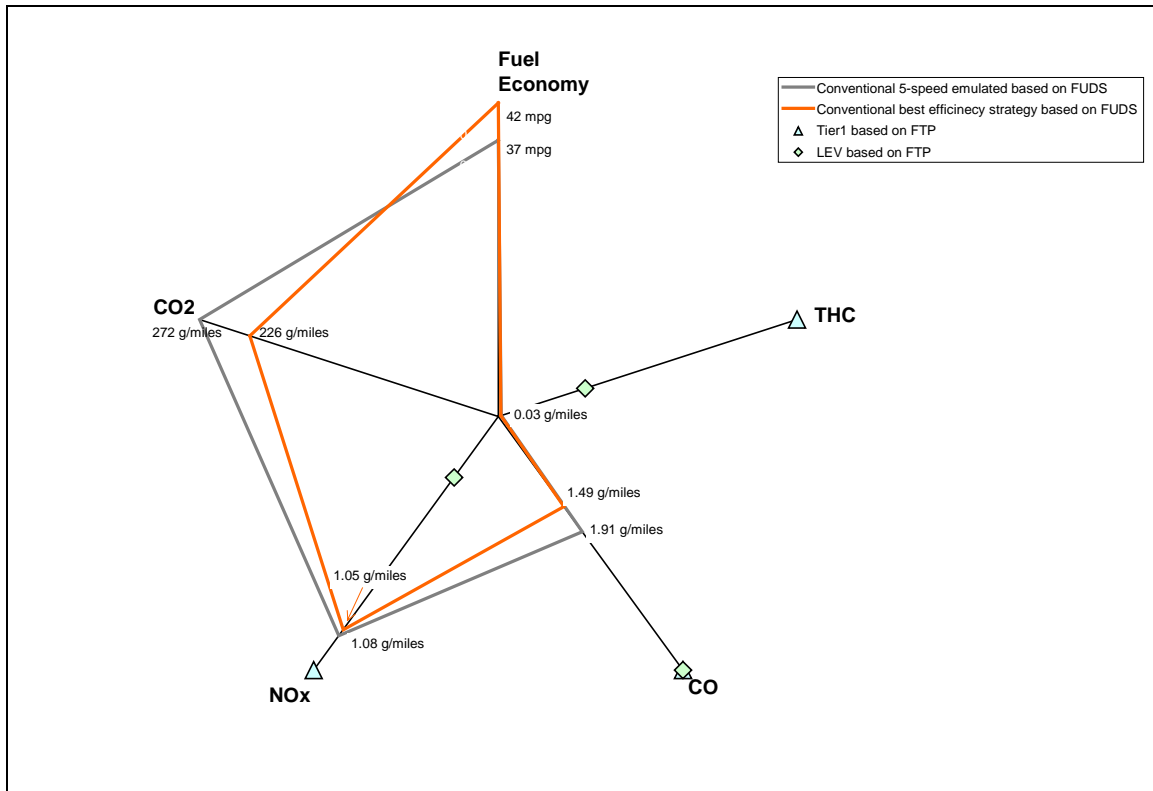


Figure 45: Comparison analysis for the conventional mode

Figure 45 shows that the control strategy has a limited impact on emissions for a conventional powertrain. In hybrid mode, we increased the degree of freedom and the potential for control impact on both emissions and fuel economy.

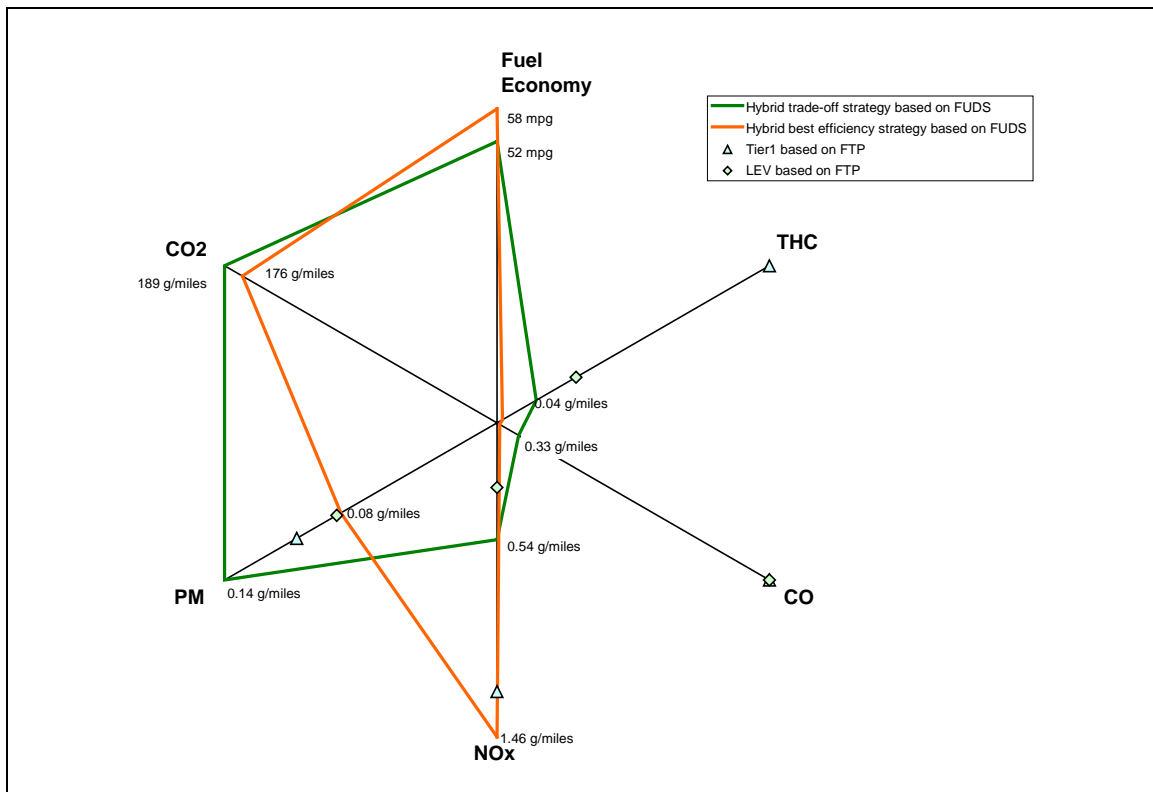


Figure 46: Comparison analysis for the hybrid mode

Figure 46 shows the trade-off between fuel economy and NO_x emissions. It demonstrates and quantifies the control strategy impact on fuel economy and emissions for diesel hybrid vehicles. To complete the evaluation of diesel hybrid technology, after-treatment devices should also be considered. Optimal control of the system would include engine calibration and advanced after-treatment devices, such as particulate filters or an NO_x absorber. At this time, particulate filter technology is more mature than the NO_x absorber. However, the development of an after-treatment control integrated to the vehicle control strategy would complete the demonstration of a diesel hybrid as a short-term bridge to a hydrogen economy.



5. Recognition

This study has been successful because of Argonne's Center for Transportation Research's (CTR's) flexible systems approach that links state-of-the-art testing and emissions measurement capabilities with accurate computer simulations (emulation) and component and vehicle testing (validation). The Advanced Powertrain Research Facility (APRF) is the U.S. Department of Energy's (DOE's) key laboratory for powertrain testing and validation.

The capabilities of our hybrid powertrain have been presented during the APRF dedication at a ribbon-cutting ceremony attended by 117 members of the U.S. Congress, officials and staff from DOE and Argonne, automobile manufacturers, the media, and others. U.S. Representative Judy Biggert (R-IL), DOE Deputy Assistant Secretary for Energy Efficiency and Renewable Energy (EERE) Richard Moorer, Argonne Laboratory Director Hermann Grunder, Argonne Associate Laboratory Director Harvey Drucker, and USCAR Executive Director Bob Culver gave opening remarks at the dedication. Others who attended the event included auto industry executives from Ford, General Motors, BMW, Honda, and DaimlerChrysler, as well as DOE sponsors Bob Kost, Vehicle Systems Team Leader, Office of FreedomCar Vehicle Technologies, and Lee Slezak, who is a member of the team.

“This facility provides researchers with the tools needed to develop and evaluate vehicle components that will meet America's changing transportation needs,” said DOE's Moorer. “The facility will help industry enhance energy efficiency and productivity by bringing clean, reliable, and affordable energy technologies to the marketplace while reducing dependence on foreign supplies of oil. This will make a difference in the everyday lives of Americans by enhancing their energy choices and their quality of life.”

Asserted Argonne's Grunder, “Argonne is an ideal place for this R&D to occur. We have one of the largest EERE transportation R&D budgets in the national laboratory system with 10 divisions actively participating in developing cutting-edge technologies in engines, fuel cells, batteries, advanced materials, heat exchangers, aerodynamic and thermal modeling, and fuel processing. We are centrally located for the automotive and truck industries, have unique scientific research facilities, and have excellent working relationships with many of the major industry players worldwide.”

“This unique combination of analytical, development and testing experience provides DOE with the latest techniques to evaluate new vehicle technologies in both emulated and real-vehicle environments,” said CTR Director Bob Larsen. “Argonne's long history in modeling, developing, and testing advanced engines, hybrid-electric vehicle powertrains and control systems, traction batteries, fuel cells, and vehicles is a large part of making Argonne an important laboratory for vehicle technology development and validation.”

This project was also presented to David Garman, Assistant Secretary for DOE's Office of Energy Efficiency and Renewable Energy (EERE), during a visit to Argonne National Laboratory. The demonstration of the diesel hybrid powertrain showed how Argonne research supports DOE's work to reduce dependence on oil imports.



(Left to right) U.S. Rep. Judy Biggert (R-IL), Argonne Laboratory Director Hermann Grunder, DOE Deputy Assistant Secretary for Energy Efficiency and Renewable Energy Richard Moorer, and Argonne Associate Laboratory Director Harvey Drucker dedicate Argonne's Advanced Powertrain Research Facility (APRF).



(Left to right): Argonne's Harvey Drucker and Hermann Grunder with Chairman of the DuPage County Board Bob Schillerstrom, USCAR Executive Director Bob Culver, DOE's Richard Moorer, and U.S. Rep Judy Biggert.



(Left to right): Argonne's Hermann Grunder, Assistant Secretary for DOE's EERE Office David Garman, Argonne's Harvey Drucker.



6. Acknowledgments

This work was supported by the U.S. Department of Energy, Office of Energy Efficiency and Renewable Energy, under contract W-31-109-Eng-38. The authors are grateful for the support of and guidance by the FreedomCAR and Vehicle Technologies Program.

Robert Larsen, Center for Transportation Research Director

Keith Hardy, Section Leader, Fuels and Vehicle Systems

John Anderson, Mechanical Engineer, Vehicle Systems and Fuel section

Geoffrey Amann, Senior Technician, Vehicle Systems and Fuel section

Ted Bohn, Engineering Assistant, Vehicle Systems and Fuel section

Roger L. Cole, Mechanical Engineer, Engine and Emission research section

Michael Duoba, Mechanical Engineer, Vehicle Systems and Fuel section

Justin Kern, Mechanical Engineer, Vehicle Systems and Fuel section

Steven S. McConnell, Mechanical Engineer, Engine and Emission research section

Gilles Monnet, Electrical Engineer, Vehicle Systems and Fuel section

Henry Ng, Mechanical Engineer, Vehicle Systems and Fuel section

Maxime Pasquier, Transportation Systems Analysis Engineer, Vehicle Systems and Fuel section

Aymeric Rousseau, Transportation Systems Analysis Engineer, Vehicle Systems and Fuel section

Phil Sharer, Electrical Engineer, Vehicle Systems and Fuel section

David Shimcoski, Automotive Emissions Testing Specialist, Vehicle Systems and Fuel section



7. References

1. Pasquier, M., Detailed Description of ANL Center for Transportation Research's Prototyping Program Activities, 2001, DOE Report.
2. Rousseau, A.; Pagerit S.; and Monnet G., The New PNGV System Analysis Toolkit PSAT v.4.1: Evolution and Improvement, SAE Paper 2001-01-2536, Future Transportation Technology Conference & Exposition, August 2001, Costa Mesa, CA, USA.
3. Pasquier, M., and Rousseau A., PSAT and PSAT-PRO, an Integrated and Validated Toolkit from Modeling to Prototyping, Proceedings of the 2001 Global Powertrain Congress, Detroit, MI, USA.
4. Pasquier, M., and Monnet G., PSAT-PRO User Guide, 2001, Hardware-In-the-Loop Control Software Documentation.
5. Duoba, M.; Ng, H.; and Larsen, R., In-Situ Mapping and Analysis of the Toyota Prius Hev Engine, SAE Paper 2000-01-3099, Future Transportation Technology Conference & Exposition, August 2000, Costa Mesa, CA, USA.
6. Duoba, M.; Ng, H.; and Larsen, R., Characterization and Comparison of Two Hybrid Electric Vehicles (HEVs) – Honda Insight and Toyota Prius, SAE Paper 2001-01-1335, SAE 2001 World Congress, March 2001, Detroit, MI, USA.
7. Oh, S.; Bohn, T.; Kern, J.; Pasquier, M.; and Rousseau, A., Axial Flux Variable Gap Motor: Application in Vehicle Systems, SAE Paper 2002-01-1088, SAE 2002 World Congress & Exhibition, March 2002, Detroit, MI, USA.
8. Min, B.; Matthews, R.; Duoba, M.; Ng, H.; and Larsen, R., Direct Measurement of Powertrain Component Efficiencies for a Light-Duty Vehicle with a CVT Operating over a Driving Cycle, SAE Paper 2003-01-3202, SAE Powertrain & Fluid Systems Conference & Exhibition, October 2003, Pittsburgh, PA, USA.
9. Pasquier, M.; Duoba, M.; and Rousseau, A., Validating Simulation Tools for Vehicle System Studies Using Advanced Control and Testing Procedures, 18th International Electric Vehicle Symposium (EVS18), 2001, Berlin, Germany.
10. Rousseau, A., and Pasquier, M. Validation Process of a Hybrid Electric Vehicle System Analysis Model: PSAT, SAE Paper 2001-01-0953, SAE 2001 World Congress, March 2001, Detroit, MI, USA.
11. Rousseau, A., and Pasquier, M., Validation of a Hybrid Modeling Software (PSAT) Using its Extension for Prototyping (PSAT-PRO), Proceedings of the 2001 Global Powertrain Congress, Detroit, MI, USA.



12. Rousseau, A., and Pasquier M., Simulation and Validation of Hybrid Electric Vehicles Using PSAT and PSAT-PRO, Advisor Conference, 2000, Costa-Mesa, CA, USA.
13. Cole, R.; Hillman, G.; and Sekar, R., Baseline Performance and Emissions of 1.7-Liter Mercedes Benz Engine, January 2002, DOE Report.
14. Pasquier, M.; Duoba, M.; Hardy, K.; Rousseau, A.; and Shimcoski, D., Evaluation of a CIDI Pre-transmission Parallel Hybrid Drivetrain with Continuously Variable transmission, 19th International Battery, Hybrid and Fuel Cell Electric Vehicle Symposium & Exhibition (EVS19), 2002, Busan, Korea.

The submitted manuscript has been created by the University of Chicago as Operator of Argonne National Laboratory (“Argonne”) under Contract No. W-31-109-ENG-38 with the U.S. Department of Energy. The U.S. Government retains for itself, and others acting on its behalf, a paid-up, nonexclusive, irrevocable worldwide license in said article to reproduce, prepare derivative works, distribute copies to the public, and perform publicly and display publicly, by or on behalf of the Government.



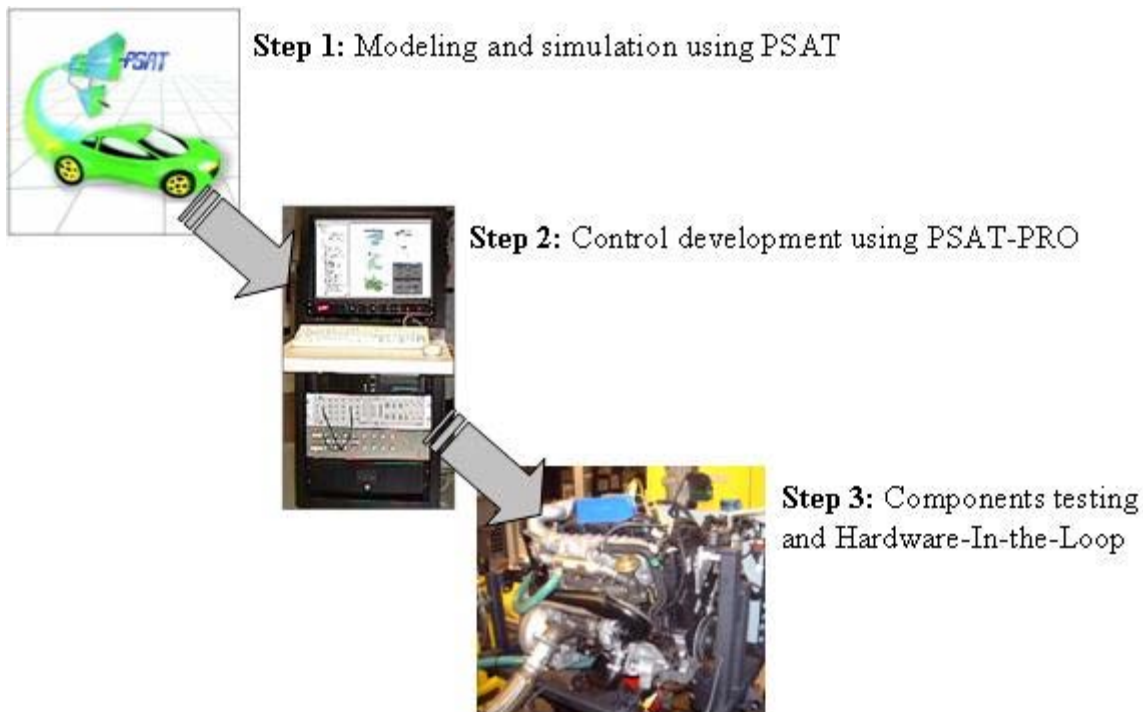
8. Appendixes

8.1. PSAT-PRO® User Guide

A1.1 Introduction

The purpose of PSAT-PRO is to facilitate the development of system controllers. PSAT, the PSAT-PRO companion for simulation, allows analysis studies and vehicle power management development.

PSAT-PRO offers you the capability to use and enhance your modeling work for control purposes. It allows the test of your power management system in a real environment or in Hardware-In-the-Loop (HIL). HIL is a technique for performing system-level tests quickly and cost-effectively. HIL can be used to test Hybrid Electric Vehicle (HEV) components when they cannot be tested or instrumented easily in their operational environments.



A1.2 Software Requirements

PSAT-PRO software has been developed to facilitate HEV control development. The software has been designed to optimize the link between modeling and prototyping, especially for the use and transfer of work from modeling to real-world applications. It uses PSAT modeling software as a base and cannot be used independently. That's why PSAT modeling software is required to use PSAT-PRO control software.

PSAT-PRO is a Matlab-based software that uses the following toolboxes:

MATLAB Toolbox	Version 5.3 (R11)	Version 6.1 (R12.1)
Simulink	Version 3.0 (R11)	Version 4.1 (R12.1)
Real-Time Workshop	Version 3.0.0 (R11)	Version 4.1 (R12.1)

PSAT-PRO INSTALLATION WITHOUT A PERSONAL MATLAB START-UP

If you have never created a personal Matlab start-up, then use the following procedure:

Open your explorer and select the drive where your installation source is located. Double-click on the installation icon (PsatProInstall).



Acknowledge the PSAT-PRO Copyright disclosure and click “OK.”



Enter the complete path where you want to install PSAT-PRO. By default, the software will be installed under c:\ASAP\PSAT-PRO (ASAP stands for Argonne National Laboratory System Analysis Program).



PSAT-PRO uses PSAT models component library. It is necessary to characterize the location of PSAT; this needs to be done when first installing PSAT-PRO. This step must also be implemented if the PSAT location changes.

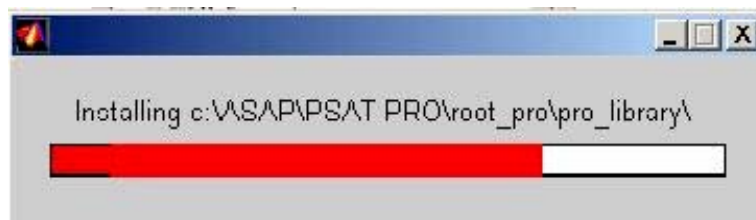
When the next window appears, select the location of the PSAT folder. Please, select only the PSAT folder and not the subdirectories.

Example:



Note: In this example, PSAT has been installed under C:\ASAP\PSAT, and now the user wants to install PSAT-PRO under the same directory C:\ASAP\PSAT-PRO. But it is not necessary to install PSAT-PRO under the same directory than PSAT.

Wait until all the PSAT-PRO directories have been installed.



Congratulations! You are ready to start a PSAT-PRO session!



A1.3 PSAT-PRO Installation with a Personal MATLAB Start-Up

If you have a personal Matlab start-up (particularly if you change the initial work directory), then you have to

Type `cd X:\psat_pro\root_pro; PsatProInstall` in your Matlab workspace:

This line will set the correct working directory and evaluate the installation file. You should replace X by the letter of the drive where your installation source is located.

Example:



Acknowledge the PSAT-PRO Copyright disclosure and click "OK."



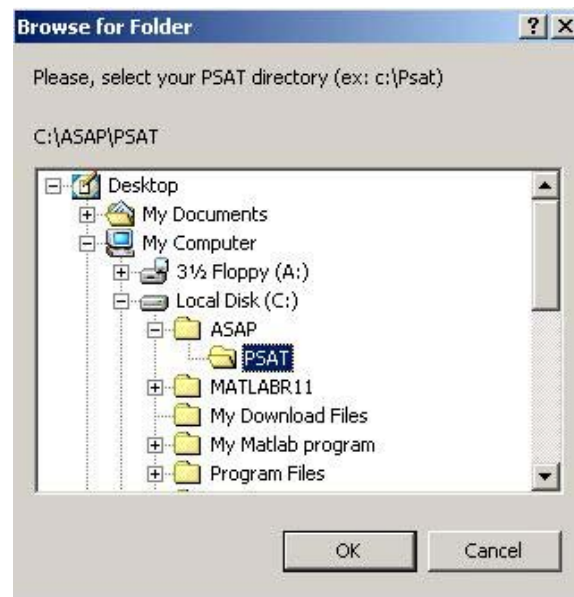
Enter the complete path where you want to install PSAT-PRO. By default, the software will be install under `c:\ASAP\PSAT-PRO` (ASAP stands for Argonne National Laboratory System Analysis Program).



PSAT-PRO uses PSAT models component library. It is necessary to characterize the location of PSAT; this needs to be done when first installing PSAT-PRO. This step must also be implemented if the PSAT location changes.

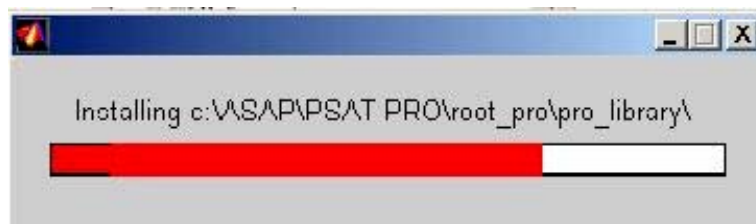
When the next window appears, select the location of the PSAT folder. Please, select only the PSAT folder and not the subdirectories.

Example:



Note: In this example, PSAT has been installed under C:\ASAP\PSAT, and now the user wants to install PSAT-PRO under the same directory C:\ASAP\PSAT-PRO. But it is not necessary to install PSAT-PRO under the same directory than PSAT.

Wait until all of the PSAT-PRO directories have been installed.



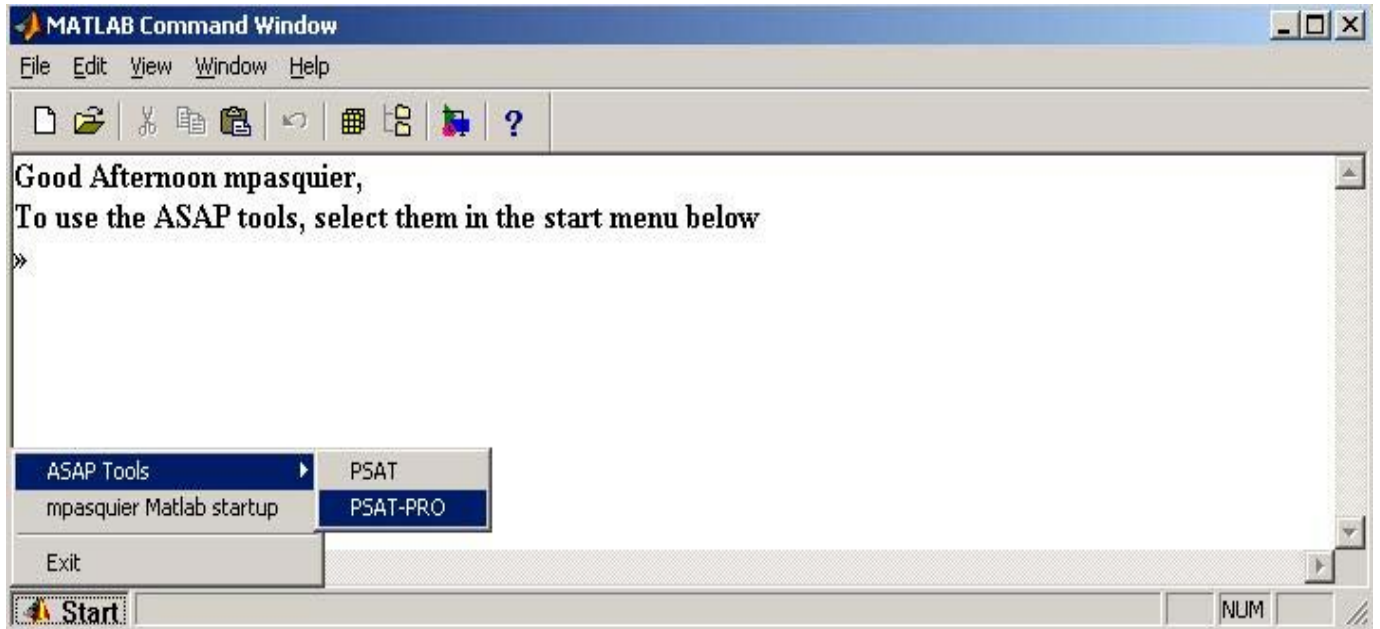
Congratulations! You are ready to start a PSAT-PRO session!



A1.4 PSAT-PRO First Start

Start a PSAT-PRO Session

To start using PSAT-PRO, you have to select it in the start menu located at the bottom of your Matlab workspace.



The start menu will appear at every Matlab session. If you want to use your personal Matlab start-up program, it has been saved as `startupsav.m`. You can still launch it by selecting "username Matlab startup" in the start menu.

Acknowledge the PSAT-PRO Copyright disclosure and click "OK."

Create a New Project

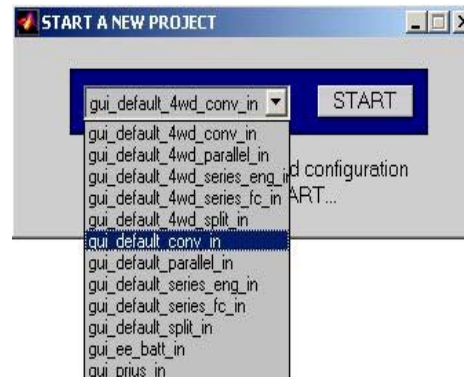
To create a new project, click on “NEW.” If it is your first session, you can only choose “NEW.” (The “BROWSE” button is disabled because no project has been created before).



Choose a name for the project you are creating; you can mix numbers and letters. Please avoid inserting a space or special characters, which may create problems (“_” and “-” are ok). Then, click “OK.”

Warning messages may appear if the project name is not correct. In this case, you have to follow the instructions.

Now, you have to choose the PSAT configuration you are interested in for control purposes. You can do this in the window: “START A NEW PROJECT.” Select the right configuration by using the popup menu and click on “START.”



The list consists of PSAT saved and default configuration. You have the option of using the particular configuration you worked on in modeling by using the PSAT graphical user interface. See:

“6 - Create and Import a Specific PSAT Configuration p. 10” for more details.

Now the Program will create your project and all requirements for you to be able to develop your own control system by using PSAT-PRO. You should not interfere with the program while it is creating the project. It is recommended to wait until the PROJECT MANAGER window appears.

Congratulations! You are ready to work with PSAT-PRO!



Create and Import a Specific PSAT Configuration

Open a PSAT session.

Set up the vehicle configuration you are interested in with the first GUI window.

Click on the save button of the same window.

A saving window opens and you have to name your file:

Make sure to respect the convention `gui*_in`.

Use the saving window browser to save the file.

Save it under your personal PSAT user folder or your personal PSAT-PRO user folder if it exists already (`/psat_pro/root_pro/users/***username***`).

Click on save.

You can close the PSAT Session and start the creation of a prototyping project by starting a PSAT-PRO Session.



Open an Existing Project

To open an existing project, click on “BROWSE.”



Select the project you want to work at, using the popup menu and click on “OPEN.” The list consists of the projects available on your user folder.

If you wish to open another existing project (created by another user), click ‘Other...’:

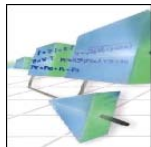
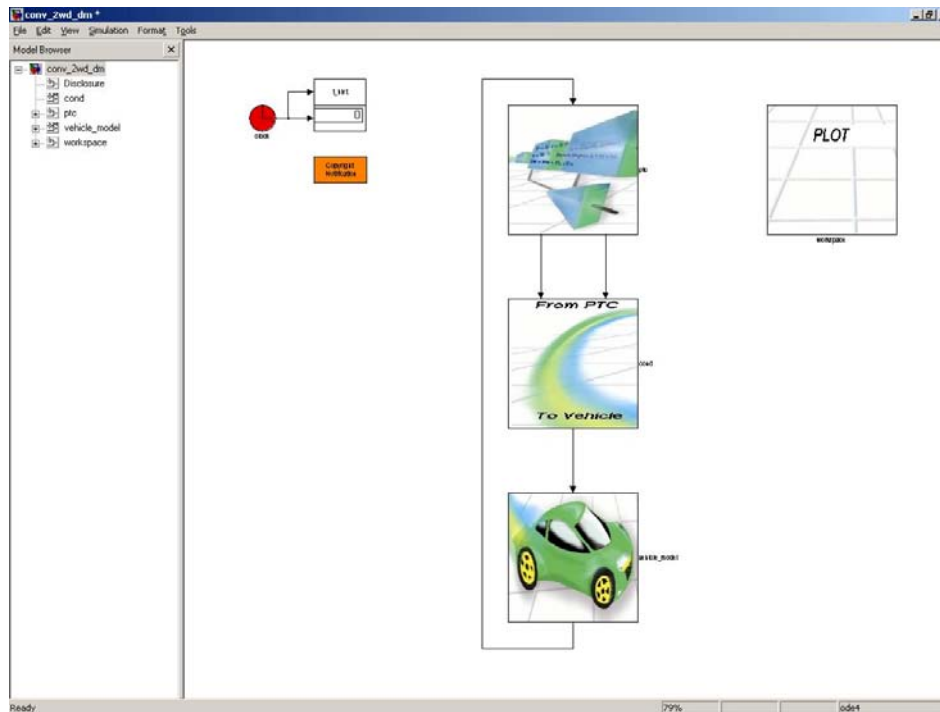
A browser window appears; use it to select the project folder you wish to open. Click open. The project you are interested in has been added to the popup menu list. You are now able to select and open it.

Note: Even if you can select this project from your popup menu, the project has not been saved under your user directory. You are working on the original project of another user. Any modifications to the project will be saved under the first user directory. Sharing work should be done with a lot of care and communication to avoid losing any work between the different users.

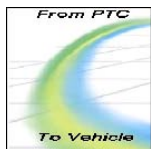
PSAT-PRO opens the latest version of the project you wish to work on.

A1.5 PSAT-PRO Description

This is PSAT-PRO top-level Simulink window



The “ptc” block (stands for PowerTrain Controller) is the controller of your system. Its only input is the measure bus, which consists of signals coming from the vehicle model block in case of simulation, from your sensors otherwise.

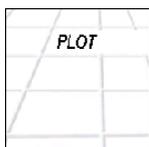


The “cond” block is a signal CONDitioning subsystem. It interfaces output signals from the “ptc” controller block to the vehicle model or the real system.



The “Vehicle_model” block is fairly similar to the PSAT powertrain model. It is built by using the PSAT component model library. The input is the command signal bus and it outputs the simulated measure bus.

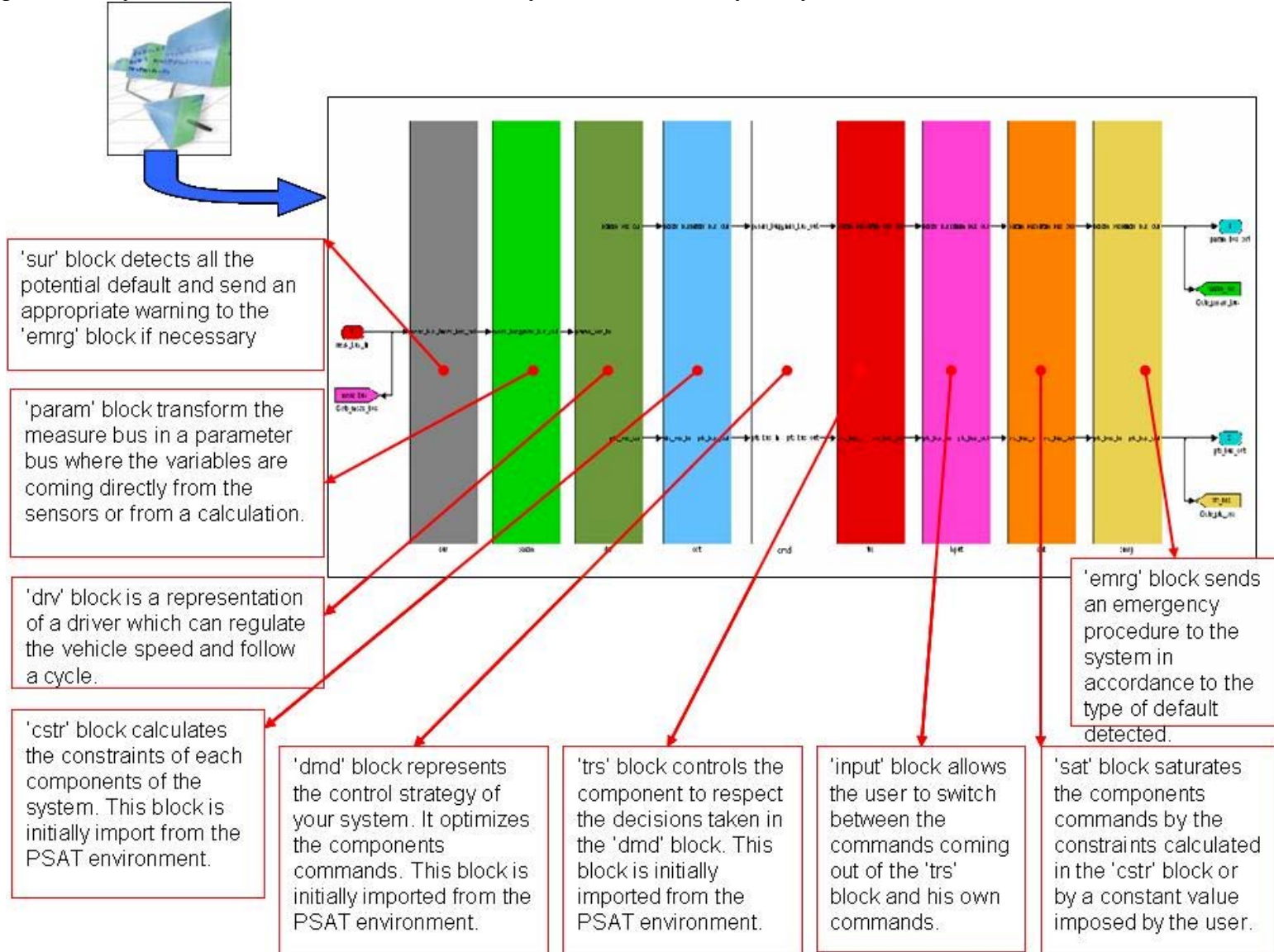
The vehicle model features specific PSAT-PRO control functionalities.



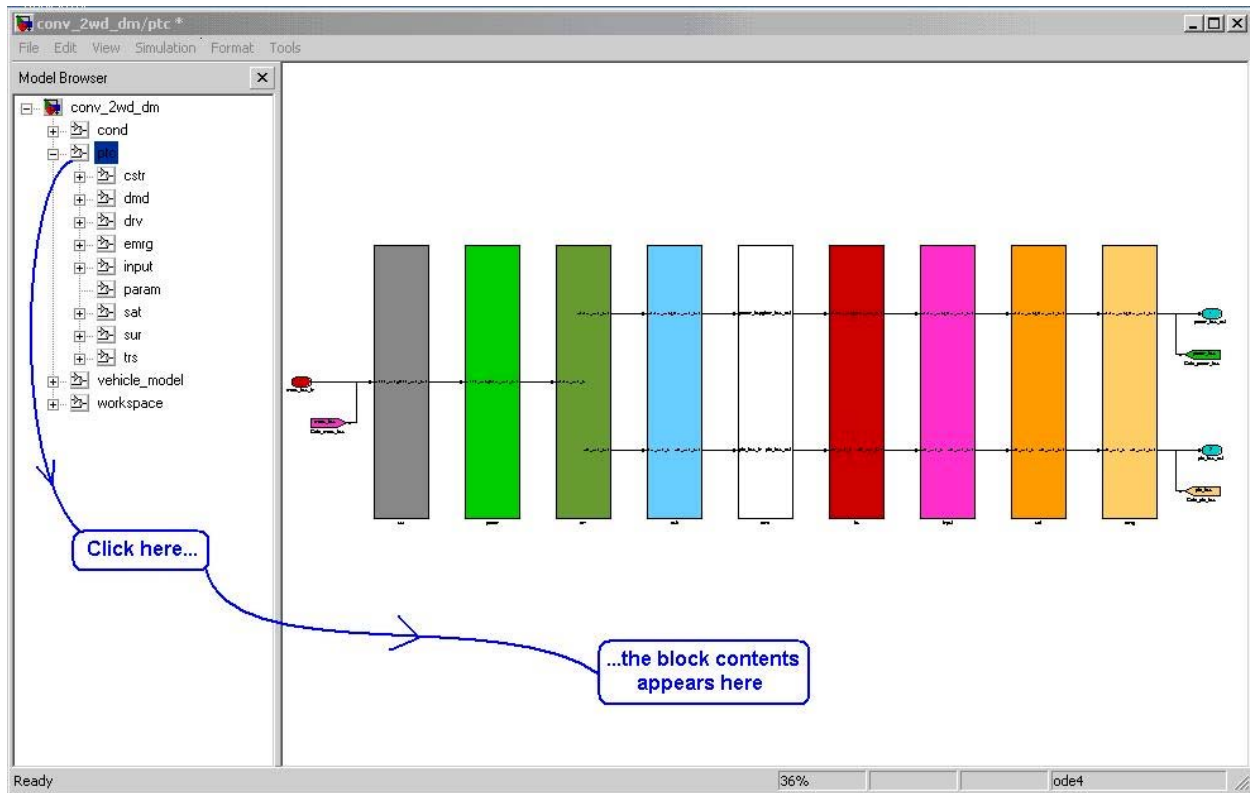
The “to_workspace” block declares all information of which the buses are made of to Matlab workspace. This block also features signal plotting.



In the 'ptc' block, you can find all the functions necessary for the control of your system.



Use the Model Browser



The model browser window on the left displays the architecture of the model. The model browser is a convenient way to navigate through the Simulink blocks.

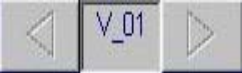
Use the Project Manager Interface

This interface was kept simple to perform project management and remote simulation.

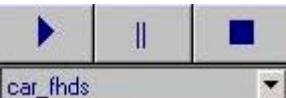
Project management consists of several main functionalities:

 Updates the different buses anytime during the development of your project. This function can be used after a modification of the bus system or when a signal has been added to a bus. See “21 – Create a new Signal and its Selector p. 26” for more details.

 Saves all the blocks and information you modified in your project. This function opens the VERSION MANAGER interface, which proposes saving and versioning of your work. See “11 – Save and Manage the Different Project Versions p. 15” for more details.

 Allows you to access the different versions of your project. The project current version is displayed between the two push buttons. It is possible to save modifications at the top version level only.

 Allows you to close the PSAT-PRO session with or without saving the last modifications.

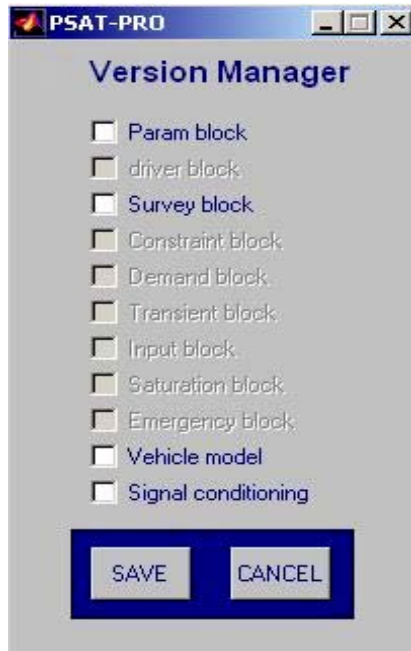
 The simulation board consists of a popup menu to choose a standard driving cycle, but also Play, Pause, or Stop the simulation.

A1.6 PSAT-PRO PROJECT DEVELOPMENT

Save and Manage the Different Project Versions



Click on the save button of the PROJECT MANAGER Interface:
The next window appears:



-There is a check box for each block of your project.

-A disabled check box indicates that the corresponding blocks have not been modified since you last opened the project.

-Parameter, Survey, Vehicle, and signal conditioning check boxes are never disabled in order to allow some of the PSAT-PRO functionalities.

The use of the CANCEL button will close the VERSION MANAGER interface without saving any block.

The information bus system is checked and updated every time you save your project.

You can decide to select or not the check boxes.

When you click on save:

-Any block corresponding to an enable and blank check box will be save in its specific library under its current top version.

-Any selected block will be saved in its specific block library under a new block version.

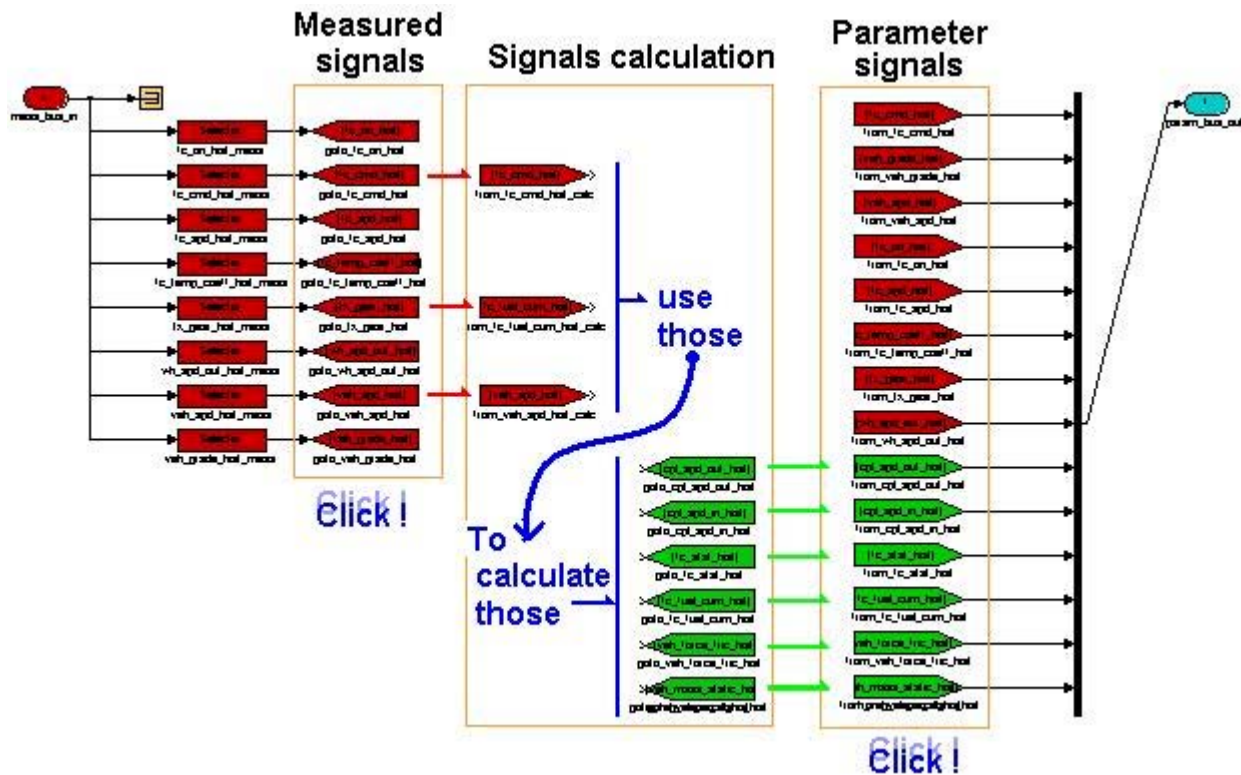
If one or more check boxes are checked: The project version will be upgraded; otherwise, the project version remains the same. Only the modifications done on the project top version can be saved.

Block versioning is hidden for the user; the user can only access project versioning (which is displayed on the PROJECT MANAGER). It is recommended that you use the versioning wisely by saving a new version at each big step of PSAT-PRO controller development. It is also highly recommended that you save regularly your project under its current version (No check box selected).

Set Up the Controller Parameters Input

Use the model browser to open the “ptc” block then the “param” block.
 See “9 – Use the Model Browser p. 13.”

Parameter signals are the signals used by the PSAT power management system. To feed those parameter signals, corresponding measurements are taken in the vehicle model. Initially, only measured and required signals are in this block. Every required signal is measured (red color) by default.



Double click on a parameter signal: It turns green and appears in the signals calculation area. The corresponding measured signal disappears.

Double click on a measured signal if you want to use it to calculate the green one; it will appear in the signal calculation area.

Both of those operations are reversible by double clicking on the green parameter signal or on the red measured signal. Basically, a green signal is calculated, and so it is removed from the measure bus.

Now you can adapt the controller to your prototype: If you do not have all of the sensors available, you have to calculate the required signals.



Example: If your controller requires two speed signals, which are linked by a constant ratio, you can use one sensor and use the measured speed to calculate the second required speed with the known ratio.

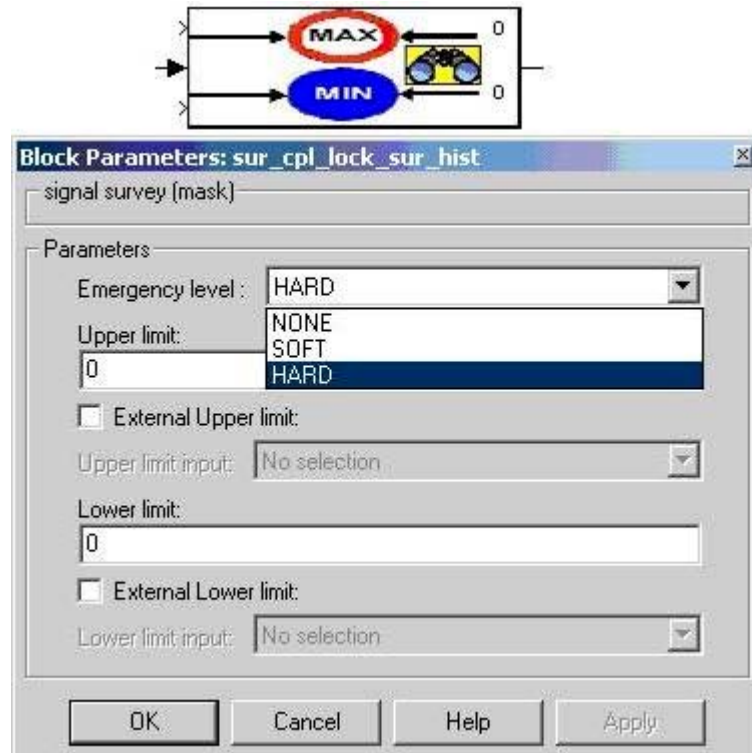
Once you are satisfied with this block or even if you did not finish this work, you can save it. By using the PROJECT MANAGER, you will be able to modify this block again in the present or future PSAT-PRO session, at any step of the project development. See “11 – Save and Manage the Different Project Versions p. 15.”

Set Up the Signal Survey

Use the model browser to open the “ptc” block then the “sur” block.

All the measured signals are surveyed in PSAT-PRO controller. It is the purpose of each “signal survey” block.

Double click on one of the “signal survey” blocks:



Set the upper and lower limit of the signal using the interface: For each limit, you can choose to write a constant or check the external upper/lower input box to choose the constraint with which you want to survey the signal. The constant values are displayed on the survey_block.

Choose the emergency level within the top popup menu. When a signal crosses one of the limits, the emergency block will react adequately.

This will allow you, for example, to detect and react to a motor over speed. You need to set the survey for each signal.

Do not forget to save your work with the PROJECT MANAGER.

Set Up the Signal Saturation

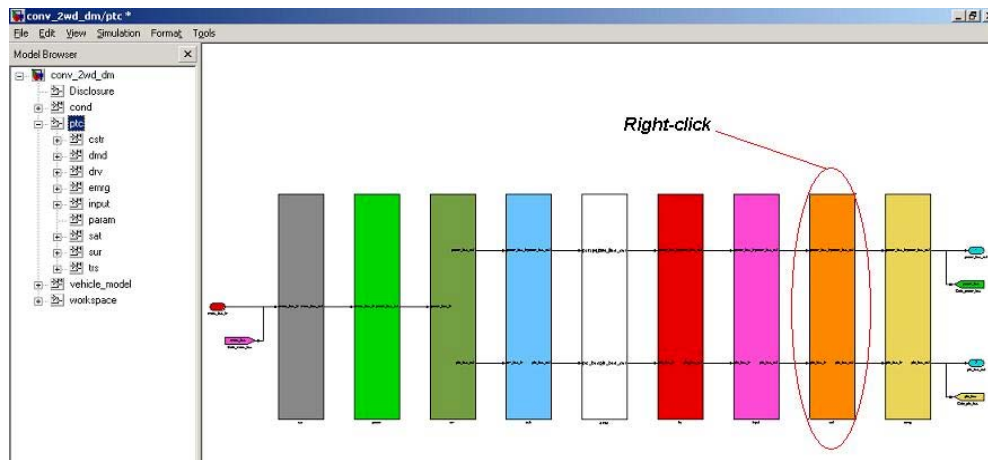
For safety purposes, all output signals of the PSAT-PRO controller must be saturated and inhibited by the emergency survey system. This will avoid sending a wrong command to the components, which may result in damage or hazards.

To modify a saturated value:

Use the model browser to open the “ptc” block.

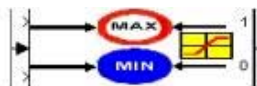
Select the “sat” block (the last but one block from the left) in the work area.

Right click and select “Break library link.”



Use the model browser to open the “sat” block.

Double-click on the block corresponding to the desired signal.



Set the upper and lower saturation limit of the signal using the interface: For each limit, you can choose to write a constant or check the external upper/lower input box to choose the constraint with which you want to saturate the signal. The constant values are displayed on the survey_block.

Set the saturation for each signal.

You can now close the block and save your project.

Warning: The saturation block is protected, and you have to break the library link to be able to modify it. It is the user’s responsibility to set the appropriate saturated values.

Set Up the Emergency Signals

The emergency block allows the user to set the commands in case of a default. The block will output the commands corresponding to the right level of emergency detected in the survey block.

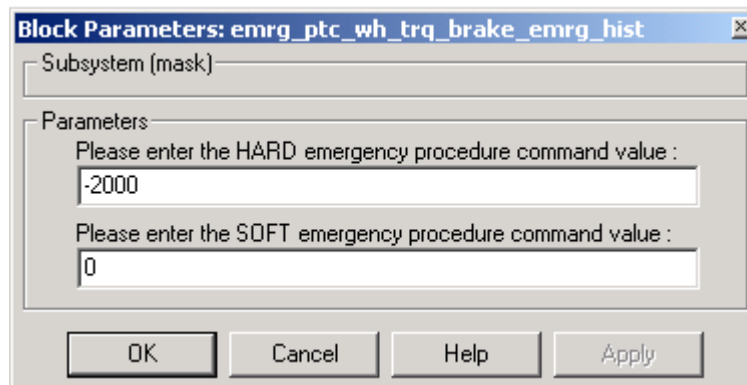
To set the commands in function of the emergency procedure:

Use the model browser to open the “ptc” block. Select the “sat” block (the last but one block from the left) in the work area.

Right click and select “Break library link.”



Double-click on the above block corresponding to the desired signal.



Set the HARD and SOFT emergency command values and click OK.

Repeat this to all signal present in the emergency block.

Do not forget to save your project.

Example: For the brake command, you may set the HARD emergency value to the max braking torque in order to stop your system motion as soon as possible; in case of a SOFT emergency, you may set the brake command to zero so that your system will stop smoothly.

Warning: The emergency block is protected and you have to break the library link to be able to modify it. It is the user’s responsibility to set the appropriate emergency procedure.

Run a Simulation Controlling the Vehicle Model

The controller is ready to be used for the simulation.

To run a simulation:

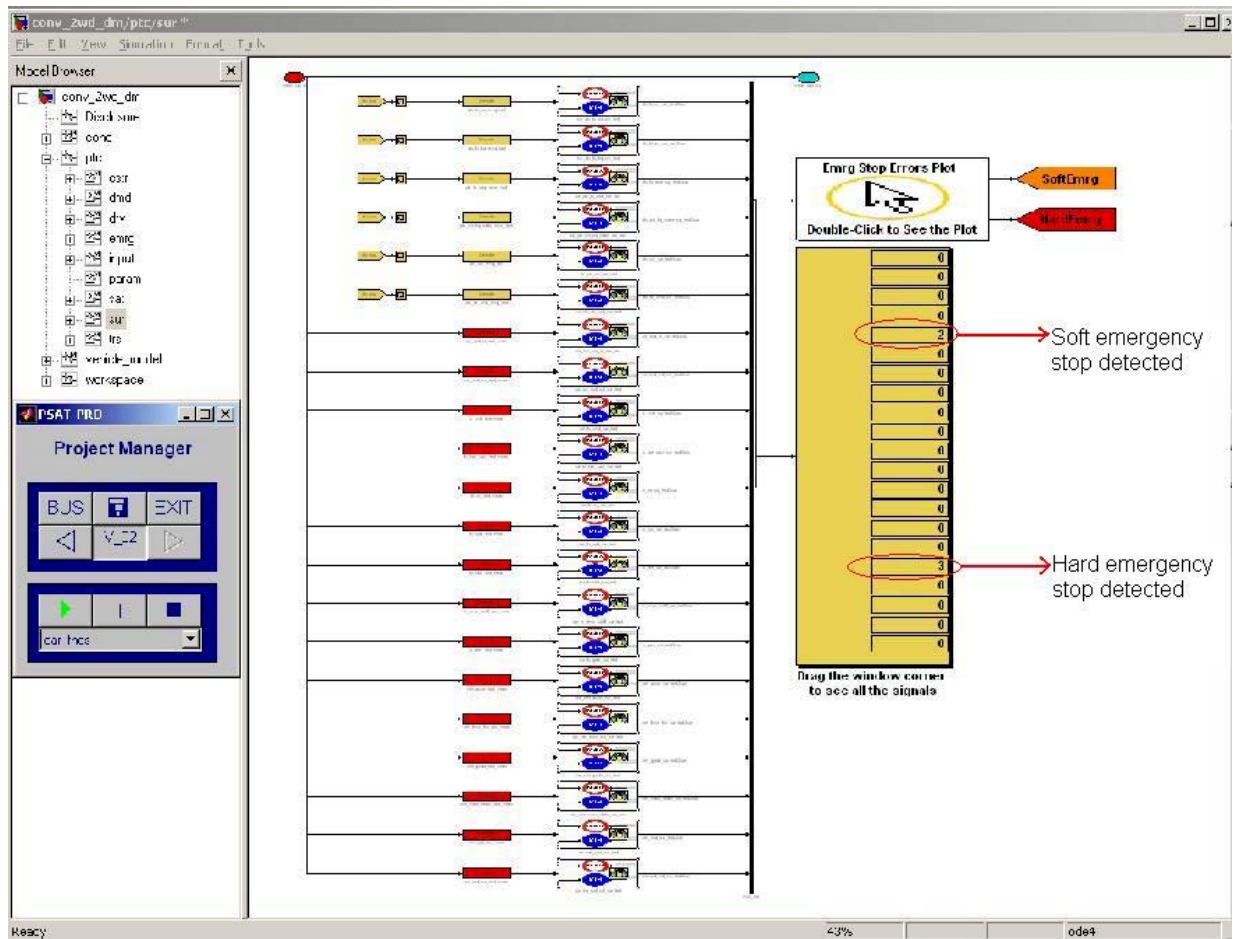
Go back to the PROJECT MANAGER interface.

Select a driving cycle within the popup menu of the simulation board.

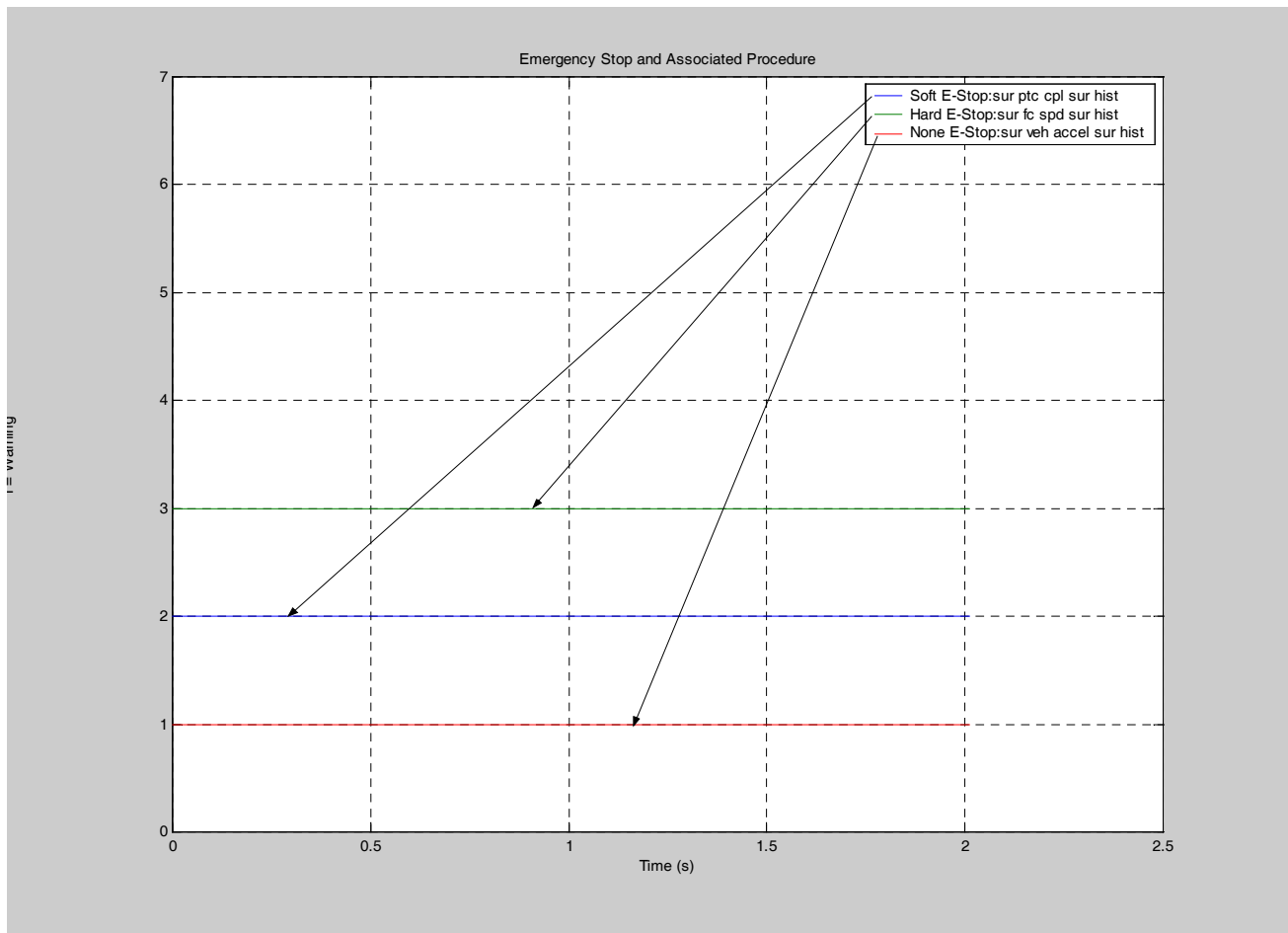
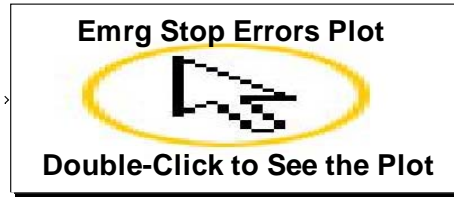
Click on play and wait while your PSAT-PRO system is being updated.

On the top-level window, the clock displays the driving cycle time.

Default detection will result in the interruption of the simulation within the next two seconds. It is then possible to check which signal crosses its limit by going in the “sur” block. A display shows the state of all the survey block output signals (1, 2, and 3 for NONE, SOFT, and HARD emergency stop).



You can also have a comprehensive plot to understand which error occurred and when it occurred by double-clicking on this push-button:



Note: For your records, the signals responsible for the emergency stop have been saved under EmrgStopHistFile.mat.

A1.7 PSAT-PRO Tools Description

Plot the Signals

PSAT-PRO proposes an easy simulation signal-plotting tool. You can use it even during a simulation pause and then keep on the simulation.

To plot a signal:

Use the browser to go in the “to_workspace” block.

You can access all the project signals. Those signal are gathered within three buses of information in the three different blocks:

- In “meas_space”: You can access the measure signals
- In “param_space”: You can access the parameter signals
- In “ptc_space”: You can access the signal generated in the controller

Go in one of those blocks by using the model browser:



Double click on the signal you wish to plot and then double click on new figure to create a new plotting window.

If you double click many signals in a row, they will appear in the same figure.

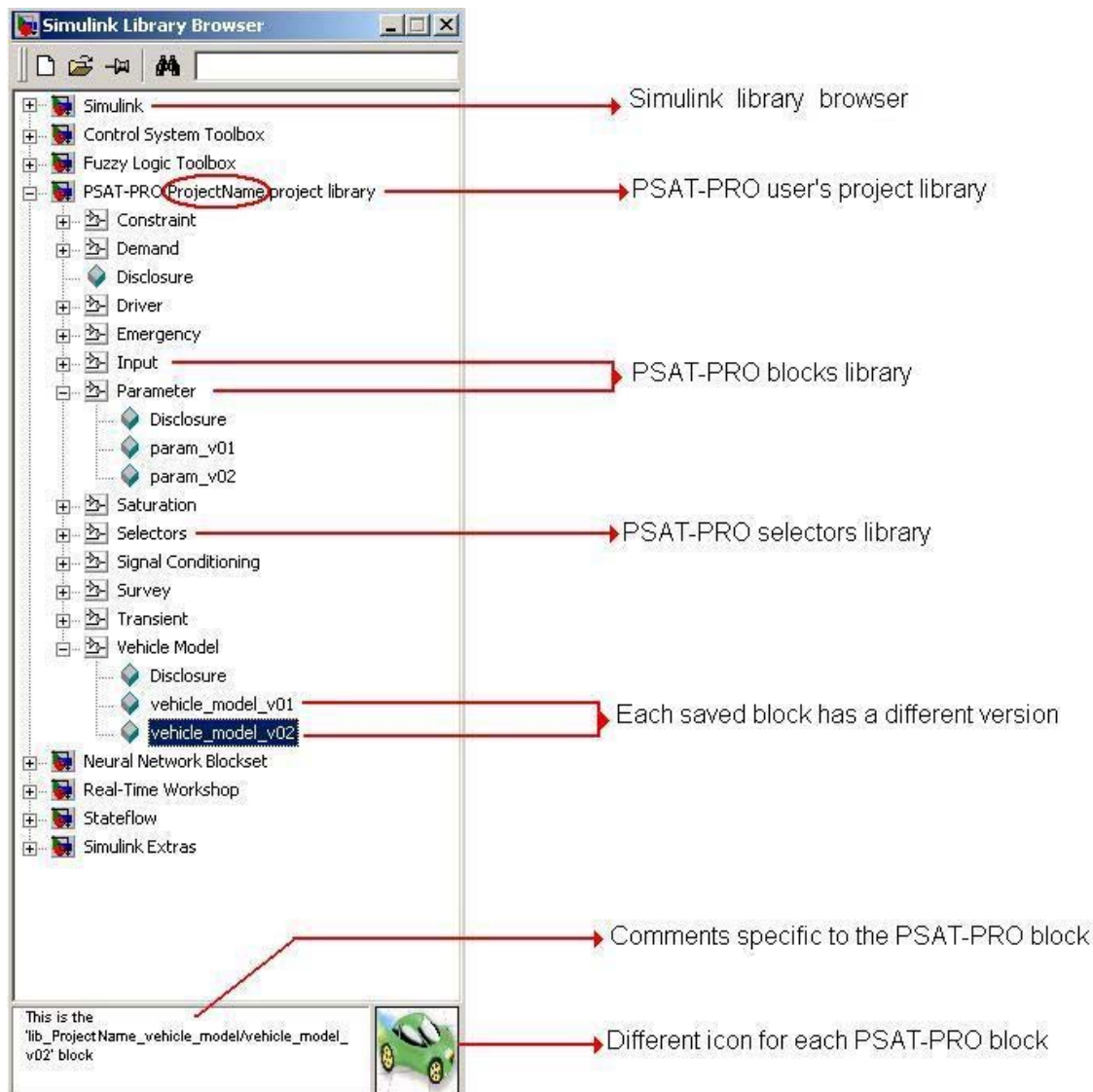
Double click on auto scale if you want the signals to be sized at the same range.

Use the PSAT-PRO User Library

PSAT-PRO facilitates the control system development. Using state-of-the-art tools, you will be able to develop your own controller, download it, and test it rapidly.

To have easy access to the PSAT-PRO blocks developed under a particular project, the library of your project has been added to the Simulink library browser. Using the library of your project, you will be able to drag and drop any block created and saved in your project library.

To open the Simulink library browser, type “simulink” on the Matlab workspace.



Note: You may have to close and re-open the Simulink library browser in order to update it.

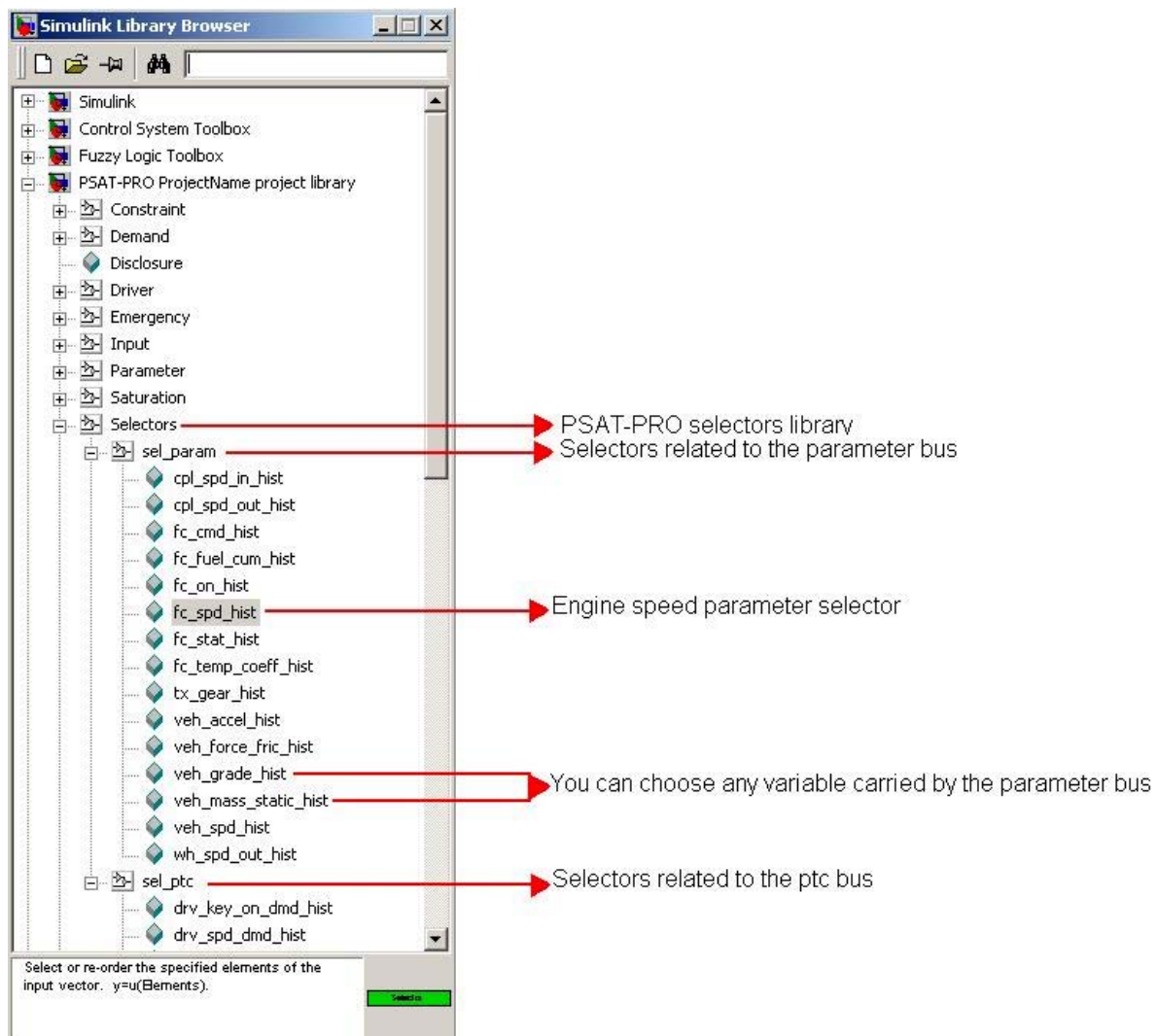
Use the PSAT-PRO Selectors Library

A selector generates as output a selective element of the input bus.

Every selector used in your model is included in your PSAT-PRO project library. This allows the user to reuse a signal previously created.

There are two types of selectors: They can be related to the ptc bus or to the parameter bus. The ptc bus carries all of the information generated by the powertrain controller, and the parameter bus carries the measures and the calculated variables.

In the Simulink library browser, select your PSAT-PRO project library and then the right selector, depending on if you need a signal coming from the ptc bus or from the parameter bus.





Use the Selector Autoplug Function

Every selector used in the model, even those newly created by the user (see “21 – Create a New Signal and its Selector p. 26”), can be plugged automatically to their related bus. This functionality avoids any mistake in the use of the variable buses.

By a simple double-click, the selector will be automatically plugged into its bus or into a feedback of the bus. In fact, you have the option of using a signal in a PSAT-PRO block before this signal has been generated. In this case, the selector will be plugged to a feedback of its related bus with a memory. The calculation will be performed by using the step before value of the signal.

Example: You need to know the engine speed measured on your system and the torque command sent to the engine to develop your control strategy.

Use the model browser to open the ptc block.

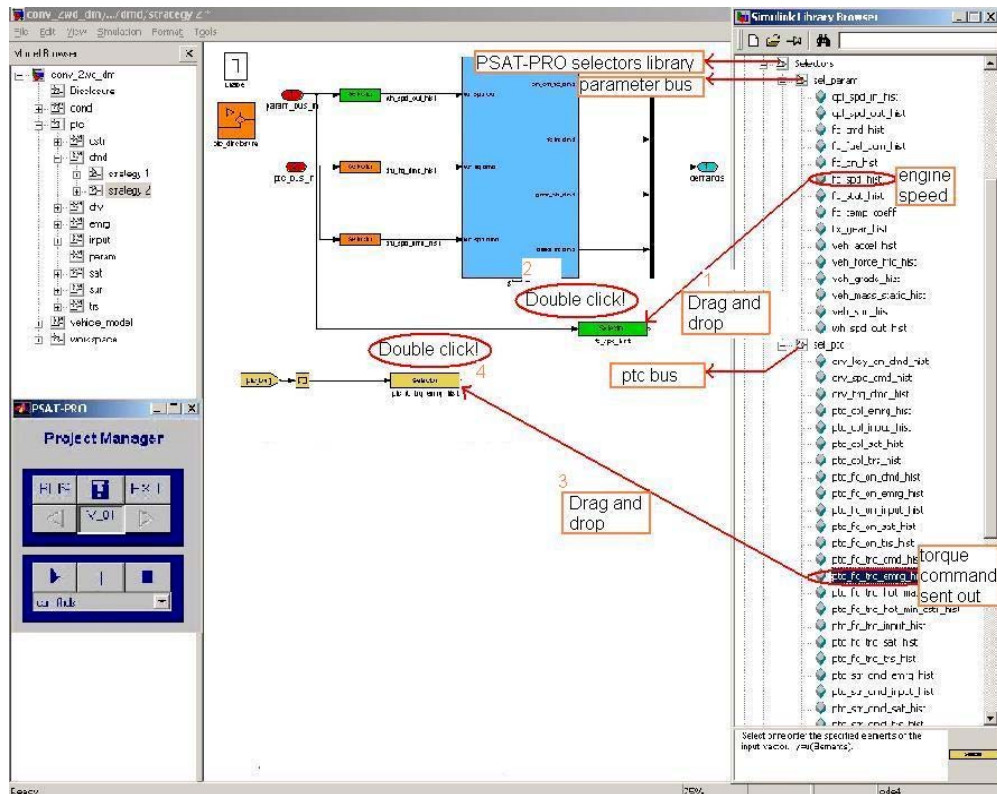
Select the dmd block (which is dedicated to the control strategy) in the work area.

Right click and select “Break library link.”

Use the model browser to open the dmd block.

Open your control strategy (strategy 2 on this example).

Open the PSAT-PRO selectors library browser.



- Drag and drop the engine speed selector from the parameter bus.
- Double-click on it and the link to the parameter bus input will appear.
- Drag and drop the selector corresponding to the engine torque command sent out from the ptc bus.
- Double-click on it and the ptc bus feedback with a memory block will appear.

Create a New Signal and its Selector

If you need to create a new selector, you must first have a new signal in one of the buses (parameter bus or ptc bus). When you add this new signal to the bus, you have to follow the rules below:

Break the library link of the block where you want to create the new signal. (Right click and select “Break library link.” Use the model browser to open this block.

Add one input to the mux block that combines the signals into the bus.

Calculate your signal and connect it to the additional input.

Label the line connected to the mux with the name of your signal. Note: This name will be used later to identify your signal in the bus.

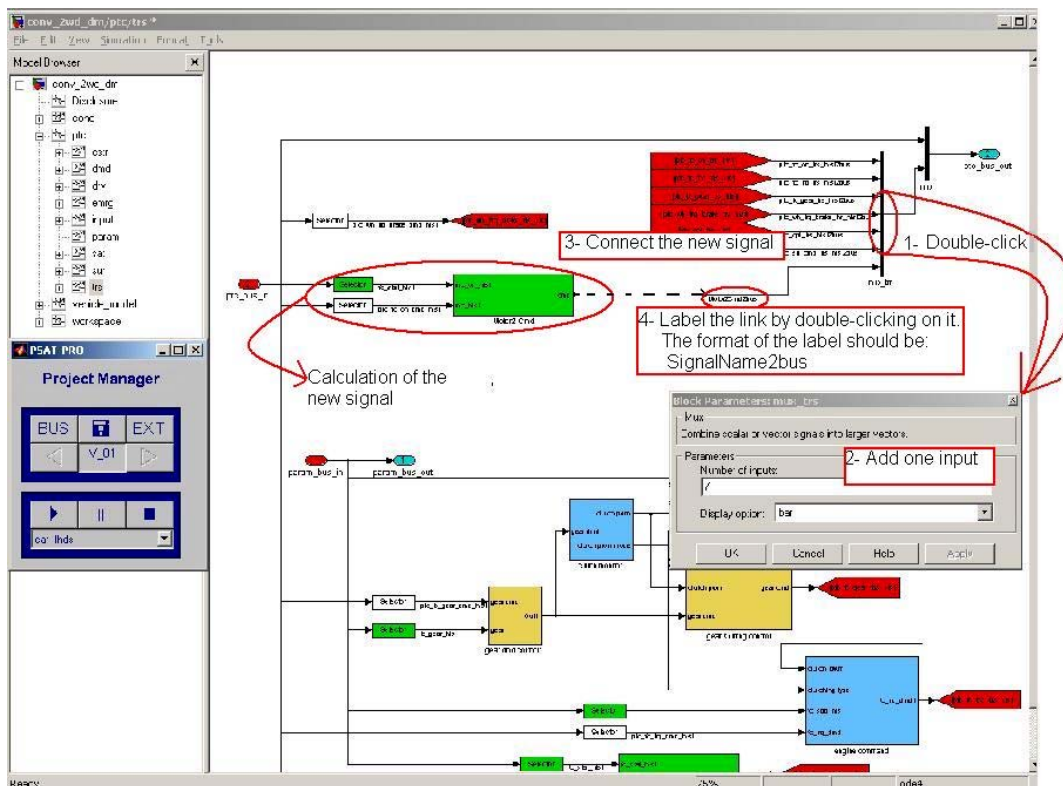
Add the string “2bus” to the label in order to generate the process that will add your signal to the bus.

Update the buses by using the Project Manager.

BUS

Congratulations! Your signal has been generated and added to the bus!

Example: You want to add a new signal to the trs block.

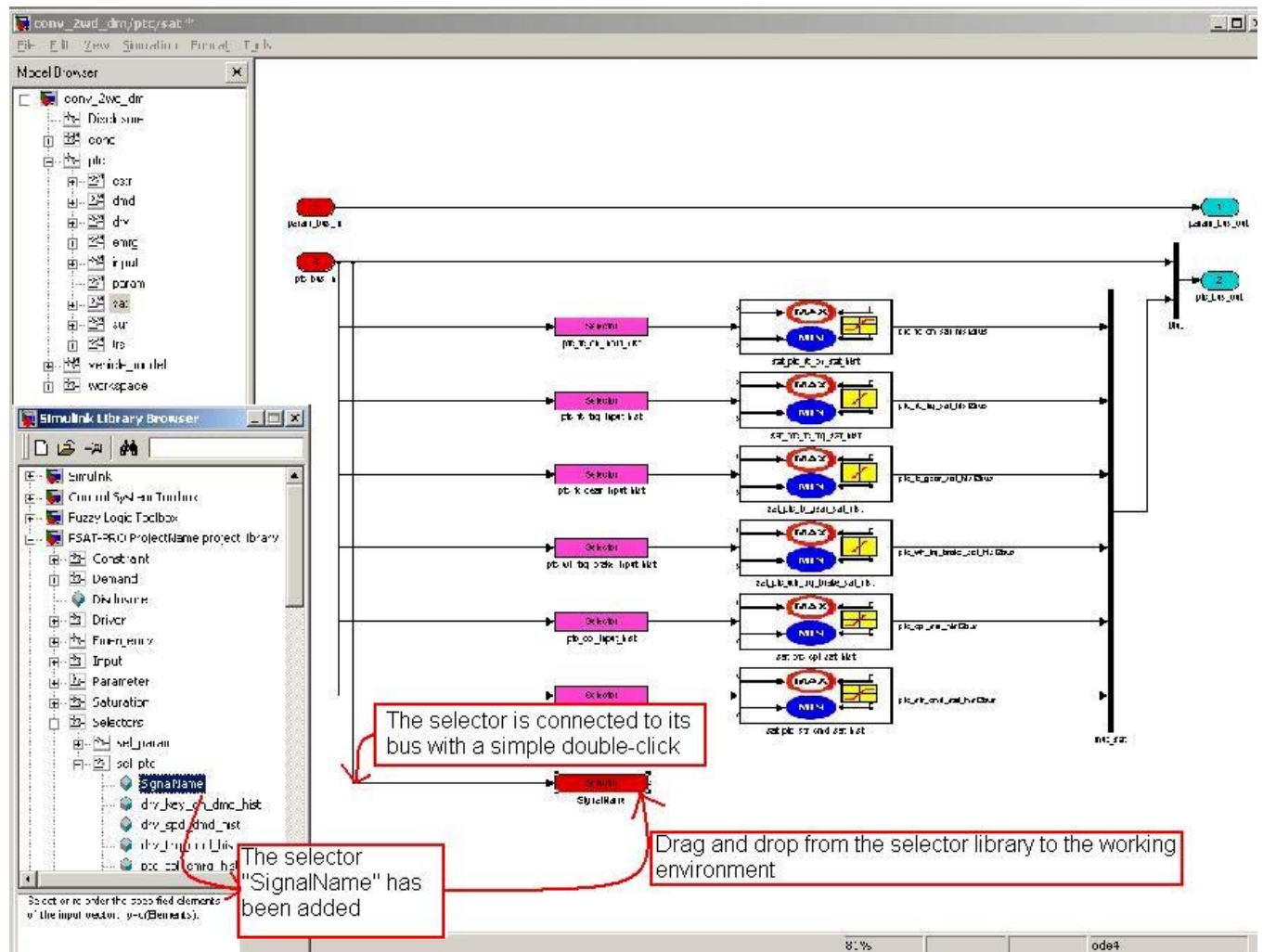




As this signal has been calculated in the trs block, it has been added to the ptc bus. You can now use this signal anywhere in your system. You just have to drag and drop the selector that has been generated.

Example: Now, you want to saturate the new signal in the sat block. You need to select your signal from the coming ptc bus.

Drag and drop the selector corresponding to your signal from the appropriate bus. Double-click on it and the link to the appropriate bus will appear.



Congratulations! Your selector has been created and you have been able to use it!



8.2. Instrumentation

MEASURE	PHYSICAL MEASUREMENT			
	Type	min	max	unit
DYNO SYSTEM				
DIGALOG SPEED CMD	SPEED	0	5000	RPM
DIGALOG TORQUE CMD	TORQUE	-542	542	Nm
DIGALOG SPEED	SPEED	0	5000	RPM
DIGALOG TORQUE	TORQUE	-814	814	Nm
AIR IN TEMP	TEMP	0	500	Deg. C
AIR OUT TEMP	TEMP	0	500	Deg. C
OIL PRESSURE	PRESSURE	0	500	PSI
CVT				
SUMP TEMP	TEMP	0	500	Deg. C
CASE TEMP	TEMP	0	500	Deg. C
OIL TEMP	TEMP	0	500	Deg. C
DRIVE PULLEY PRESSURE	PRESSURE	0	1000	PSI
DRIVEN PULLEY PRESSURE	PRESSURE	0	1000	PSI
SUPPLY PRESSURE	PRESSURE	0	1000	PSI
INPUT SPEED	SPEED	0	4500	RPM
OUTPUT SPEED	SPEED	0	2000	RPM
INPUT TORQUE	TORQUE	-500	500	N.m
OUTPUT TORQUE	TORQUE	-5000	5000	N.m
EXHAUST				
PRE TURBO	TEMP	0	1000	Deg. C
PRE CATALYST	TEMP	0	500	Deg. C
MID CATALYST	TEMP	0	500	Deg. C
POST CATALYST	TEMP	0	1000	Deg. C
FUEL & EMISSION				
VOLUME	VOLUME	0	60	L/h
AMBIANTE TEMP	TEMP	0	500	Deg. C
CO2	CONCENT.	0	1000000	ppm
CO	CONCENT.	0	1000000	ppm
O2	CONCENT.	0	1000000	ppm
CH4	CONCENT.	0	1000000	ppm
NOX	CONCENT.	0	1000000	ppm
THC	CONCENT.	0	1000000	ppm
CVS PRESS.	PRESSURE	-20	20	PSI
CVS TEMP.	TEMP.			Rankine

MEASURE	PHYSICAL MEASUREMENT			
	Type	min	max	unit
ENGINE				
SPEED	SPEED	0	4500	RPM
COOLANT RETURN TEMP	TEMP	0	500	Deg. C
COOLANT SUPPLY TEMP	TEMP	0	500	Deg. C
AIR INTAKE TEMP	TEMP	0	500	Deg. C
OIL TEMP	TEMP	0	500	Deg. C
MANIFOLD AIR PRESSURE	PRESSURE	0	100	PSI
OIL PRESSURE	PRESSURE	0	100	PSI
PRE-TURBO PRESSURE	PRESSURE	0	100	PSI
POST-TURBO PRESSURE	PRESSURE	0	100	PSI
PRE INTERCOOLER TEMP	TEMP	0	500	Deg. C
POST INTERCOOLER TEMP	TEMP	0	500	Deg. C
FUEL SUPPLY TEMP	TEMP	0	500	Deg. C
FUEL RETURN TEMP	TEMP	0	500	Deg. C
AIR INTAKE MASS FLOW	AIR FLOW	0	530	SCFM
BRAKE				
COMMAND	TORQUE	0	400	Nm
PRESSURE	PRESSURE	0	1000	PSI
PAD TEMP	TEMP	0	500	Deg. C
UQM				
FIRST TEMP	TEMP	0	500	Deg. C
SECOND TEMP	TEMP	0	500	Deg. C
COOLANT IN TEMP	TEMP	0	500	Deg. C
COOLANT OUT TEMP	TEMP	0	500	Deg. C
INVERTER IN TEMP	TEMP	0	500	Deg. C
INVERTER OUT TEMP	TEMP	0	500	Deg. C
SPEED	SPEED	0	8000	RPM
TORQUE	TORQUE	-200	200	N.m
INVERTER CURRENT	CURRENT	-300	300	A
VOLTAGE	VOLTAGE	0	200	V
CLUTCH				
COMAND SIGNAL	POSITION	0	1	Deg. C
FALK 4:1 Speed increaser				
TEMP	TEMP	0	500	Deg. C
OIL PRESSURE	PRESSURE	0	50	PSI

8.3. Design of the Constant Velocity Sampler

Critical Flow Venturi

Constant velocity sampling is achieved when an emission sample is extracted out of a constant and homogeneous flow; the known flow and the concentration readings give emission flow mass. A Critical Flow Venturi (C.F.V.) will be used to achieve constant velocity sampling: The CFV is a specially designed orifice with a smoothly curved geometry (see Figure 3.1)

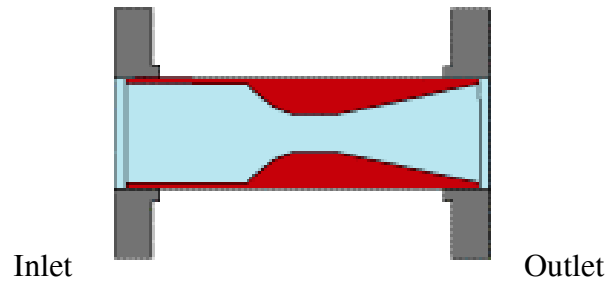


Figure 3.1: Critical Flow Venturi

The property of the CFV is to ensure constant flow at the throat when the pressure or vacuum of the outlet reaches a certain level. When the critical flow is reached, the venturi is operating in choked mode and ensures sonic flow. The flow value can be calculated accurately by using a venturi -geometry-related calibration constant and the pressure and temperature affecting fluid density at the inlet of the venturi.

The CFV that will be used for the design of the CVS is a stainless-steel HORIBA design recovered from decommissioned CVS-40 equipment. The Throat diameter of the venturi is 1.2865 in. (32.7 mm)

The flow can be calculated as follows: $V_{mix} = (C1 \cdot P_{in}) / \sqrt{T_{in}}$

V_{mix} : Choked flow in Standard Cubic Feet per Minute (SCFM)

$C1$: Calibration constant: $10.631 \text{ SCFM} \cdot \text{R}^2 \cdot \text{mmHg}^{-1}$

P_{in} : Inlet pressure in millimeter of mercury (mmHg)

T_{in} : inlet Temperature in Degree Rankin (R)

Under standard conditions of $P_{in} = 760 \text{ mmHg}$ and $T_{in} = 527.69 \text{ R}$, the venturi standard flow is $V_{mix_std} = 350 \text{ SCFM}$.

The main issue with CFV is to make sure that the blower pulls enough air to choke the venturi. The manufacturer usually provides CFV operating pressure conditions. Those conditions are usually a vacuum level at the venturi outlet and/or a pressure differential ratio between inlet and outlet. Another way to verify that the venturi is choked is to verify that the pressure inlet in the venturi is not affected by pressure change at the venturi outlet. When choked, the flow at the venturi is constant, and pressure in the dilution tunnel only depends on dilution tunnel geometry.

A propane shot calibration test will certify that the CFV is choked because sonic flow is used to recalculate injected propane mass. If sonic flow is not achieved, the result of the propane shot test will be irrelevant.

Dilution Tunnel

Both exhaust gas and dilution air must be well mixed to have a meaningful concentration reading of a homogeneous sample. To do so, a dilution tunnel collects and mixes both exhaust and dilution air before the sample is routed to an analyzer. The dilution tunnel consists of a pipe connected to the venturi inlet on one side and a collecting exhaust flow and dilution air on the other side. A mixing device is installed on the collecting side of the tunnel. This ensures dilution of exhaust in air by creating turbulences. The sample probes must be placed closer to the venturi, where mixing turbulences are dampened by their travel throughout the tunnel and where the sample will most likely be homogeneous. The general rule of thumb for dilution tunnel dimensioning is that the length separating mixing device and sample probe must be at least 10 times the diameter of the tunnel (see Figures 3.2 and 3.3).

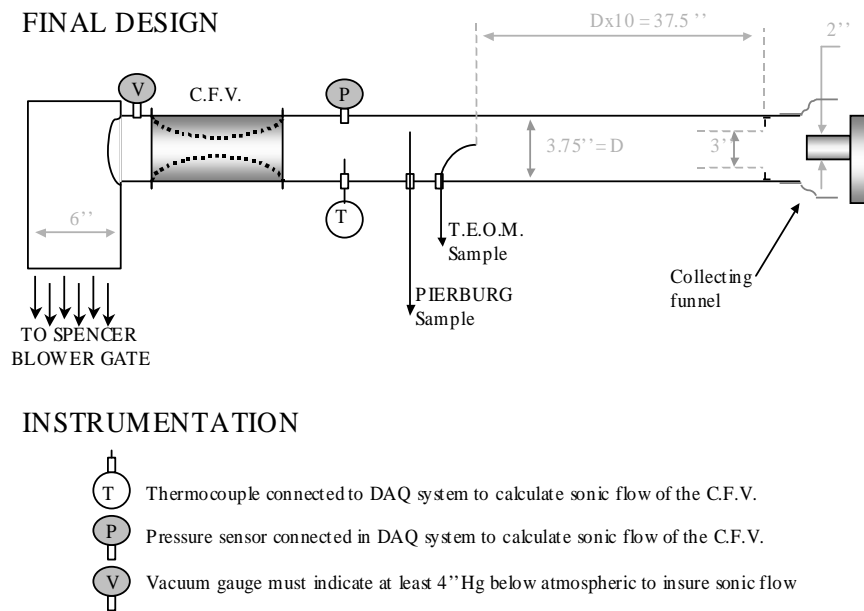


Figure 3.2

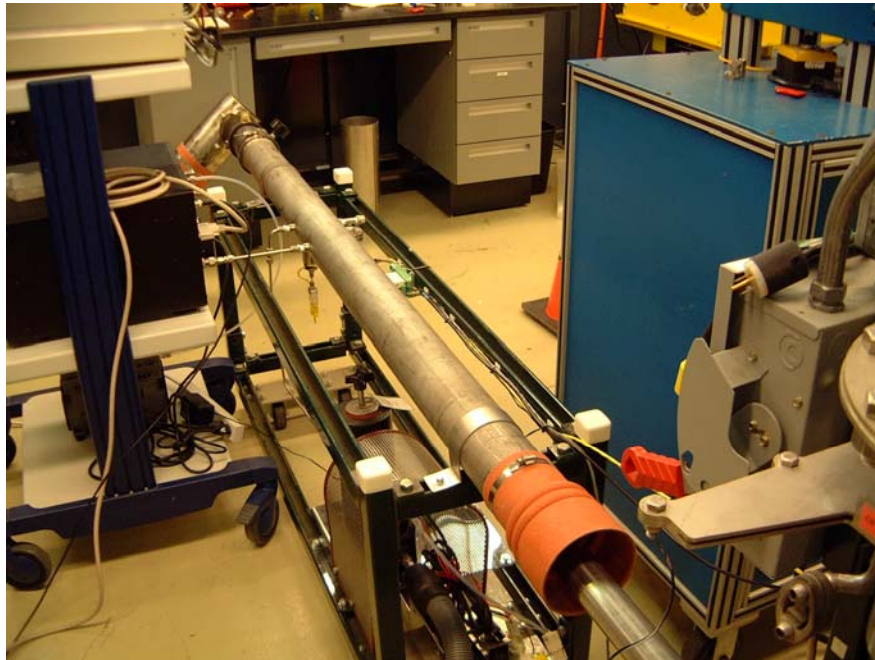


Figure 3.3

The tunnel diameter should be approximately the same as the diameter of the venturi inlet for assembly compatibility. To simplify design, the tunnel must be a straight pipe; in addition, this will minimize the loss of particulates that are more likely to be trapped in a complex geometry. A mixing device will create turbulences near the tailpipe gases and ambient dilution air inlet.

Mixing Device and Collecting Funnel

The mixing device is an aluminum reduced-diameter choking plate that is fitted near the inlet of the dilution tunnel. The diameter is 1 in. smaller than the inside diameter of the dilution tunnel. The plate has been secured with rivets. The reduced diameter of the mixing device creates a pressure drop at the inlet of the CFV. It is important that the reduced diameter remains bigger than the diameter of the venturi throat, or Venturi flow might be disturbed (see Figure 3.4).

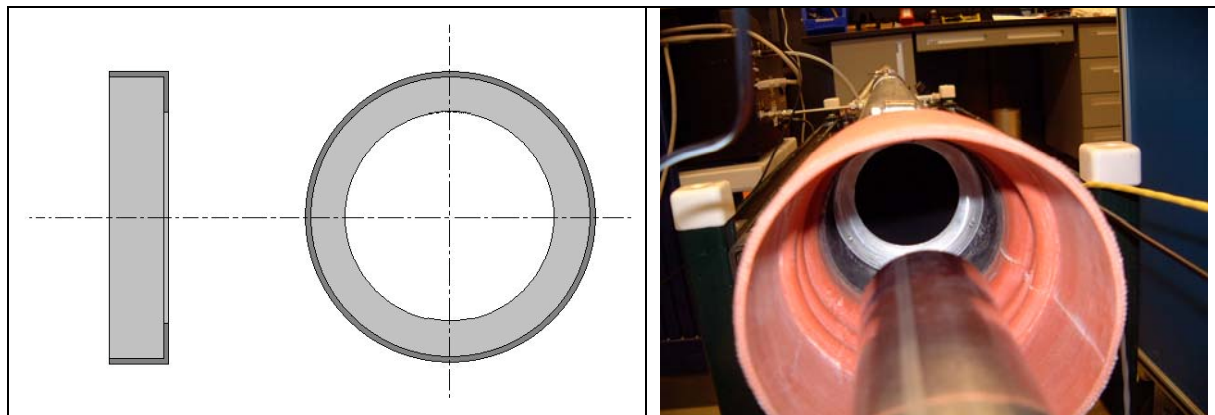


Figure 3.4

The propane shot calibration procedure demonstrated the importance of a mixing device. Propane was first injected into a dilution tunnel without a mixing plate. Then, injection was performed with mixing device in place. Figure 3.5 demonstrates how a mixing device affects stable concentration.

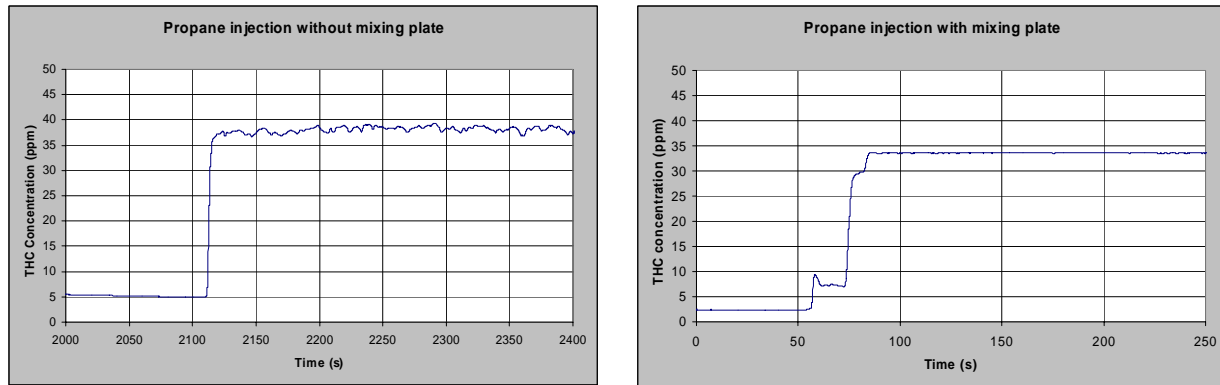


Figure 3.5

A collecting funnel has been installed to reduce air speed flowing along the tailpipe. In this way, the funnel helps maintain near-atmospheric pressure at the tailpipe. If the tailpipe were directly inserted in tunnel, exhaust gases would be non-realistically pulled from the exhaust line because tailpipe and tunnel diameter are fairly close.

Sampling Probes

The Pierburg probe collects a sample to read the concentration of the dilute sample gas. The probe is plumbed by using a stainless-steel line to the end of line filter. The Pierburg line is heated between the end of line filter and concentration bench (see Figure 3.6 and 3.7).

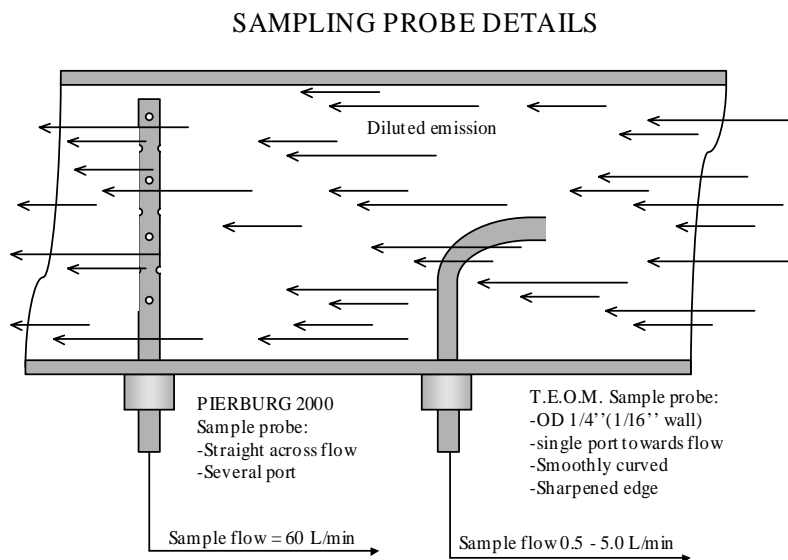


Figure 3.6



Figure 3.7

Ideally, the TEOM probe should be designed to have iso-kinetic PM mass measurement sampling. This means that dilute sample would enter the TEOM probe at the same speed that sample is flowing in the tunnel. This way, the sample probe would collect particulate species without creating turbulences in the flow. Iso-kinetic sampling can be achieved in the following condition: $Q_s/Q_t = (R_s/R_t)^2$

- Qs: Flow of the TEOM sampling
- Qt: Flow of the dilution tunnel
- Rs: Radius of the TEOM probe inlet port
- Rt: Radius of the dilution tunnel

In addition, the collecting probe should have a diameter of at least ½ in. Because of the tunnel diameter and Q_s/Q_t ratio value, iso-kinetic sampling could not be achieved with the developed setup. However, a design effort has been made to minimize travel between inlet port and TEOM analyzer. Reducing this travel contributes to decreasing the amount of particulate losses on the inside wall of the line. The final probe design makes the particulate travel through a single smooth 90° curve and less than a foot of line to the instrument (see Figure 3.8).

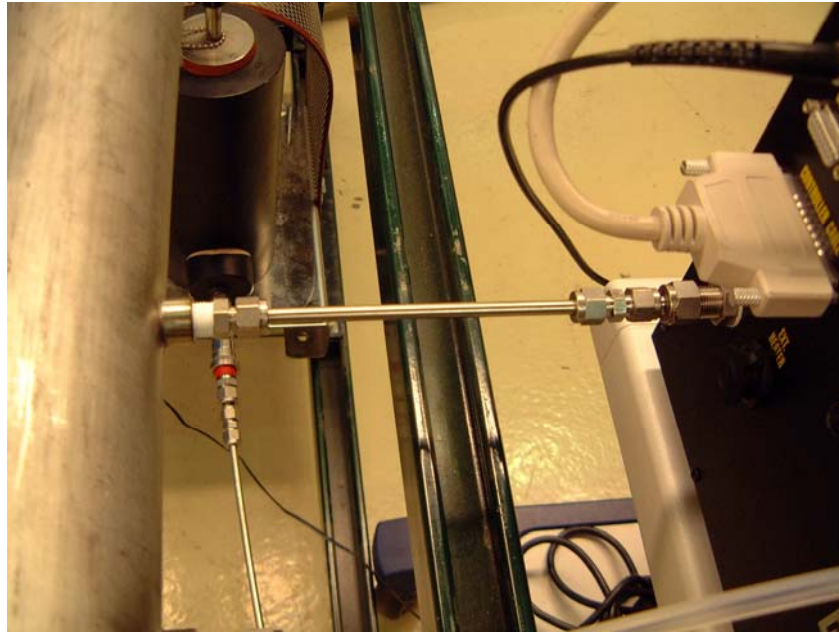


Figure 3.8

Emission Mass and Fuel Consumption Calculation

The Pierburg 2000 emission bench provides dilute emission concentration in particles per pillion (ppm). The critical flow will be used to calculate emission mass in grams. The calculation will be processed on-line by using the data acquisition system based on CFR 40 Part 86 calculation theory.

The emitted masses are calculated according to the following equation:

$$M_i = V_{mix} * Q_i * C_i / 1000000$$

M_i : Mass of exhaust pollutant

Q_i : Density of the pollutant g/L at standard temperature and standard pressure

C_i : Pollutant concentration expressed in ppm

V_{mix} : Corrected dilute exhaust volume corrected to standard conditions

The data acquisition system is connected to the Pierburg 2000 concentration bench through the RS232 series interface so that the mass of each pollutant can be calculated on-line during powertrain operation. Exhaust gas is diluted by using ambient air, and so background pollutant concentration is collected while the engine is not operating. At each sample time, the program computes pollutant and background concentration values, sample temperature, and pressure that yield instantaneous pollutants in g/s for the following species: CH₄, THC, CO₂, CO, O₂, and NO_x.



At the end of a test, all data are saved and post-processed by using integrated instantaneous vehicle speed (driving distance). Finally, pollutant emissions in g/mi are used to calculate vehicle fuel consumption in mpg by using the following formula:

$$\text{Diesel fuel consumption (mpg)} = 2778 / (0.866 * \text{HC} + 0.429 * \text{CO} + 0.273 * \text{CO}_2)$$

HC: Total hydrocarbon mass g/mi

CO: Total carbon monoxide g/mi

CO₂: Total carbon dioxide g/mi



8.4. Data Acquisition Code to Calculate g/mi Emissions

```
/*                               CSV THEORY                               */

float C1;

// float NOXbckgnd; float CObckgnd; float THCbckgnd; float CH4bckgnd;
// float CO2bckgnd; float O2bckgnd;
float QNOX;float QCO; float QTHC; float QCH4; float QCO2; float QO2;
float SCFM2LPS; float QFuel; float gallon2L; float V; float Vmix; float DF;
float NOXcorrected; float COcorrected; float THCcorrected; float CH4corrected; float
CO2corrected; float O2corrected;
float Fuelgallonsec;

/*Declares constants*/

QNOX=1.913;QCO=1.164;QTHC=0.5768;QCH4=0.6672;
QCO2=1.83;QO2=1.3136;QFuel=837;

SCFM2LPS=28.316847/60;
gallon2L=3.785412;
C1=10.631;

/*Calculates total flow in venturi*/

V=(C1*DilPress)/sqrt(DilTemp); /* Venturi SCFM */
Vmix=V*SCFM2LPS; /* Venturi choke flow in L/s */

/*Calculates the dilution factors */

DF=13.4/((CO2+THC+CO)/10000);

/*Calculates corrected concentrations*/

NOXcorrected = NOX - NOXbckgnd *(1-(1/DF));
Cocorrected = CO - Cobckgnd *(1-(1/DF));
THCcorrected = THC - THCbckgnd *(1-(1/DF));
CH4corrected = CH4 - CH4bckgnd *(1-(1/DF));
CO2corrected = CO2 - CO2bckgnd *(1-(1/DF));
O2corrected = O2 - O2bckgnd *(1-(1/DF));
```



/* Mass of emissions */

$NOXg = V_{mix} * Q_{NOX} * NOX_{corrected} / 1000000;$

$COg = V_{mix} * Q_{CO} * CO_{corrected} / 1000000;$

$THCg = V_{mix} * Q_{THC} * THC_{corrected} / 1000000;$

$CH4g = V_{mix} * Q_{CH4} * CH4_{corrected} / 1000000;$

$CO2g = V_{mix} * Q_{CO2} * CO2_{corrected} / 1000000;$

$O2g = V_{mix} * Q_{O2} * O2_{corrected} / 1000000;$

/* Calculates fuel flow measured using fuel scale signal*/

$FuelgsecMeas = FuelIN * Q_{Fuel} / 3600;$

/* Calculates fuel flow using emission concentrations */

$Fuelgallonsec = (0.866 * THCg + 0.429 * COg + 0.273 * CO2g) / 2778; /* gallon per sec */$

$FuelgsecCalc = Fuelgallonsec * gallon2L * Q_{Fuel};$

8.5. A, B, C Coefficients Calculation

Powertrain Specifications:

We estimated the powertrain rotational inertia at 139 kg/m^2 , which would correspond to a vehicle of 1410 kg (curb weight) with an assumed wheel radius of 0.316 m .

Mercedes-Benz C 220 CDI Vehicle Specifications:

Curb Weight: 1410 kg

Wheel Radius: 0.316 m (estimated from tires specifications 195/65 R 15 H)

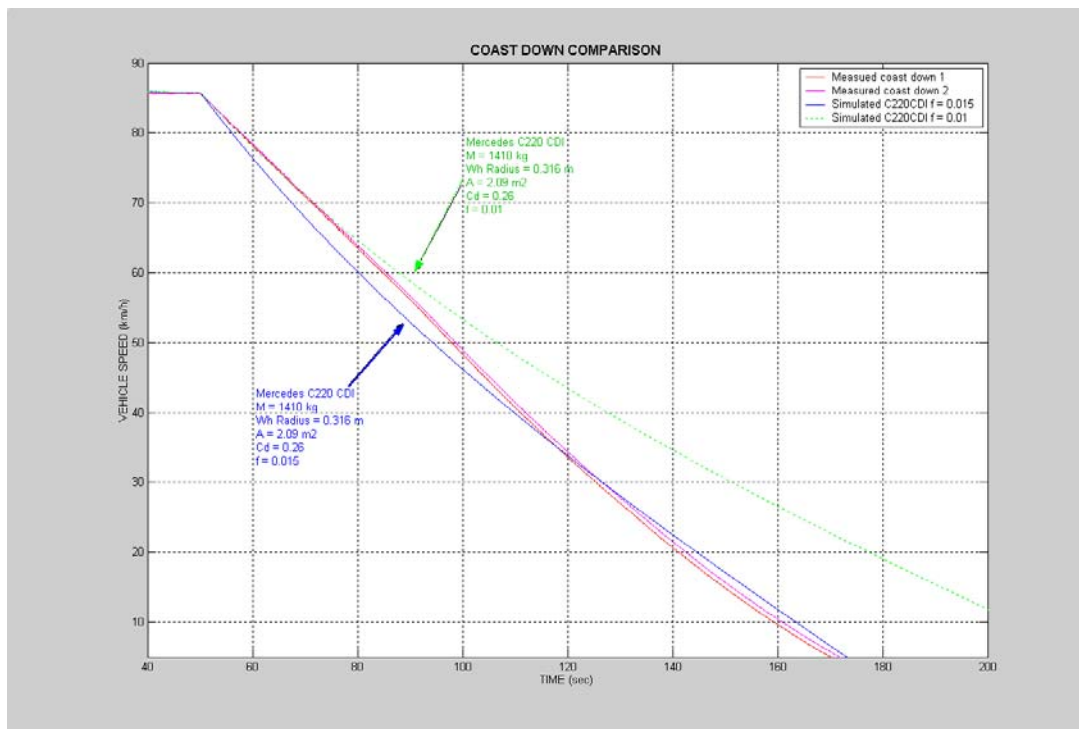
Frontal Area: 2.09 m^2

The rolling coefficient depends on the road surface, vehicle speed, and type of tires used. Simulation tools have been used to demonstrate the important impact of the rolling coefficient.

Simulations of coast down have been performed for two different values to demonstrate the important impact of the rolling coefficient:

$f = 0.01$ for low-rolling resistance car tire on dry pavement

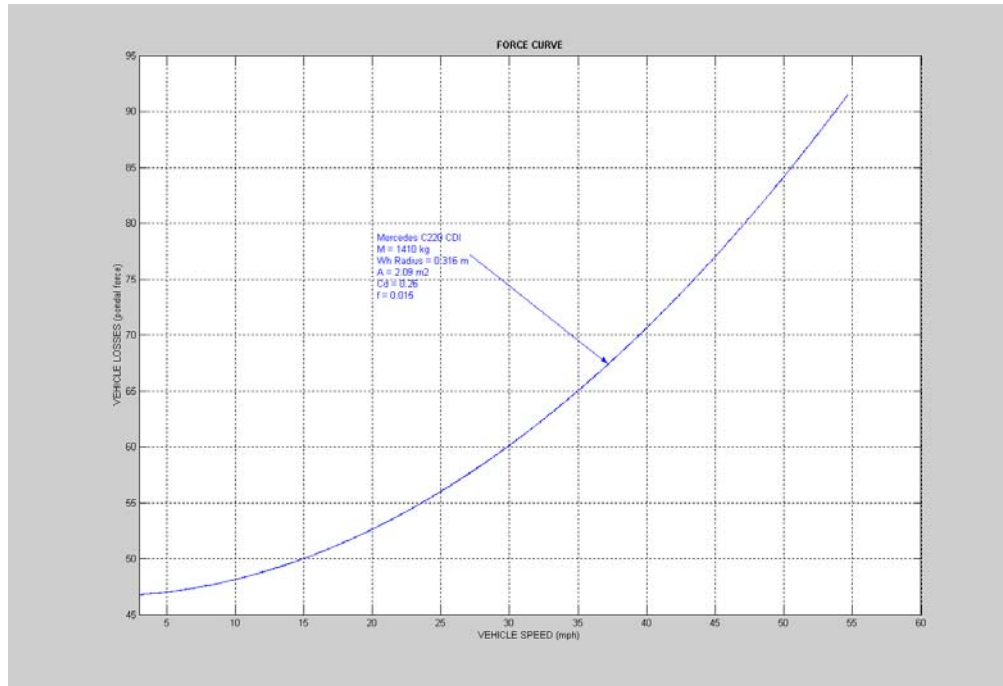
$f = 0.015$ for ordinary car tire on dry pavement



A coast down of the powertrain was performed so that we could compare the results of the simulation and determine the corresponding rolling coefficient value for the powertrain. The curves clearly show that the performance of a Mercedes C220 CDI with a rolling coefficient of 0.015 can be accurately compared with the performance of a hybrid powertrain.

The following curve has been generated by simulation using a model of the Mercedes C220 CDI with a rolling coefficient of 0.015. This curve allows the calculation of the A, B, and C target coefficient of the chassis dynamometer by using a polynomial fit algorithm.

A, B, C Target Calculation from Simulated Vehicle Data with $f = 0.015$



The polynomial fit algorithm gives:

$$A = 46.64$$

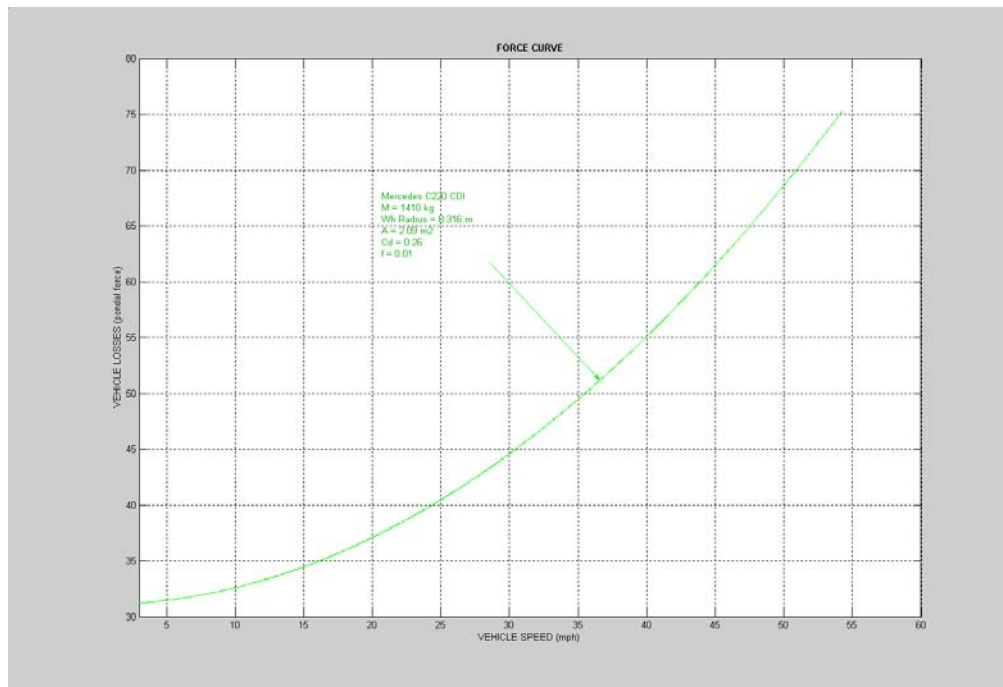
$$B = 0.00$$

$$C = 0.02$$

$$\text{with } P = A + B \cdot v + C \cdot v^2$$

The same process was applied for a vehicle with a rolling coefficient of 0.01.

A, B, C Target Calculation from Simulated Vehicle Data with $f = 0.01$



The polynomial fit algorithm gives:

$$A = 31.10$$

$$B = 0.00$$

$$C = 0.02$$

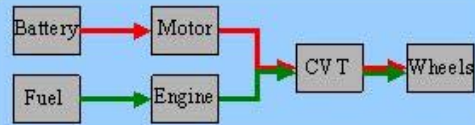
$$\text{with } P = A + B \cdot v + C \cdot v^2$$

The previous A, B, and C calculations were obtained from a simulation of a Mercedes C220 CDI with different rolling coefficients. Those A, B, and C coefficients were used as a target for the emulated vehicle. But we would not be completely accurate if we were using the same coefficient during vehicle testing because of the potential gap between the target and the actual emulated vehicle A, B, and C: We need to measure the emulated vehicle losses that could be different from the target A, B, and C.



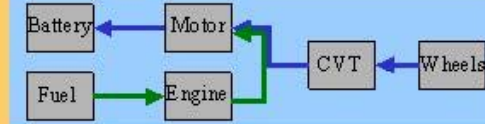
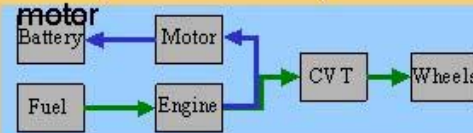
8.6. Different Mode of Operation of the Powertrain

DRIVING MODE	MODE	SPEED	SOC	ENGINE	DETAILS
<p>EV Mode Accel.</p>	EV1	Increases	Decreases	Disabled	Vehicle launch mode. Might be used during cruising if battery SOC allows. Mechanical brakes are used as well to slow down the vehicle.
<p>EV Mode Decel.</p>	EV2	Decreases	Increases	Disabled	Vehicle stop mode. Also used during deceleration when engine is off.
<p>HEV Mode Accel.</p>	HEV1	Increases	Decreases	Enabled	Mode used when engine power is too low to match driver acceleration demand.
<p>HEV Mode Accel.</p>	HEV2	Increases	Increases	Enabled	Cruising mode used when engine power is higher than driver demand. Motor absorbs a part of engine power in order to charge the battery.
<p>HEV Mode Decel.</p>	HEV3	Decreases	Increases	Enabled	Motor absorbs both engine power and regenerative power coming from the wheels. Mechanical brakes are used as well to slow down the vehicle.



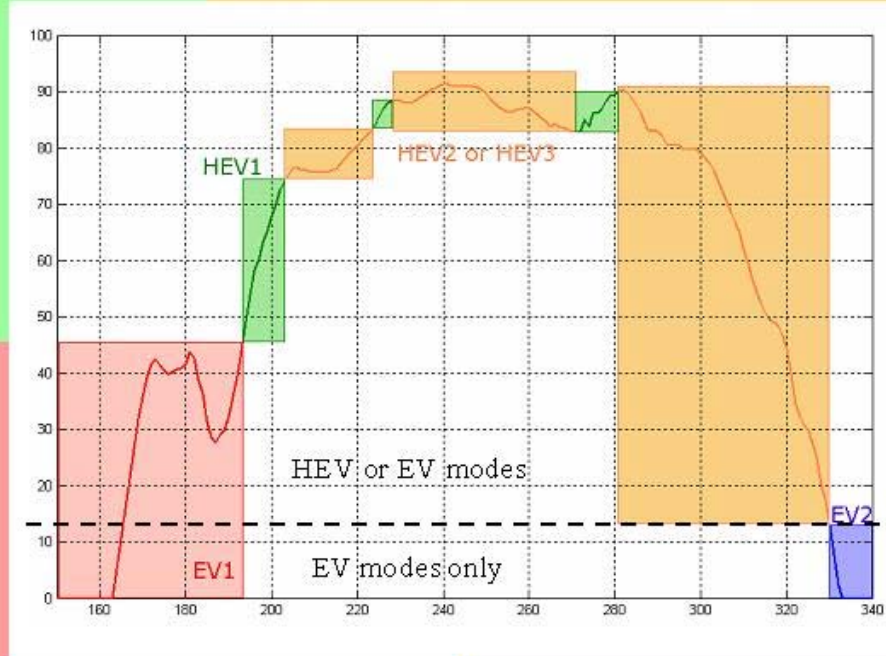
Acceleration might require both motor and engine to provide torque at the wheels

While cruising, engine power can operate vehicle and charge the battery simultaneously thru the motor

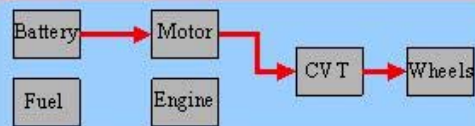


During deceleration, battery absorbs both powers coming from the engine the vehicle regenerative power

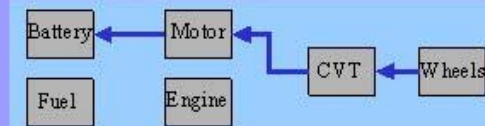
Depending on Battery Control Unit BCU and State-Of-Charge SOC, vehicle will switch from EV to HEV mode



As engine cannot be operated below idle speed clutch is opened and vehicle comes to a complete stop in EV mode



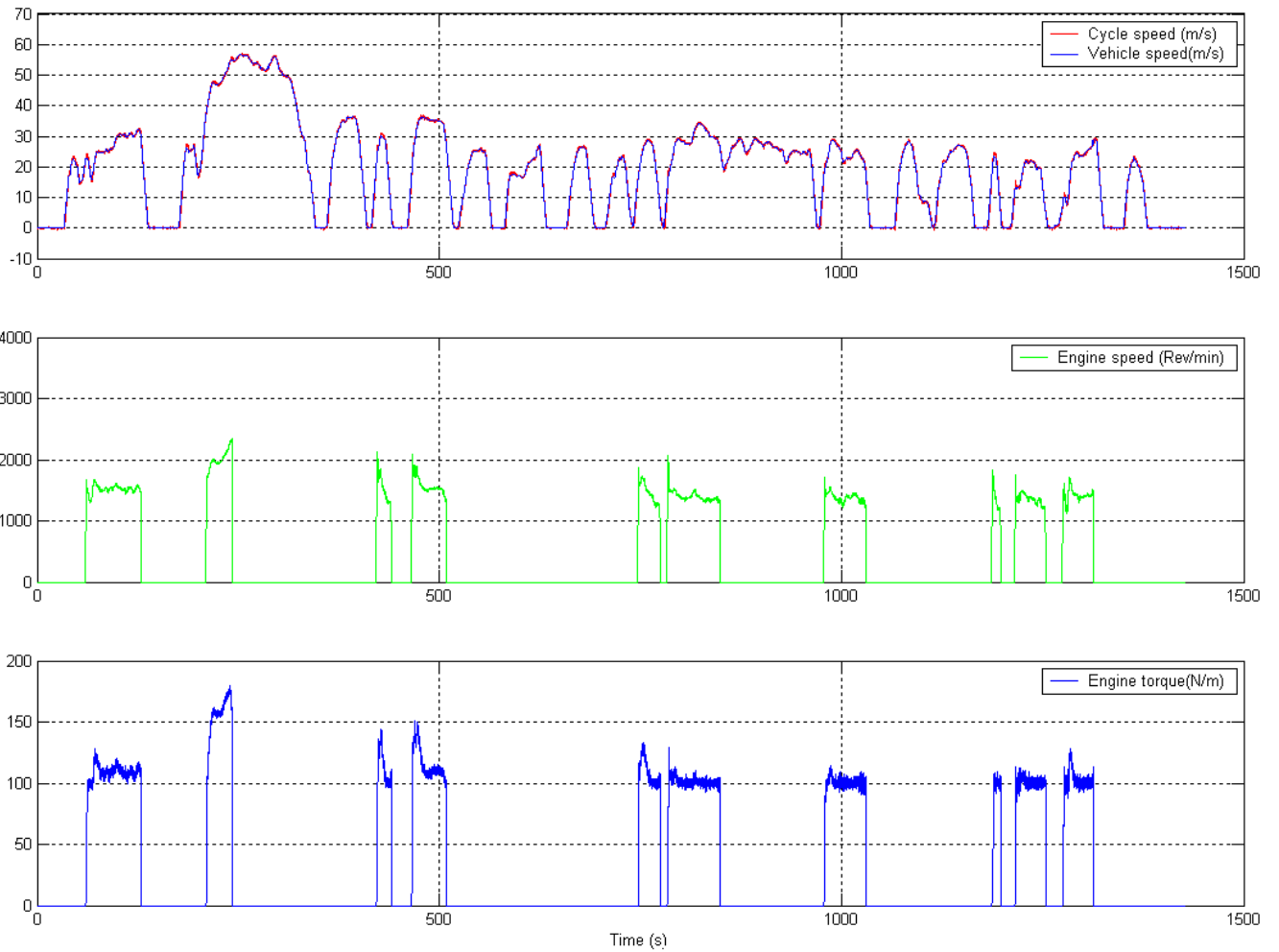
Below a certain speed, vehicle is operated in EV mode



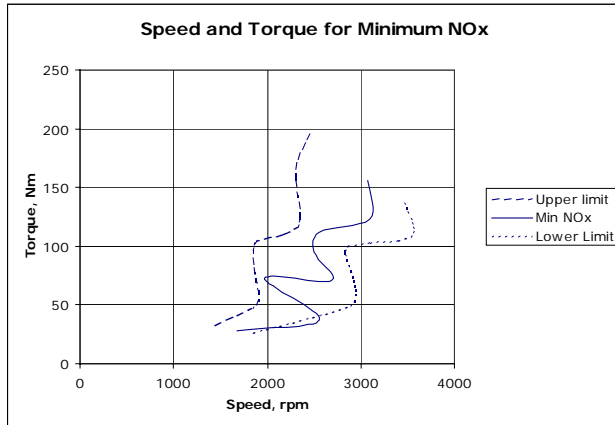
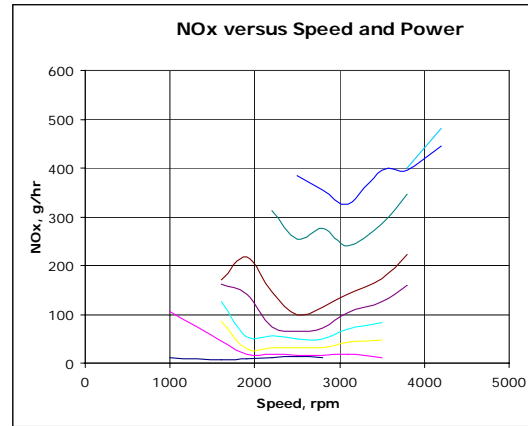
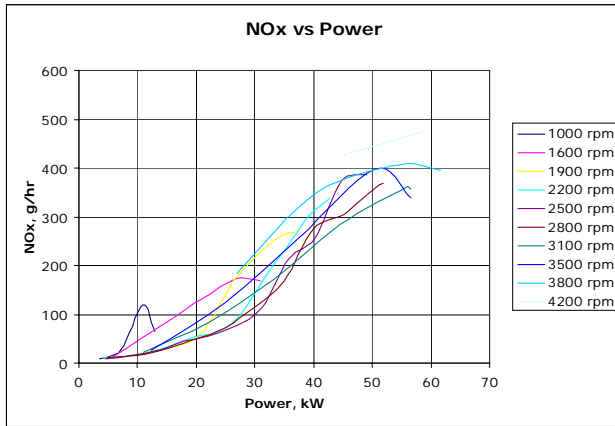


8.7. Engine Torque and Speed Using Best Efficiency Control

FUDS cycle

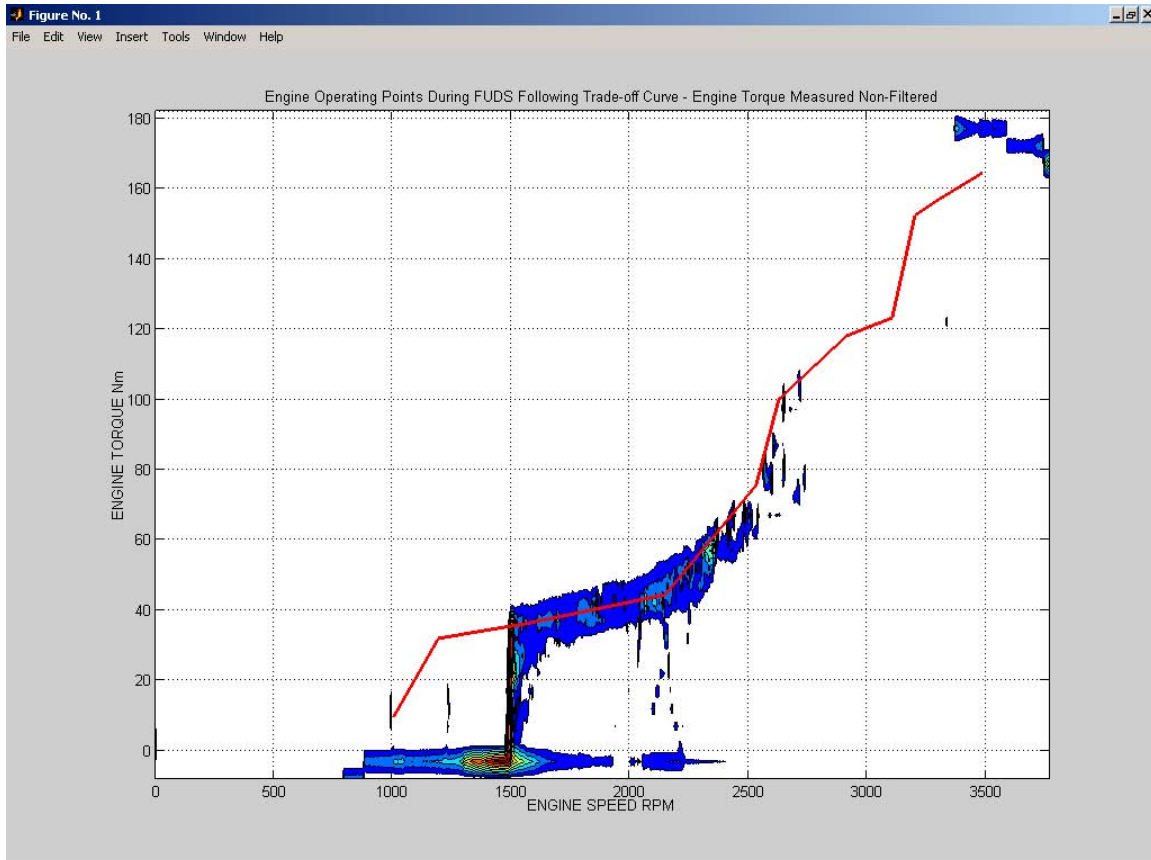


8.8. NO_x Emissions Results from Engine Steady-State Tests



8.9. Simulation Results Trade-Off Control Operation

The simulation results show a good ability for the control to keep the engine on the trade-off curve.



As for the best efficiency curve, it is more accurate to use the engine torque measured in order to determine the speed target that will allow the engine to operate at the desired operating point.

Improvements to the CVT model have been done to take into account the dynamic of the CVT, represent more realistically the behavior of the transmission, and correlate the test results.

8.10. Engine Torque and Speed Using Trade-Off Control

FUDS cycle

